UNIVERSIDADE FEDERAL DO RIO GRANDE DO SUL
INSTITUTO DE CIÊNCIAS BÁSICAS DA SAÚDE
PROGRAMA DE PÓS-GRADUAÇÃO EM CIÊNCIAS BIOLÓGICAS:
BIOQUÍMICA

Vítor Rocco Torrez

Disfunções retículo endoplasmático-mitocondriais induzidas pela inibição de PP2A e o papel astrocitário na neuroproteção em doenças neurodegenerativas

Porto Alegre
2019

Vítor Rocco Torrez

Disfunções retículo endoplasmático-mitocondriais induzidas pela inibição de PP2A e o papel astrocitário na neuroproteção em doenças neurodegenerativas

Tese apresentada ao Programa de Pós-Graduação em Ciências Biológicas: Bioquímica do Instituto de Ciências Básicas da Saúde da Universidade Federal do Rio Grande do Sul como requisito parcial para a obtenção do título de doutor em Bioquímica.

Orientador: Prof. Dr. Diogo Onofre Gomes de Souza
Coorientador: Prof. Dr. Luis Valmor Cruz Portela

Porto Alegre
2019

"Não desejo suscitar convicções. O

que desejo é estimular o

pensamento e derrubar

preconceitos."

Sigmund Freud

Agradecimentos

Ao meu orientador, Professor Diogo Onofre Gomes de Souza, por me mostrar que podemos ser diferentes e fazer a diferença. Por me mostrar, na primeira aula da faculdade, que a única busca realmente importante na vida é aquela pelo "amor verdadeiro". Tu mudaste minha vida.

Ao meu co-orientador, Professor Luis Valmor Cruz Portela, por sempre colocar-se ao lado de seus orientandos e amigos. Também por me mostrar que a vida pode ser mais leve, sem tantas formalidades.

Ao Professor Eduardo Rigon Zimmer, meu mestre e grande amigo. Por contagiar a mim e a todos ao seu redor com o seu ânimo e felicidade. Me inspiro em ti muito mais do que imaginas.

Aos meus amigos-irmãos, por todas as noites de longas conversas que me animaram nos momentos mais difíceis. Formamos o melhor grupo que alguém pode ter, independente do tempo e das circunstâncias.

Ao Sushi, o melhor cão e amigo que já existiu. Pelas lambidas, alegria e amor após cada noite estendida no laboratório. Tua amizade está nessa tese.

A Gabriela Wandscher, minha vida e meu amor, pela companhia, apoio e compreensão diária. Tu me fazes melhor a cada dia. Obrigado por nossa vida juntos.

À minha família, a base de tudo, por todo amor e carinho durante a vida.

Aos meus irmãos, Ariane e Danilo. Cresci e cresço a cada dia tendo vocês como inspiração.

À minha mãe, Gisele, pela dedicação e amor irrestritos e infinitos. Tu és o alicerce de cada conquista em minha vida.

Ao meu pai, Francisco. Sem ti, não seria nada. Te tenho como espelho a cada dia e escolha em minha vida. Obrigado por tudo.

APRESENTAÇÃO

Esta tese constitui-se de três partes, sendo elas:

Parte I: Resumo, Resumo em inglês (*abstract*), Lista de abreviações, Introdução e Objetivos;

Parte II: Resultados, que estão divididos em capítulos, cada um com um breve prefácio seguido de um artigo científico;

Parte III: Discussão, Conclusão, Anexos e Referências bibliográficas.

Na seção "Anexos", constam os artigos científicos que foram realizados durante o período de doutoramento, divididos em Anexo I (com conteúdo relacionado ao tema da tese) e Anexo II (conteúdo não diretamente associado ao tema da tese).

Os trabalhos elaborados nesta tese foram desenvolvidos no Laboratório de Neurotrauma e Biomarcadores, no Departamento de Bioquímica da Universidade Federal do Rio Grande do Sul (UFRGS), sob a orientação do Prof. Dr. Luis Valmor Cruz Portela, como também no Laboratório 26 deste mesmo departamento, sob a orientação do Prof. Dr. Diogo Onofre Gomes da Souza.

Sumário

PARTE I

Resumo

Torrez, Vítor Rocco. **Disfunções retículo endoplasmático-mitocondriais induzidas pela inibição de PP2A e o papel astrocitário na neuroproteção em doenças neurodegenerativas.** Tese de Doutorado, Programa de Pós- graduação em Ciências Biológica: Bioquímica, Universidade Federal do Rio Grande do Sul. Porto Alegre, Brasil, 2019.

As doenças neurodegenerativas constituem um grupo de doenças marcadas pela progressiva morte neuronal e consequente disfunção cognitiva. A prevalência dessas patologias tem aumentado rapidamente com o crescimento da expectativa de vida da população, fazendo do desenvolvimento de tratamentos efetivos e métodos de diagnóstico precoce uma questão de saúde pública a nível global. Entretanto, a evolução dessas pesquisas aparece como um grande desafio, visto a grande variedade de apresentações clínicas e distintos achados neuropatológicos presentes nessas doenças, tornando ainda mais difícil a compreensão dos mecanismos envolvidos na patogênese e evolução de seus processos neurodegenerativos. Alguns achados comuns à maior parte desses distúrbios e ainda pouco esclarecidos são a redução no metabolismo energético celular e disfunções na proteostase celular que levam ao acúmulo de diferentes proteínas patológicas. Na presente tese, avançamos na elucidação das alterações presentes nos circuitos de sinalização desses mecanismos e no entendimento da associação destes com outro achado frequente nas doenças neurodegenerativas: a redução da atividade da proteína fosfatase 2A (PP2A). Além disso, também ampliamos o entendimento sobre possíveis mecanismos neuroprotetores para esses distúrbios, demonstrando a necessidade de modular a interação astrócito-neurônio para a ação preventiva alcançada no tratamento com memantina em nosso modelo de inibição da atividade da PP2A. Dessa forma, buscamos progredir no contexto da busca por um diagnóstico precoce e por tratamentos eficazes para as doenças neurodegenerativas.

Palavras-chave: Doenças neurodegenerativas; proteína fosfatase 2A; estresse do retículo endoplasmático; disfunção mitocondrial; reatividade astrocitária; apoptose

Abstract

Torrez, Vítor Rocco. **Endoplasmic reticulum-mitochondrial dysfunctions induced by inhibition of protein phosphatase 2A and the astrocytic role in neuroprotection in neurodegenerative diseases.** PhD Thesis, Post-graduation Program of Biological Sciences: Biochemistry, Universidade Federal do Rio Grande do Sul. Porto Alegre, Brazil, 2019.

Neurodegenerative diseases are a group of disorders marked by progressive neuronal death and consequent cognitive dysfunction. The prevalence of these pathologies has raised rapidly with the increase in the life expectancy of the population, making the development of effective treatments and methods of early diagnosis a public health issue at a global level. However, the evolution of these researches presents a challenge, considering the great variety of clinical presentations and different neuropathological findings present in these diseases, making it even more difficult to understand the mechanisms involved in the pathogenesis and evolution of their neurodegenerative processes. Some findings common to most of these disorders and still unclear are the reduction in cellular energy metabolism and dysfunctions in the cellular proteostase that lead to the accumulation of different pathological proteins. In the present thesis, we advanced the elucidation of the alterations present in the signaling circuits of these mechanisms and in the understanding of the association of these with another frequent finding in the neurodegenerative diseases: the reduced activity of protein phosphatase 2A (PP2A). In addition, we also broadened our understanding of possible neuroprotective mechanisms for these disorders, demonstrating the need to modulate the neuron-astrocyte interaction for the preventive action achieved in the treatment with memantine in our model of inhibition of PP2A activity. Thus, we seek to progress in the context of the search for an early diagnosis and effective treatments for neurodegenerative diseases.

Keywords: Neurodegenerative diseases; protein phosphatase 2A; endoplasmic reticulum stress; mitochondrial dysfunction; astrocytic reactivity; apoptosis

Lista de Abreviaturas

ATF4 Fator ativador de transcrição 4

ATF6 Fator ativador de transcrição 6

BiP Proteína de Acoplamento

CDK5 Ciclina dependente de cinase 5

CHOP Fator de transcrição homólogo ao C/EBP

DA Doença de Alzheimer

DP Doença de Parkinson

EIF2α Fator de Iniciação Eucariótico 2α

FDA Food and Drug Administration

GLT-1 Transportador de Glutamato do tipo 1

GRP78 Proteína regulada por glicose, de 78kDa

GSK3β Glicogênio sintase cinase 3-beta

ICV Intracerebroventricular

IRE1α Proteína cinase dependente de inositol 1α

IH Intrahipocampal

LCR Líquido cefalorraquiano

MAM Membranas do retículo endoplasmático associadas à mitocôndria

mGluR Receptores metabotrópicos de glutamato

MN Memantina

NFTs Emaranhados neurofibrilares

NMDA N-metil D-aspartato

OKA Ácido ocadáico

PERK Proteína cinase do retículo endoplasmático semelhante à proteína cinase do RNA

P-tau Proteína tau fosforilada

PP2A Proteína fosfatase 2A

RE Retículo endoplasmático

Ser Serina

SNC Sistema nervoso central

Tre Treonina

UPR Resposta a proteínas desenoveladas

Introdução

Doenças Neurodegenerativas

As doenças neurodegenerativas são um grupo heterogêneo de doenças com fenótipos clínicos distintos e influências genéticas diversas, caracterizadas por disfunção global progressiva e perda de neurônios (Heemels, 2016). A variedade de mecanismos patogênicos envolvidos nestes distúrbios está associada a um amplo espectro de apresentações clínicas. Essas apresentações são definidas pelo envolvimento distinto dos sistemas funcionais e não indicam necessariamente o fundo patológico molecular, o que acaba por dificultar o diagnóstico desses pacientes e atrasa o início de tratamentos.

Devido ao crescimento visto atualmente na prevalência dessas doenças, em parte explicado pelo aumento da expectativa da população, cresce na mesma proporção o interesse na evolução de métodos de diagnóstico precoce e de tratamentos para elas. O diagnóstico de categorias neuropatológicas de doenças neurodegenerativas por biomarcadores *in vivo* detectáveis é apenas parcialmente alcançado nos dias de hoje, mas diversas pesquisas são realizadas para se aproximar desse objetivo (Kovacs, 2017).

Uma característica presente na maior parte dessas doenças é a deposição de proteínas com propriedades físico-químicas alteradas, também conhecidas como proteínas desenoveladas. As proteínas mais frequentemente envolvidas na patogênese dessas doenças são β-amiloide, tau, proteína priônica e α-sinucleína. Existem outras proteínas associadas principalmente a distúrbios hereditários, tais como proteínas codificadas por genes ligados a distúrbios de repetição de trinucleotídeos e amiloidoses cerebrais familiares. A alta frequência da presença dessas alterações proteicas nas doenças neurodegenerativas tem levado a um crescente interesse no estudo do

envolvimento de mecanismos intracelulares de formação e dobramento proteico na patogênese desses distúrbios (Hoozemans e Scheper, 2012; Roussel et al, 2013).

Ainda não há cura conhecida para nenhuma dessas doenças, porém, o avanço no entendimento dos mecanismos moleculares envolvidos em suas patogêneses aproxima-nos cada vez mais do desenvolvimento de métodos diagnósticos precoces, para possibilitar então uma intervenção em um momento em que a doença ainda se encontre em processo reversível, ou, ao menos, controlável a um ponto que impeça sua neuroprogressão.

Além disso, a fim de aumentar o rol de possíveis alvos para o desenvolvimento de tratamentos, um outro ramo dos estudos atuais busca compreender os mecanismos adaptativos de neuroproteção desencadeados pelos danos iniciais decorrentes desses distúrbios.

Mecanismos envolvidos nas doenças neurodegenerativas

Nas seções seguintes, discutiremos alguns dos mecanismos moleculares envolvidos na patogênese e na evolução das doenças neurodegenerativas. Dentre os mecanismos estudados nessa tese, ganham destaque os distúrbios na função proteostática do retículo endoplasmático, na comunicação entre essa organela com as mitocôndrias e a consequente ativação apoptótica. Além disso, também procuramos abordar as conhecidas alterações do sistema de neurotransmissão glutamatérgico que ocorrem nessas doenças e a importância da atividade astrocitária no processo de neuroproteção.

Estresse do Retículo Endoplasmático

Nas células eucarióticas, a organela responsável pelo controle do dobramento proteico, dentre outras funções essenciais para o metabolismo celular, é o retículo endoplasmático (RE).

O RE é necessário para o dobramento e correção de todas as proteínas secretadas e de membrana. Danos ou disfunções que prejudicam sua função induzem um estado patológico conhecido como estresse do RE. O estresse do RE desencadeia um processo adaptativo chamado de resposta a proteínas desenoveladas (UPR – do inglês, *unfolded protein response*). Essa resposta se constitui de cascatas de sinalização do RE ao núcleo a fim de aumentar o controle de qualidade e a degradação das proteínas terminalmente mal dobradas (Paschen e Mesgendorf, 2005; Hoozemans et al, 2012).

Em condições fisiológicas, a proteína chaperona BiP (ou GRP78) mantém-se ligada a três proteínas principais presentes na membrana do RE: PERK, IRE1α e ATF6. Essa ligação se desfaz com o aumento da presença de proteínas mal dobradas no lúmen do RE, que atraem mais fortemente essa chaperona para ajudar no processo de correção das mesmas. Isso promove uma mudança na conformação das proteínas da membrana do RE, o que possibilita a fosforilação da PERK e da IRE1α, além da clivagem da ATF6, iniciando assim os três ramos da cascata de sinalização que resulta na regulação da expressão de diversos genes (Walter e Ron, 2011; Ferreiro e Pereira, 2012). Apesar de inicialmente promover citoproteção, quando a disfunção é muito grande e a UPR torna-se demasiadamente prolongada, podem ocorrer alterações nocivas à célula, como prejuízo na homeostase de cálcio, com a liberação de suas reservas intracelulares, além de ativação de vias proapoptóticas (Szegezdi et al, 2006).

A UPR combina a inibição precoce da síntese proteica com uma regulação posterior de genes que promovem o dobramento ou o descarte de proteínas, assim

protegendo os neurônios de serem sobrecarregados por proteínas mal dobradas (Roussel et al, 2013). Embora muitas células estejam razoavelmente bem protegidas do acúmulo de proteínas mal dobradas durante a diluição continuada do RE pela replicação celular, este processo deixa de estar disponível para neurônios pós-mitóticos, que dependem exclusivamente da UPR para sobrevivência frente a tais danos ou disfunções. Mesmo as células da glia, que podem se replicar, são suscetíveis ao estresse do RE devido às suas vias secretoras bastante desenvolvidas (Verfaillie et al, 2012).

O processo da UPR pode ser melhor visto esquematicamente na figura abaixo:

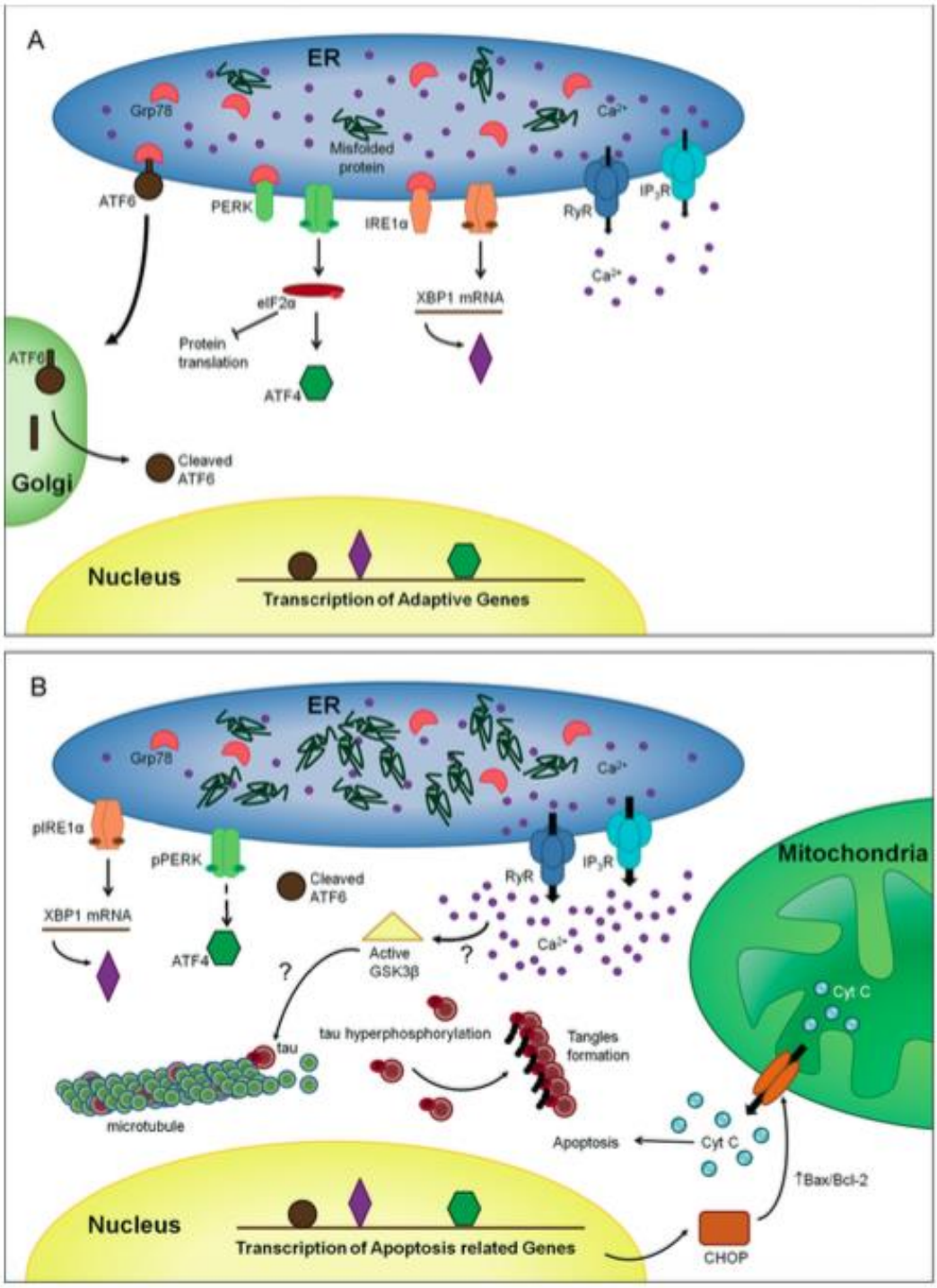

Figura 1 – Resposta ao estresse do RE. (A) UPR adaptativa: o acúmulo de proteínas mal dobradas no lúmen do RE leva ao início da resposta devido à ativação de seus três "sensores" – PERK, ATF6 e IRE1α – e suas cascatas de sinalização correspondentes. (B) Apoptose induzida pela UPR prolongada: quando as células não conseguem resolução dos problemas na síntese proteica com as respostas iniciais da UPR, o estresse do RE leva

a ativação de vias apoptóticas. A homeostase do cálcio é perdida, levando a uma liberação das reservas do RE para o meio citoplasmático. O Ca2+ liberado pode levar a ativação de CDK5 e GSK3b, cinases que levam à hiperfosforilação da proteína tau e sua saída dos microtúbulos. Além disso, há uma up-regulation de genes pró-apoptóticos, principalmente CHOP, que leva a translocação da proteína Bax para a mitocôndria e consequente liberação de citocromo c, além da down-regulation do gene antiapoptótico Bcl2, causando a eliminação das células irreversivelmente danificadas. (Adaptada de Ferreiro e Pereira, 2012)

Sabe-se que o estresse do RE pode induzir a hiperfosforilação da proteína tau e esta causar o prolongamento da UPR, formando um círculo vicioso (Ho et al, 2012; Hoozemans et al, 2012). Estudos *in vitro* e *in vivo* demonstraram aumento da ativação de GSK3β induzida pela UPR (Song et al, 2002; Kim et al, 2005). Além disso, o estresse do RE prolongado pode levar à liberação de cálcio das reservas intracelulares, uma potencial via de ativação da CDK5 (Saito et al, 2007). A GSK3β e a CDK5 são as principais cinases da proteína tau e estão envolvidas no processo de hiperfosforilação desta proteína nas taupatias e doença de Alzheimer (DA).

Há crescente evidência de que o estresse do RE está envolvido na patogênese da DA e de outras doenças neurodegenerativas (Hoozemans et al, 2009; Duran-Aniotz et al, 2014; Li et al, 2014), tornando-se assim objeto para o estudo de novos alvos terapêuticos. Entretanto, ainda é necessário melhor elucidar os mecanismos pelos quais a UPR está relacionada à neurodegeneração.

Disfunção Retículo Endoplasmático-Mitocondrial e Apoptose

As mitocôndrias e o RE desempenham um papel crucial nos processos fundamentais para a sobrevivência celular, como síntese proteica e respiração celular e

são peças-chave para a manutenção do metabolismo energético das células (Tubbs et al, 2017).

A literatura atual torna crescente a ideia de que ambas as organelas não são independentes, mas estruturas intracelulares interconectadas, compartilhando interações estruturais e funcionais, permitindo uma regulação recíproca. Os estreitos contatos entre o ER e mitocôndrias, conhecidos como membranas do retículo endoplasmático associado a mitocôndrias (MAM – do inglês *mitochondria-associated membranes*), abrigam várias proteínas com diferentes funções e desempenham um papel fundamental em diferentes processos, que vão da sinalização de cálcio (Ca2+), transporte lipídico e estresse do RE até morfologia mitocondrial (Giorgi et al, 2015). Dentre as funções exercidas pelas proteínas da MAM, destaca-se um papel-chave na iniciação e amplificação da morte celular. A participação em mecanismos de apoptose ainda não é completamente elucidada, porém recentes estudos têm auxiliado no entendimento da atuação de diversas proteínas nessa complexa regulação, como pode ser observado na figura abaixo.

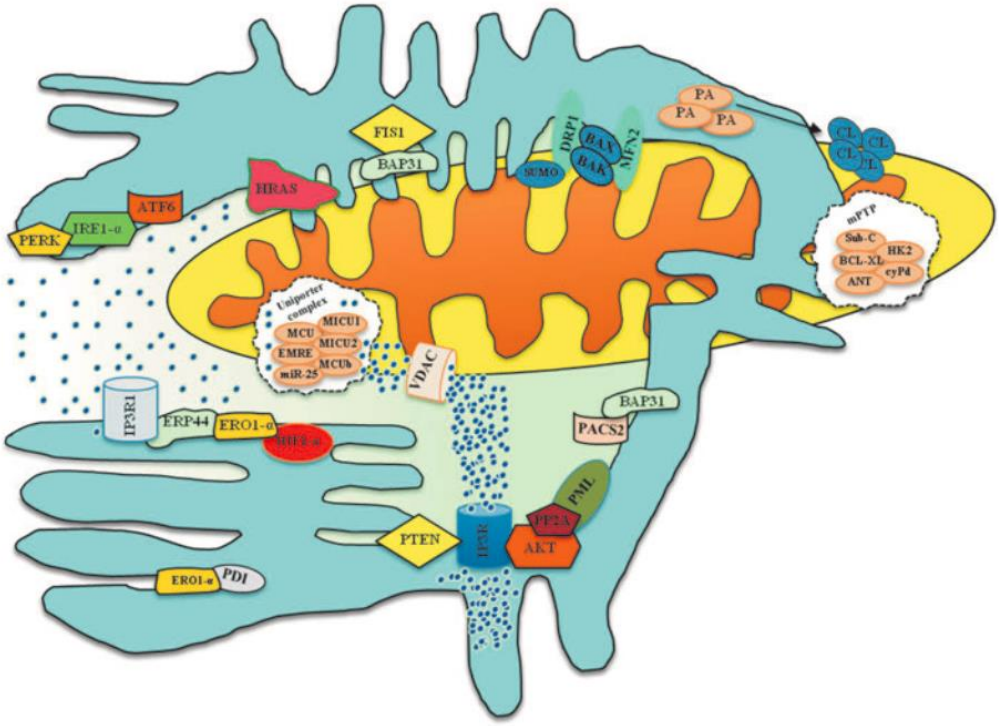

Figura 2 – Representação esquemática das principais proteínas associadas às MAM envolvidas na apoptose. Um número crescente de estudos destaca a importância de diversas proteínas associadas às MAM na regulação da cascata apoptótica. Essas proteínas conseguem modular a apoptose através de complexos mecanismos, ainda não plenamente elucidados, tendo entre eles a geração de ROS e o recrutamento e regulação de proteínas de fissão/fusão mitocondrial. (Adaptado de Giorgi et al, 2015)

A via intrínseca da apoptose opera na superfície das organelas intracelulares, dentre as quais a mitocôndria tem sido a mais estudada (Lin e Beal, 2006). Entretanto, crescentes evidências demonstram um envolvimento do RE e, mais precisamente, das proteínas presentes na MAM, em processos apoptóticos. Diversas proteínas regulatórias da apoptose, como a pro-apoptótica Bax e a anti-apoptótica BCL-2, também demonstraram operar nas MAM, e possuem função importante na interação dessas duas organelas.

Sobre essa relação, é sabido também que a UPR muito prolongada induz estresse oxidativo – majoritariamente por via mitocondrial - e consequente produção de espécies reativas de oxigênio (ROS). Em última análise, essas alterações levam a aumento da liberação do Ca2+ do RE e a uma sinalização de "suicídio celular". Esse mecanismo é ativado principalmente pela elevação sustentada de CHOP e ROS (Verfaillie et al, 2012). Alguns destes mecanismos estão presentes na figura 2B, outros podem ser melhor observados de forma esquemática na figura a seguir.

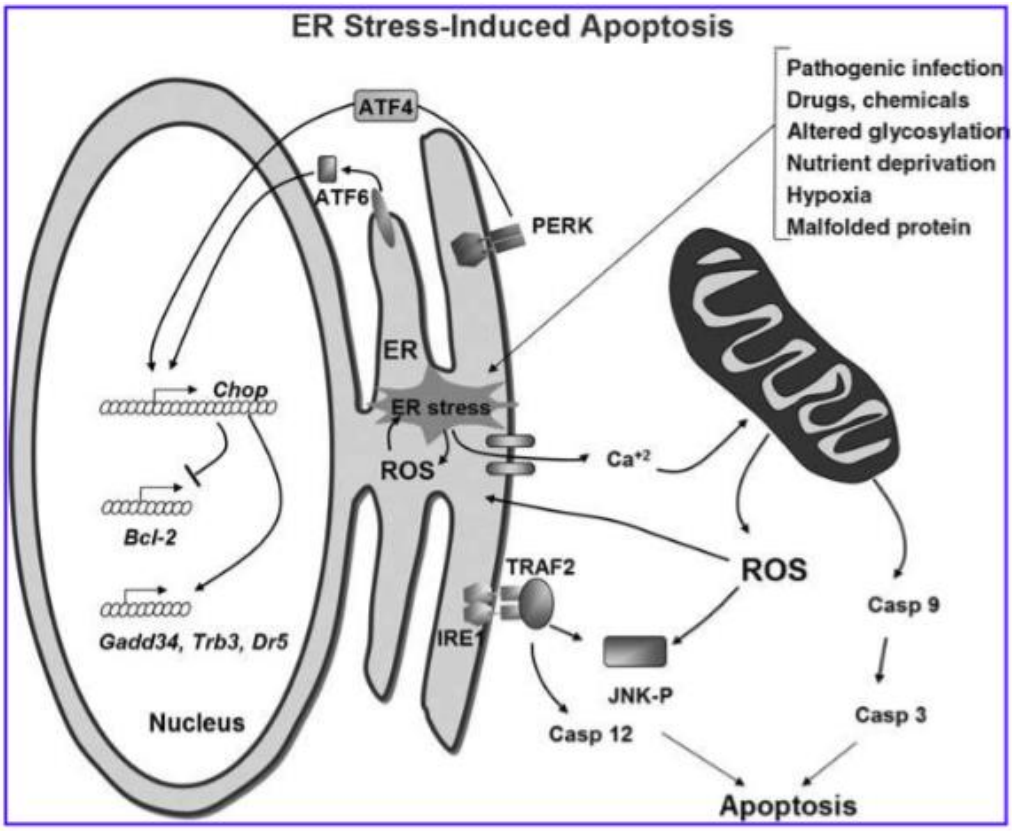

Figura 3 – Apoptose induzida pelo estresse do RE. O estresse do RE leva a liberação de Ca2+ na MAM, levando a disfunção mitocondrial, produção de ROS e ativação da procaspase 9, que participa da clivagem da caspase 3 e consequente apoptose. Uma segunda via apoptótica ocorre pela ativação da transcrição de CHOP, que induz apoptose, entre outros, por inibir a expressão do gene antiapoptótico Bcl2. Com isso, a

associação do estresse oxidativo com o estresse do RE não-resolvido pode levar à morte celular por diversas vias (adaptado de Malhotra e Kaufman, 2007).

Atividade da Proteína Fosfatase 2A

A proteína fosfatase 2A (PP2A) pertence à classe das serina/treonina fosfatases e tem sido identificada como a mais envolvida na regulação de processos de neurogênese e neurodegeneração. Basicamente, as proteínas fosfatases são moléculas nucleofílicas e atacam os grupos fosfato de resíduos de aminoácidos fosforilados e desfosforilam-nos na presença de água.

A PP2A é expressa em todas as células de mamíferos e contribui com cerca de 0,3 a 1% do total de proteínas celulares (Shi, 2009). Tem um papel em numerosas funções celulares importantes, tais como crescimento neural, replicação, transcrição, tradução, ciclo celular, transformação celular, glicólise, metabolismo lipídico e síntese de catecolaminas. Além disso, a PP2A afeta a apoptose, atua como um supressor de tumor e é relatado como inativado no câncer (Chen et al, 2013).

A redução da atividade de PP2A é característica de diversas doenças neurodegenerativas, como demências, doença de Parkinson, transtorno do humor bipolar e câncer cerebral (Nematullah et al, 2017). Visto sua interferência em importantes processos celulares, há diversos anos, a redução da atividade de fosfatases é apontada como um dos mecanismos principais no desenvolvimento da doença de DA (Placido et al, 2017), como demonstrado na figura abaixo.

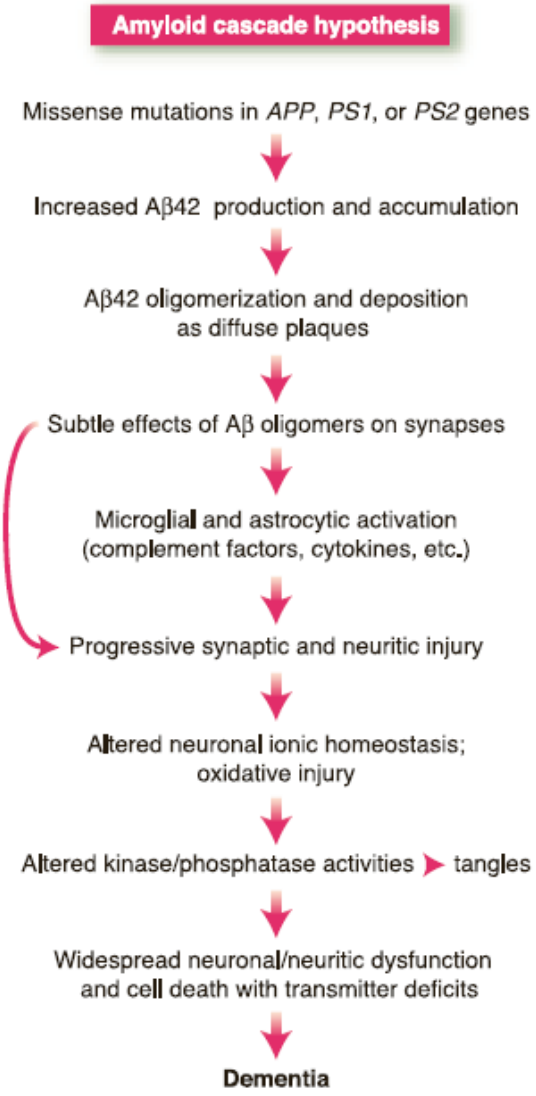

Figura 4 – A hipótese da cascata amiloide para o desenvolvimento da DA. Hardy colocava em sua hipótese um envolvimento da redução da atividade de fosfatases após a ação dos oligômeros de β-amiloide e dano sináptico e neuronal. As hipóteses mais recentes colocam essa alteração como um possível evento prévio a esses danos. (Adaptada de Hardy e Selkoe 2002)

Nos últimos anos, muito tem-se estudado sobre a função da PP2A na fosforilação e desfosforilação da proteína tau (Taleski e Sontag, 2018; Sontag et al, 2014). Entretanto, essas alterações não explicam a importância da redução da atividade de PP2A nas não-taupatias.

Nesse sentido, diversos estudos têm apontado para um possível papel dessa fosfatase na regulação da homeostase do RE e da mitocôndria (Kamat et al, 2011), em parte pelo controle da ativação de proteínas envolvidas na regulação da interação entre essas organelas (Tubbs et al, 2017), em parte pela promoção de alterações na dinâmica mitocondrial e na estrutura de suas membranas (Placido et al, 2017). Além disso, a atividade da PP2A tem demonstrado função fisiologicamente essencial na ativação da UPR (Hetz et al, 2006) e de vias anti-apoptóticas (Lin et al, 2006).

Também, a literatura recente demonstra relação entre a diminuição da atividade da PP2A com aumento dos níveis de glutamato e excitotoxicidade (Kamat et al, 2014; Zimmer et al, 2015). Esta relação, porém, ainda precisa de mais estudos para melhor compreensão.

Excitotoxicidade e Reatividade Astrocitária

O L-glutamato é o principal neurotransmissor excitatório no SNC dos mamíferos (Meldrum, 2000). O sistema glutamatérgico de neurotransmissão desempenha um papel fundamental em muitas funções neurofisiológicas. Por exemplo, em condições normais, o glutamato é o principal neurotransmissor envolvido em processos cognitivos, como a formação de memória. Esta resposta é iniciada após uma interação do glutamato com seus receptores presentes em canais iônicos.

Em excesso, essa ativação pode ser nociva, tornando, dessa forma, o glutamato também uma neurotoxina (Dong et al, 2009). A retirada do glutamato do espaço extracelular é realizada principalmente pela absorção mediada por transportadores glutamatérgicos. Os transportadores de glutamato são expressos por muitos tipos de células no SNC, incluindo astrócitos, neurônios, oligodendrócitos, microglia e endotélio. Parte desse metabolismo encontra-se esquematizado na figura abaixo.

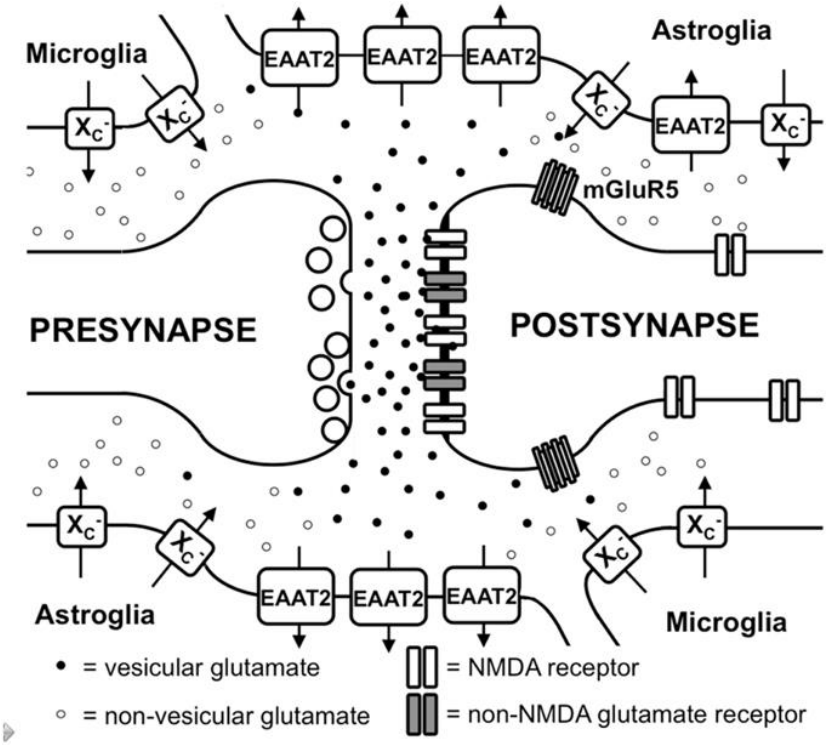

Figura 5 - Metabolismo glutamatérgico no cérebro. O glutamato vesicular é liberado na sinapse e rapidamente liga-se aos receptores ionotrópicos pós-sinápticos. Ele é rapidamente reabsorvido pelos transportadores glutamatérgicos astrocitários, principalmente EAAT2. Resquícios de glutamato excedente podem ativar receptores perisinápticos, como mGluR5. Microglia e astrócitos podem liberar glutamato de forma não vesicular fora do espaço sináptico, onde ele pode ativar receptores NMDA extrasinápticos (adaptado de Lewerenz e Maher, 2015)

Destes, a absorção pelos astrócitos é quantitativamente mais importante para manter as concentrações normais de glutamato extracelular, principalmente devido à ação do transportador glutamatérgico EAAT2. A captação astrócitária também pode ser fundamental na formação da cinética da atividade sináptica glutamatérgica (Anderson e Swanson, 2000)

Os níveis de glutamato persistentemente elevados na fenda sináptica podem causar hiperativação de receptores glutamatérgicos e morte celular, um processo fisiopatológico conhecido como excitotoxicidade (Meldrun et al, 2000). A ativação excessiva de receptores de glutamato por aminoácidos excitatórios leva a várias consequências deletérias, incluindo comprometimento do tamponamento de cálcio, geração de radicais livres, aumento de permeabilidade mitocondrial e excitotoxicidade secundária. Estudos recentes implicam excitotoxicidade em uma variedade de condições neuropatológicas, sugerindo que doenças neurodegenerativas com etiologias genéticas distintas podem compartilhar a excitotoxicidade como uma via patogênica comum (Dong et al, 2009). Devido à perda de neurônios glutamatérgicos em estágios iniciais da doença de Alzheimer (DA), há muitos anos o papel da excitotoxicidade tem sido estudado nas demências e em outras doenças neurodegenerativas (Greenamyre et al, 1988). Mais recentemente, foram descobertas alterações na plasticidade e na transmissão dessas sinapses presentes ainda antes do início da morte neuronal em diversos modelos da DA, o que aumenta a possibilidade de intervenções nesse sistema ainda em estágios reversíveis dessas doenças (Hu et al, 2012).

Em condições fisiológicas, os astrócitos são responsáveis pela primeira linha de defesa contra a excitotoxicidade, liberando substâncias tróficas como a proteína S100B e, predominantemente, removendo o excesso de glutamato da fenda sináptica, mantendo assim regulada a estimulação excitatória nos receptores de glutamato (Anderson et al, 2014).

Os astrócitos se tornam reativos em resposta a praticamente todas as condições patológicas no sistema nervoso central (SNC), tanto após lesões agudas quanto durante doenças progressivas (Haim et al, 2015). Essa reatividade foi inicialmente caracteriazada

pelas alterações morfológicas e aumento na expressão da proteína citoesquelética GFAP (do inglês, *glial fibrillary acidic protein*).

Além dessa alteração morfológica, a reatividade dos astrócitos é caracterizada pelo aumento de diversas moléculas neuroativas que podem determinar a sobrevivência ou a morte das células neurais adjacentes.

Em contraste, os astrócitos reativos liberam fatores que podem atuar também como substâncias neuroinflamatórias, o que pode contribuir para exacerbar a morte neuronal (Mayhew et al, 2009; Fernandez et al, 2012). Considerando essa perspectiva, a proteína S100B, que no cérebro é secretada predominantemente por astrócitos, exerce efeitos reparativos e neurodegenerativos, e está fortemente associada a mudanças na morfologia dos astrócitos (Verkhratsky et al, 2010). Em estudos clínicos e experimentais, a avaliação da S100B e da proteína glial fibrilar ácida (GFAP) em fluidos biológicos são considerados biomarcadores da reatividade dos astrócitos (Chaves et al, 2010; Böhmer et al, 2011).

Van Eldik e Wainwright propuseram, em 2013, que o principal fator a determinar se a ação da S100B seria benéfica ou deletéria ao cérebro é o nível de ativação astrocitária induzido por algum estímulo nocivo ou pela própria S100B em suas diferentes concentrações. (Van Eldik e Wainwright, 2003). O esquema proposto por eles aparece na figura a seguir:

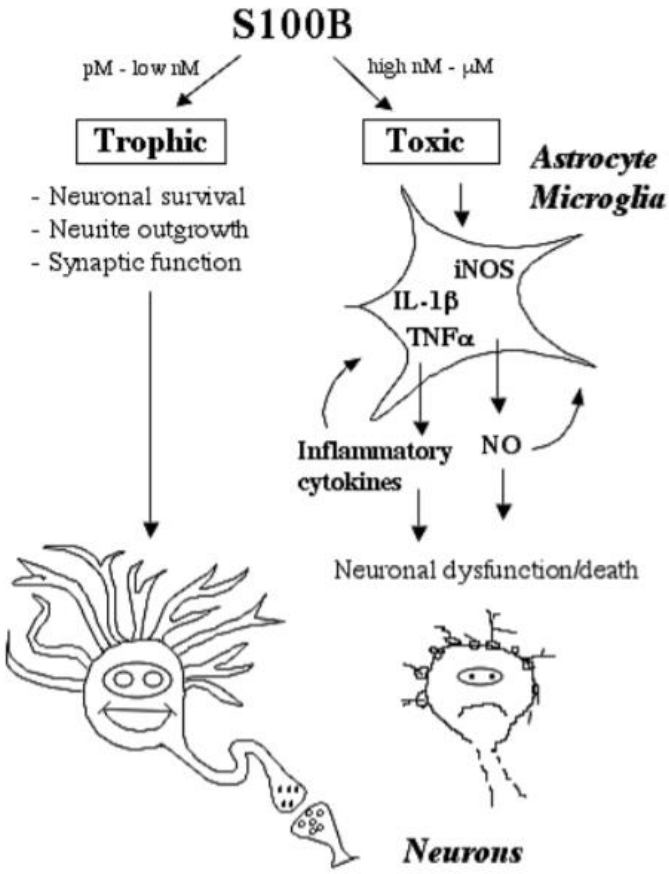

Figura 6 – Representação dos possíveis papéis da S100B no cérebro. No cérebro adulto e em desenvolvimento normal, a S100B extracelular tem atividades tróficas benéficas para aumentar a sobrevivência neuronal, estimular o crescimento de dendritos e modular a função sináptica. No entanto, após lesão cerebral aguda ou crónica ou em condições neurodegenerativas, a produção e liberação excessivas de S100B a partir de astrócitos podem ter consequências tóxicas. A S100B pode estimular os astrócitos e a microglia a produzir citocinas pró-inflamatórias e NO, o que pode levar à disfunção neuronal ou à morte. S100B em altas concentrações também pode ser diretamente neurotóxico (adaptado de Van Eldik e Wainwright, 2003).

Objetivos

Investigar mecanismos fisiopatológicos intracelulares de controle da proteostase e seu envolvimento na progressão de processos neurodegenerativos associados à redução da atividade de PP2A, além de avaliar a possível modulação astrocitária como mecanismo neuroprotetor para esses distúrbios.

Objetivos Específicos

- Investigar os efeitos da inibição da atividade da PP2A sobre a sinalização da UPR, a comunicação RE-mitocondrial, produção energética mitocondrial e a ativação de apoptose;

- Avaliar a reatividade astrocitária e a recaptação glutamatérgica como parte do mecanismo preventivo e neuroprotetor da MN frente a inibição da PP2A.

PARTE II

CAPÍTULO I – *Inhibition of protein phosphatase 2A exacerbates endoplasmic reticulum-mitochondria apoptotic responses*

No capítulo I, apresentamos o artigo submetido para publicação no periódico *BBA – Molecular Basis of Disease*

Neste estudo, investigamos a influência da redução da atividade de PP2A em outros mecanismos comuns no desenvolvimento e avanço da maior parte das doenças neurodegenerativas: o estresse do RE, disfunções na interação RE-mitocôndria e a consequente ativação de apoptose. Para isso, inibimos a PP2A através do modelo de infusão intrahipocampal de OKA. O uso de OKA levou a redução de 43% da atividade da PP2A e a disfunção cognitiva demonstrada pelo teste de reconhecimento de objetos, além de aumento de pEIF2α^{ser51}/EIF2α e CHOP. Concomitantemente, no teste de respirometria hipocampal, foi encontrada redução da síntese de ATP devido a disfunção mitocondrial evidenciada pela diminuição da atividade do complexo V mitocondrial, vazamento de prótons e produção de H_2O_2. Além disso, houve aumento de marcadores apoptóticos e redução da viabilidade celular. Considerando esses diversos fatores, fizemos uma análise estatística (PCA) para verificar os principais componentes envolvidos no dano causado, cujo resultado foi produção de H_2O_2. Esses resultados nos levam a sugerir que a redução da atividade de PP2A leva a um distúrbio da comunicação RE- mitocôndria através do aumento do estresse do RE, disfunção bioenergética mitocondrial e produção de H2O2, levando a consequente ativação de mecanismos apoptóticos. Essas alterações podem ser peças-chave para o entendimento da patogênese, evolução e possível tratamento das doenças neurodegenerativas.

Elsevier Editorial System(tm) for BBA - Molecular Basis of Disease

Manuscript Draft

Manuscript Number: BBADIS-19-143

Title: Inhibition of protein phosphatase 2A exacerbates endoplasmic reticulum-mitochondria apoptotic responses

Article Type: Regular Paper

Keywords: MAMs; Mitochondrial dysfunction; Bioenergetics impairment; Eukaryotic initiation factor 2α; H2O2; Apoptosis.

Corresponding Author: Dr. Luis V. Portela, Ph.D.

Corresponding Author's Institution: Federal University of Rio Grande do Sul

First Author: Afonso Kopczynski

Order of Authors: Afonso Kopczynski; Vitor R Torrez; Randhall Bruce K Carteri; Marcelo S Rodolphi; Paula A Barcellos; Luana Strapazzon; Marco A De Bastiani; Nathan R Strogulski; Mônia Sartor; Fábio Klamt; Harm H Kampinga; Diogo O Souza; Luis V. Portela, Ph.D.

Abstract: Endoplasmic reticulum and mitochondria (ER-mitochondria) functional interactions may be regulated by protein phosphatase 2A (PP2A). The unfolded protein response (UPR) is upregulated in neurodegenerative disorders; however, the bioenergetics mechanisms behind these events were not elucidated. Our hypothesis is that brain PP2A inhibition heightens ER-mitochondria dysfunction and cause hierarchical neurochemical abnormalities that drive apoptotic neurodegeneration. Hence, we inhibited brain PP2A activity in mice with okadaic acid (OKA) and assessed memory fitness, and molecular markers of ER stress coupled with mitochondrial outcomes. We showed that a single i.c.v. infusion of OKA inhibits PP2A activity (43%) and impaired recognition memory. Simultaneously, there increased hippocampal levels of pEIF2αSer51/EIF2α and CHOP, which highlights that PP2A is a key regulator of ER-stress and recognition memory processing. Concomitant hippocampal respirometry analysis showed decreased ATP synthesis due to downregulation of the mitochondrial complex V activity, increased proton leak and H2O2 production, markers of mitochondrial dysfunction. Also, apoptotic markers BAX/Bcl2, cytochrome c and cleaved caspase-3/caspase 3 were increased, whereas cell viability was significantly decreased. Considering these multiple elements involved in the ER-mitochondrial stress responses due to PP2A inhibition we performed principal component analysis (PCA) in which the H2O2 was hierarchized as the highest effector. Decreased PP2A activity impairs ER UPR mechanistically associated with mitochondrial bioenergetics uncoupling and H2O2 production, implying in ER-mitochondria miscommunication. Also, the PCA analysis highlights H2O2 as an important effector of ER-mitochondrial dysfunction leading to cells death and memory impairment.

Suggested Reviewers: Khalid Iqbal Ph. D.
Professor, Department of Neurochemistry, New York State Institute for Basic Research in Developmental Disabilities

moc.liamg@rbi.labqi.dilahk
He is a world expert in basic neurochemistry and models of neurodegenerative disorders.

Jennifer Rieusset Ph. D.
Professor, INSERM UMR-1060CarMeN Laboratory, Lyon University
jennifer.rieusset@univ-lyon1.fr
She is an expert in the functional aspects of Mitochondria-Associated Endoplasmic Reticulum Membrane (MAM) in pathological conditions.

Claudio Hetz Ph. D.
Professor, Department of Cellular and Molecular Medicine, University of Chile
chetz@med.uchile.cl
He is a renowned researcher in the field of cell biology.

Raghu Vemuganti Ph. D.
Professor, Department of Neurological Surgery, University of Wisconsin
vemuganti@neurosurgery.wisc.edu
Expert in brain disorders

Inhibition of protein phosphatase 2A exacerbates endoplasmic reticulum–mitochondria apoptotic responses

Afonso Kopczynski[1#], Vitor R. Torrez[1#], Randhall B. Carteri[1], Marcelo S. Rodolphi[1], Paula A. Barcellos[1], Luana Strapazzon[1], Marco A. De Bastiani[2], Nathan R. Strogulski[1], Mônia Sartor[1], Fabio Klamt[2], Harm H. Kampinga[3], Diogo O. Souza[4] and Luis V. Portela[1*].

[1] Laboratório de Neurotrauma e Biomarcadores, Departamento de Bioquímica, Programa de Pós Graduação-Bioquímica, Universidade Federal do Rio Grande do Sul-UFRGS, Porto Alegre, RS, Brasil.

[2] Laboratório de Bioquímica Celular, Departamento de Bioquímica, Programa de Pós Graduação-Bioquímica, Universidade Federal do Rio Grande do Sul-UFRGS, Porto Alegre, RS, Brasil.

[3] Department of Cell Biology, University Medical Center Groningen, University of Groningen, Groningen, The Netherlands.

[4] Departamento de Bioquímica, Programa de Pós Graduação-Bioquímica, Universidade Federal do Rio Grande do Sul-UFRGS, Porto Alegre, RS, Brasil.

[#] Both authors contributed equally.

*** Corresponding author:**

Luis Valmor Portela, Ph.D.

Department of Biochemistry, ICBS, UFRGS
2600 Ramiro Barcelos street, 90035-003, Porto Alegre, RS, Brazil
Email: roskaportela@gmail.com
Telephone: 55 51 33085558
Fax: 55 51 33085544

Abstract

Endoplasmic reticulum and mitochondria (ER-mitochondria) functional interactions may be regulated by protein phosphatase 2A (PP2A). The unfolded protein response (UPR) is upregulated in neurodegenerative disorders; however, the bioenergetics mechanisms behind these events were not elucidated. Our hypothesis is that brain PP2A inhibition heightens ER-mitochondria dysfunction and cause hierarchical neurochemical abnormalities that drive apoptotic neurodegeneration. Hence, we inhibited brain PP2A activity in mice with okadaic acid (OKA) and assessed memory fitness, and molecular markers of ER stress coupled with mitochondrial outcomes. We showed that a single i.c.v. infusion of OKA inhibits PP2A activity (43%) and impaired recognition memory. Simultaneously, there increased hippocampal levels of pEIF2α^{Ser51}/EIF2α and CHOP, which highlights that PP2A is a key regulator of ER-stress and recognition memory processing. Concomitant hippocampal respirometry analysis showed decreased ATP synthesis due to downregulation of the mitochondrial complex V activity, increased proton leak and H_2O_2 production, markers of mitochondrial dysfunction. Also, apoptotic markers BAX/Bcl2, cytochrome c and cleaved caspase-3/caspase 3 were increased, whereas cell viability was significantly decreased. Considering these multiple elements involved in the ER-mitochondrial stress responses due to PP2A inhibition we performed principal component analysis (PCA) in which the H_2O_2 was hierarchized as the highest effector. Decreased PP2A activity impairs ER UPR mechanistically associated with mitochondrial bioenergetics uncoupling and H_2O_2 production, implying in ER-mitochondria miscommunication. Also, the PCA analysis highlights H_2O_2 as an important effector of ER-mitochondrial dysfunction leading to cells death and memory impairment.

Keywords: MAMs; Mitochondrial dysfunction; Bioenergetics impairment; Eukaryotic initiation factor 2α; H_2O_2; Apoptosis.

Declarations of interest: none

1. Introduction

The integrity of interorganelle communications is a fundamental biological aspect behind the maintenance of cell functional homeostasis. Accordingly, the endoplasmic reticulum (ER)–mitochondria contact sites, defined as mitochondria-associated membranes (MAM), encompasses multiple molecular components mechanistically linked with diverse functions [1]. MAM possess proteins sharing functions in complementary manner like calcium signaling, mitochondrial dynamics and bioenergetics [2]. From this functional interplay arises the principle that cellular stressful events leading to MAM miscommunication can potentially designate cells to die [3,4].

ER is particularly involved in the correct folding and processing of newly synthesized proteins. Environmental disturbances affecting protein folding may cause ER stress, characterized by the accumulation of unfolded proteins in ER lumen coupled with a complex ER-to-nucleus protein response that works to reestablish the quality control, folding capacity and degradation of terminally misfolded proteins[5,6]. This ubiquitous process is called unfolded protein response (UPR), and usually initiates by decoupling of chaperone glucose-regulated protein 78 (GRP78 or BiP) from ER transmembrane proteins thereby resulting in activation of the transcription factor 6 (ATF6), inositol-requiring enzyme 1α (IRE1α) and RNA-dependent protein kinase (PKR)-like ER kinase (PERK) [7]. Unsolved and persistent ER stress may “switch on” apoptotic cascades in brain pathologies associated with the loss of proteostasis, like Alzheimer disease (AD)

[8,9]. Actually, in pathological conditions, PERK branch of this response triggers persistent phosphorylation of eukaryotic initiation factor-2a (EIF2α) and subsequent increased expression of the transcription factor C/EBP homologous protein (CHOP) [10,11]. Such response subsequently heightens mitochondrial apoptotic effectors[12,13] and ROS production, which further support ER stress[14-16]. Although increased ROS seems a feed-forward mechanism sustaining ER-mitochondria dysfunction [17] and conceptually might represent bioenergetics disturbances, the mitochondrial mechanism behind this hypothesis was not properly addressed yet. Therefore, MAM integrate a variety of intracellular adaptive signals within the brain and consequently it requires a fine-tuning regulation of the UPR responses, otherwise the signals will be converted into proapoptotic cellular responses[18,19].

Protein phosphatase 2A (PP2A), a serine/threonine phosphatase, contributes to the dynamic state of phosphorylation and dephosphorylation of Tau, a major microtubule-associated protein. Actually, the reduction in the PP2A expression and activity was reported in the brain of AD patients[20,21]. However, reduction of PP2A activity and increased neuronal death is also present in non-related tauopathy disorders, which highlights that this enzyme also targets molecular components beyond those directly involved in the control of Tau phosphorylation [22]. This is the case of the regulatory effects of PP2A on the dephosphorylation of EIF2α, which is an event necessary to avoid ER stress and in parallel, to conserve MAM homeostasis [23,24]. However, abnormal PP2A inhibition could sustain increased EIF2α phosphorylated state ultimately serving as a molecular trigger to disrupt MAM homeostasis and to cause neurological disorders [23,25]. Currently, this intricate relationship is not fully understood and requires better comprehension in terms of mechanisms. Moreover, considering the multitude of MAM

components, it would be useful to rank the relative importance of PP2A inhibition regarding brain molecular and functional outcomes.

In this study, we aimed to further explore mechanisms underlying brain PP2A and MAM communication. Our hypothesis is that PP2A inhibition heightens MAM miscommunication and cause hierarchical neurochemical abnormalities that drive cells to death. Therefore, we inhibited brain PP2A activity and assessed memory fitness, and molecular markers of ER stress coupled with mitochondrial outcomes.

2. Material and Methods

2.1. Animals

Three-month old CF1 mice were housed in standard cages (48 x 26 cm). Animals were kept in a room with controlled temperature (22ºC) under a 12 h light/12 h dark cycle (lights on 7 am) and had free access to food and water. Mice were randomized into two groups: okadaic acid (OKA, n=6) and control (CT, n=6). To avoid social isolation, we maintained four animals per cage [26]. All experiments were conducted according to official governmental guidelines in compliance with the Federation of Brazilian Societies for Experimental Biology and were approved by the Ethical Committee of the Federal University of Rio Grande do Sul, Brazil (CEUA#31443).

2.2. Treatment, Surgical Procedure and PP2A activity

Animals were anesthetized using i.p. injection of ketamine (Cetamin, Schering-Plough Coopers, Brazil, 100 mg/kg body weight) and xylazine (Coopazine, Syntec, Brazil, 30 mg/kg body weight). OKA (Ref. O8010, Sigma, USA) was dissolved in artificial cerebrospinal fluid (aCSF) [27]. OKA causes high-affinity inhibition of the enzyme serine/threonine phosphatase 2A (PP2A) relative PP1[28]. Thus, the molecular

and behavioral abnormalities induced by OKA in vivo have been predominantly attributed to PP2A inhibition. Actually, the inhibition of PP2A by OKA is achieved at concentrations up to 100 times lower than those required to inhibit PP1 [29]. A single intracerebroventricular (i.c.v.) infusion of 2 μL OKA (100 ng) or aCSF (vehicle) was made into the right hemisphere in the lateral ventricle region at the following coordinate location, with reference to bregma: A -1.0, L 1.0, and V 2.5[30]. Animals received appropriate post-surgery care and were left to rest during 24 h and 48 h. The activity of PP2A was measured in hippocampal extracts at 24 h and 7 days after i.c.v. injection. We used a commercially available kit (Cat.# V2460) (Serine/Threonine Phosphatase assay system, Promega Corporation, Madison, WI, USA) to measure PP2A activity. Prior to PP2A assay, the endogenous phosphate present in these sample preparations was eliminated using spin columns (sephadex resin), which remove free phosphate and other low-molecular-weight inhibitors from the sample. The assay detects free phosphate released from a synthetic phosphopeptide (RRA(pT)VA), which is a highly specific substrate for the action of PP2A enzyme. The amount of free phosphate is measured through the absorbance of a molybdate:malachite green:phosphate complex[31].

2.3. Open Field Task (OF):

On the 3rd day, animals were submitted to an open field task. The apparatus was made of a black-painted box measuring 50 cm × 50 cm and was surrounded by 50 cm high walls. The experiments were conducted in a quiet room under low-intensity light (12 lx). Each mouse (n=6 per group) was placed in the same site in the arena and the distance travelled (total and central zone), time spent in central zone and mean speed were measured during 5 min[32]. The experiment was recorded with a video camera positioned

above the arena. The analysis was performed using a computer-operated tracking system (Any-maze, Stoelting, Woods Dale, IL).

2.4. Novel Object Recognition Task (OR)

This task serves to investigate recognition memory fitness. The training session of OR was performed 24 h after the OF task. The short-term memory testing session was performed 90 min after training, and the long-term memory testing was performed 24 h after training. The duration of each session was 5 min. During training session the apparatus contained two identical objects, while in the test session two different objects were present: a familiar and a novel one. The session starts when a mouse is placed in the apparatus facing the wall at the middle of the front segment. At the end of session, the mice were immediately put back in its home cage. Recognition object index (ROI) were calculated for the short-term (SROI) and long-term (LROI) testing by the following ratio: the time spent exploring novel object (TN) by the time spent exploring the familiar (TF) and the novel one in the test session (index = TN/TN + TF). Recognition was defined as directing the nose to the object at a distance of no more than 2 cm and/or touching the object with the nose. Sitting on the object was not considered recognition [33].

Animals were euthanized two-days after long-term OR tests and their hippocampi were dissected for neurochemical and bioenergetics assessments (See Experimental design and model validation, Figure 1A).

2.5. Western blotting

Soon after the euthanasia, one hippocampus was dissected and homogenized in a buffer solution (EDTA 2 mM, protease and phosphatase inhibitor cocktails I and II (Sigma, St. Louis, USA) 0.001 %, Tris HCl 50 mM, (pH 7,4), glycerol 10 % and Triton

X-100 1 %) and centrifuged (15000 g/ 10 min). Supernatant was collected and diluted in an appropriated sample buffer. Samples of 20 µg of protein from each hippocampus (n=6 per group) were separated by electrophoresis on a 10 % polyacrylamide gel and electrotransferred to Nitrocellulose membranes (Amersham, GE Healthcare, Little Chalfont, UK) as previously reported [26]. Blocking procedures were performed according to the manufacturer instructions. Primary antibodies against PP2A subunits A and C (Cell Signalling Technology, Denver, USA, 1:1000) Tau (Abcam, Cambridge, UK, 1:1000), $pTau^{ser396}$(Abcam, Cambridge, UK, 1:1000), GRP78(Abcam, Cambridge, UK, 1:1000), PERK (Abcam, Cambridge, UK, 1:1000), $pPERK^{thr981}$ (Abcam, Cambridge, UK, 1:1000), EIF2α (ENZO Life Sciences, Farmingdale, USA, 1:1000), $pEIF2\alpha^{Ser51}$(ENZO Life Sciences, Farmingdale, USA, 1:1000), CHOP (Cell Signaling Technology, Denver, USA, 1:1000), ATF6 (Abcam, Cambridge, UK, 1:1000), IRE1α (Abcam, Cambridge, UK, 1:1000), Bax (Abcam, Cambridge, UK, 1:1000), Bcl-2 (Abcam, Cambridge, UK, 1:1000), Cytochrome-c, Caspase-3 (Cell Signaling Technology, Denver, USA, 1:1000) and cleaved Caspase-3 (Cell Signaling Technology, Denver, USA, 1:1000) were incubated overnight followed by 2 h incubation with horseradish peroxidase-conjugated anti-rabbit or anti-mouse IgG (1:5000) (GE, Little Chalfont, UK) secondary antibodies. Membranes were incubated with Amersham ECL Western Blotting Detection Reagent (GE Healthcare Life Sciences, Little Chalfont, UK) for 5 min and the immunodetection was made by chemoluminescence using Image Quant LAS 4000 (GE, Little Chalfont, UK). The protein expression was quantified using Image J® software (Rockville, USA). The values of optic density were expressed as % of control.

2.6. Mitochondrial function

High Resolution Respirometry: Oxygen (O_2) measurement was performed in homogenates of cells dissociated from one hippocampus in Sucrose Medium' (320 mM sucrose, 1mM EDTA, 0.25 mM dithiothreitol, pH 7.4). The respirometry protocol was performed in a standard respiration buffer (100 mM KCI, 75 mM mannitol, 25 mM sucrose, 5mM phosphate, 0.05 mM EDTA, and 10 mM Tris-HC1, pH 7.4). Oxygen consumption was measured using the high-resolution Oxygraph-2k system (Oroboros, Innsbruck, Austria). The results were normalized relative to the protein content. All the experiments were performed at 37°C in a 2-mL chamber through a multi-substrate titration protocol [34]. The titration consisted of the sequential addition of pyruvate, malate, and glutamate (PMG; 10, 10, and 20 mM, respectively); succinate (S, 10 mM); adenosine diphosphate (ADP, 2.5 mM); oligomycin (Oligo, 2 μg/ml); carbonyl cyanide p-(trifluoromethoxy) phenylhydrazone (FCCP, 1 μM); rotenone (R, 2 μM); and cyanide (KCN, 5 mM). The states related to mitochondrial function were calculated as follows: State II was obtained before PMG+S addition; State III to measure OXPHOS capacity was obtained after ADP titration in the presence of PMGS, State IV was obtained after Oligomycin addition; State V to measure ETS Capacity after FCCP titration, and non-mitochondrial respiration (ROX) after Rotenone, Antimycin-A and KCN.

The respiratory control ratio was calculated as State III-State IV/State III (ADP-Leak/ADP). Proton leak was calculated by the difference between leak respiration and ROX. Oxygen concentration was expressed as nmol/ml and the O_2 flux was expressed per mass [pmol / (s*mg)].

Mitochondrial H_2O_2 production and mitochondrial membrane potential ($\Delta\Psi m$): the mitochondrial production of hydrogen peroxide (H_2O_2) was assessed in homogenates of cells dissociated from the hippocampus using the Amplex Red oxidation method (n = 6 per group). The level of H_2O_2 was measured using the same protocol of respirometry.

Fluorescence was monitored at excitation (563 nm) and emission (587 nm) wavelengths with a Spectra Max M5 microplate reader (Molecular Devices, USA). The ΔΨm was measured using the fluorescence signal of the cationic dye, safranin-O. Hippocampal cells were dissociated and supplemented with 10 μM safranin-O. The fluorescence was detected with an excitation wavelength of 495 nm and an emission wavelength of 586 nm (Spectra Max M5, Molecular Devices). Data are reported as arbitrary fluorescence units (AFUs) [34].

2.7. Cellular viability (MTT assay)

The assessments of cells viability were performed by the colorimetric [3(4,5-dimethylthiazol-2-yl)-2,5-diphenyl tetrazolium bromide]. Homogenates of cells dissociated from hippocampus were pre-incubated adding 0.5 mg/ml of MTT, followed by incubation at 37 °C during for 45 min. The formazan product generated during the incubation was solubilized in dimethyl sulfoxide and measured at 560 and 630 nm (Spectra Max M5 (Molecular Devices, USA)[35].

2.8. Hierarchical Clustering (HC) and Principal Component Analysis (PCA)

Original variable data was centered and scaled. Unsupervised hierarchical clustering (HC) was performed using normalized data, computed in *R* statistical environment, applying euclidean distance and average linkage agglomeration methods [36].

Original variable data was centered and scaled. Principal component analysis was performed using normalized data, computed with the FactoMineR and factoextra packages in R statistical environment [36-38].

2.9. Statistical Analysis

The comparisons between OKA and CT groups were performed through Student t test. For the mitochondrial parameters we used Two-way ANOVA for multiple comparisons followed by the post hoc test of Tukey. Bivariate correlation analysis was performed by Pearson's correlation test. We used the package PASW Statistics 18. Statistical significance was considered when $p < 0.05$.

3. Results

3.1. PP2A inhibition impairs OR and increases Tau phosphorylation

Initially, we checked whether i.c.v. OKA infusion actually inhibits PP2A activity in the hippocampus. We found that the enzyme activity was significantly decreased at 24 h after OKA infusion (Figure 1A, 63 % inhibition), and remained lower than CT at day 7 (Figure 1B, 40 % inhibition). Also, protein expression levels of PP2A subunits A (constitutive) and C (catalytic) were decreased at day 7 after OKA infusion ($p<0.0384$ and $p<0.006$, Figure 1C and D, respectively).

In the OF task, there was no significant difference between groups in the distance traveled and average speed between groups (Supplementary Figure 1A). OKA did not affect the total time exploration of both objects in the training session of OR (Supplementary Figure 1B). In the testing sessions (short- and long-term memory), the CT group spent more time exploring the novel object compared to old object (CT old *vs.* CT novel object, Supplementary Figure 1C and D). In contrast, OKA group explored similarly both objects (OKA old *vs.* OKA novel object, Supplementary Figure 1C and D). Likewise, SROI and LROI confirmed a significant deficit in recognition memory caused by OKA (Figure 1E and F, for both comparisons $p< 0.0001$). Phosphorylated Tau at Ser^{396} /Tau total ratio was significantly increased in the OKA compared to CT group ($p<$

0.0299, Figure 1G). These results confirm the relevance of physiological PP2A activity/protein level in the hippocampus for the regulatory mechanisms of memory formation and Tau dynamics.

3.2. PP2A inhibition triggers endoplasmic reticulum stress

Next we characterized the impact of PP2A inhibition on endoplasmic reticulum stress responses seven days after OKA i.c.v. infusion. The well-known molecular markers of active unfolded protein response (UPR), to date GRP78, pPERK^{Thr981}/PERK total ratio, pEIF2α^{Ser51}/EIF2α total ratio and CHOP (PERK branch), and ATF6 and IRE1α were assessed in the hippocampal tissue preparations. There were statistically significant increases in the immunocontent of GRP78, pEIF2α^{Ser51}/ EIF2α total ratio, CHOP, ATF6 and IRE1α in the OKA relative to CT group (OKA *vs.* CT: GRP78, $p< 0.0006$; pEIF2α^{Ser51}/ EIF2α, $p< 0.0061$; CHOP, $p< 0.0009$; Figures 2A, C, and D, respectively). The phosphorylation of PERK at threonine 981 in OKA was not different from CT group ($p>0.0938$, Figure 3B); however the ratio (pEIF2α^{Ser51}/EIF2α) / (pPERK^{Thr981}/PERK) was significant different from CT group (Supplemental Figure 2A). Also, the expression levels of ATF6 and IRE1α were significantly different in OKA relative to CT group ($p< 0.0182$ and $p< 0.042$, Figures 2E and F, respectively). These results imply that a moderate (40%) inhibition of PP2A activity triggered parallel molecular alterations associated with ER stress response.

3.3. PP2A inhibition alters mitochondrial bioenergetics

Considering the proposed functional coupling between ER and mitochondria, here we checked whether the ER stress might influence specific metabolic mitochondrial responses associated with the activity of electron transport system. Therefore, we

performed *ex-vivo* respirometry analysis in homogenates of hippocampus incubated with a mitochondrial uncoupler, metabolic substrates and inhibitors of the electron transport system complexes (Figure 3). There were no significant differences between OKA and CT in terms of oxygen concentration (Supplementary Figure 2B) whereas mitochondrial membrane potential ($\Delta\Psi_m$) dynamics (formation and dissipation) does not respond properly after addition of succinate and succinate+ADP (Figure 3B and D), while the oxygen flux did not increased significantly in OKA after addition of ADP (Supplemental Figure 2C). Moreover, OKA displayed a significant reduced Respiratory Control Ratio linked to ATP synthesis (RCRa) ($p< 0.0001$, Figure 3A) concomitant with increased proton leakage ($p< 0.0001$, Figure 3C). These settings of results reinforce specific sites of the ETS influencing the RCRa impairment. The variations of mitochondrial membrane potential after addition of substrates and inhibitors (Succinate-basal, ADP-Succinate, Rotenone-ADP, KCN-Rotenone, FCCP-KCN), demonstrated that there was no appropriated formation of membrane potential after addition of succinate and ADP (Figure 3B).

Bearing in mind the mechanistically relevance of mitochondrial proton leakage for the production of reactive oxygen species (ROS) we assessed H_2O_2 production. There was significant increase in the H_2O_2 levels induced by succinate and FCCP in OKA compared to CT ($p< 0.0001$ and $p< 0.0001$ respectively, Figure 3D). Overall, these functional parameters are consistent neurobiological indicators of mitochondrial dysfunction, which then seeds a pro-oxidative cell microenvironment.

3.4. PP2A inhibition induces apoptosis

Additionally, we characterized the impact of ER stress and mitochondrial dysfunction on apoptotic markers (Figure 4). Therefore, the BAX/BCL2 ratio,

cytochrome c, and cleaved caspase 3/caspase total ratio were used as molecular indicators of MAM dysfunction and apoptosis. OKA significantly increased the expression levels of proteins associated with apoptotic outcomes (OKA *vs.* CT: BAX/BCL2 ratio, $p < 0.0014$, Figure 4A; cytochrome c, $p < 0.0023$, Figure 4B and cleaved caspase 3/caspase total ratio, $p < 0.0003$, Figure 4C).

The ER-stress upregulation coupled with mitochondrial apoptotic responses culminates with decreased cell viability in the OKA relative to CT group ($p < 0.0147$, Figure 4D). Therefore, hippocampal PP2A deficiency integrate ER-mitochondria disturbances leading to decreased cells viability and function.

3.5. Bivariate correlation analysis between UPR and mitochondria outcomes

We tested the degree of interaction between representative parameters of ER stress and mitochondrial dysfunction, and cell viability through correlation analysis (Figure 5). Primarily, we reinforce the connection of ER-mitochondria dysfunction in OKA group through the demonstration of significant positive correlation between BAX/BCL2 and the expression of a pivotal molecular component of ER stress, namely pEIF2α^{Ser51}/Eif2α (Figure 5A). To further characterize this concept we showed that key aspects of mitochondrial function like RCRa and H_2O_2 production, also correlated with pEif2α^{Ser51}/ Eif2α (Figure 5B and C).

Moreover, pEif2α^{Ser51}/Eif2α and the levels of mitochondrial H_2O_2 are both correlated with decreased cell viability (MTT) (Figure 5D and E, respectively). The expression levels of pTau^{Ser396}/Tau, a hallmark molecular marker of neurodegeneration and a substrate of PP2A activity, did not significantly correlate with cell viability (Figure 5F). The degree of PP2A activity showed high level of correlations with the parameters linked with ER-stress, mitochondria dysfunction and apoptosis (Supplementary Figure 3).

Overall, these results emphasize that PP2A exerts key influence on components of ER-mitochondria communication, which dependent on the level of activity determine the fate of cells survival and death. The correlations between memory parameters (SROI and LROI), neurochemical, neuroenergetics and molecular variables within the CT group do not show statistical significance (data not shown).

3.6. ER-mitochondria dysfunction and bioinformatics analysis

Aiming to categorize the similarities between the variables, we performed hierarchical clustering (HC) analysis (Figure 6), which resulted in a distance matrix displayed in a heatmap (Figure 6A). The color key values display mice separated into distinct groups according the similarity among variables - CT mice: 1-6, OKA mice: 7-12 corroborating the magnitude of OKA effects. Within the OKA group there are two clusters of variables. The neurochemical markers of MAM dysfunction represent the first cluster (in red); meanwhile the respiratory control efficiency (RCRa) comprises the second cluster (blue). Remarkably, the increase neurochemical markers induced by OKA in the first cluster likely decrease markers in the second cluster. Moreover, the proximity between the markers of ER stress and mitochondrial malfunction strongly suggests MAM dysfunction.

Operating under the assumption that the entire neurochemical data would better account for the differences between OKA and CT groups, we used Principal Component Analysis (PCA). This statistical multivariate procedure analyzes inter-correlated quantitative dependent variables creating a new set of variables called principal components (PC), in which the first component has the largest possible variance. Indeed, the chosen neurochemical variables created a novel one (PC1) that alone could explain nearly 80 % of data variance (Figure 6B). The main contributors to PC1 were eight

variables, which move to the right of dashline in the Figure 6C. Also, among the eight variables in the PC1, the H_2O_2 was graded as the highest contributor. Moreover, comparison of PC1 analysis between CT and OKA was able to confirm that this variable strongly discriminates both experimental groups (Figure 6D). We also showed that PC1 (OKA) data significantly correlates with PP2A activity, memory fitness and cell viability (Figure 6E, F, G and H respectively). Correlations analysis was also performed between PC1 (CT) with neurochemical, molecular and memory variables and do not shown statistical significance. Hence, we highlight the H_2O_2 as an important neurochemical player mechanistically associated with MAM dysfunction.

4. Discussion

We have demonstrated that PP2A inhibition with a single i.c.v. infusion of OKA impaired ER and mitochondrial responses in the hippocampus. Taking advantage of molecular, functional and bioinformatics approaches we provided mechanistic insights to further integrate such responses within a unique entity namely MAM dysfunction, which compromised cells viability and recognition memory.

Actually, many neurodegenerative diseases including Parkinson and AD involve the accumulation of protein aggregates associated with ER-stress and an adaptive UPR response trying to restore the proteostasis. Unsolved UPR response leads to abnormal ER stress linked with detrimental consequences for the cells survival and brain function [39]. As expected, decreased PP2A activity duplicates Tau hyperphosphorylation and caused object recognition memory impairment, which is coincident with previous molecular and behavioral evidences for PP2A deficiency reported in AD patients and rodent models [40-42]. Beyond Tau dynamics, PP2A inhibition also mediates the activity of key elements participating in the ER stress responses and MAM interactions. Actually, we

found that the PP2A inhibition in the hippocampus of mice resulted in the increased expression levels of pEIF2α^{Ser51}, which is a well-recognized molecular marker of ER stress associated with UPR. This effect was likely dependent of PERK; an upstream enzyme activating EIF2α kinase. Indeed, endogenous PP2A limiting role against pEIF2α^{Ser51} accumulation is achieved predominantly through the control of EIF2α kinase activity. As already showed, when PP2A was inhibited the EIF2α kinase overcome phosphatase activity thereby supporting the accumulation of pEIF2α^{Ser51} [43,23]. Also, the accumulation of pEIF2α^{Ser51} provides the mechanistic link for the observed concomitant increased levels of CHOP, a downstream nuclear transcription factor that upregulates the abundance of mitochondrial apoptotic proteins[10,3]. It has been consistently demonstrated that high levels of CHOP due to ER-stress mediate apoptotic mechanism in several neurodegenerative disorders, particularly AD[44]. In opposite to the apoptotic CHOP signaling, we also detected an upregulation of GRP78 levels in the hippocampus that mirrors an adaptive response targeting proteins to degradation hence avoiding the accumulation and aggregation of misfolding proteins within the lumen as consequence of the ER-stress induced by PP2A inhibition. Actually, upregulation of GRP78 tend to shift the balance to the pro-survival branches of the UPR[45,46]. Therefore, it seems that PP2A activity exerts a homeostatic dominance upon key molecular effectors governing the ER-stress responses, to date the pEIF2α^{Ser51} and CHOP. A failure in this dominance over the PERK branch may exacerbate ER stress coupled with mitochondria dysfunction and additionally, may impacts ATF6 and IREα branches likely to oppose these responses (Claudio Hetz, 2017 Nature Reviews Neurology). While Plácido and colleagues (2017)[24] demonstrated that the PP2A inhibition disrupted ER-mitochondria communication, here we highlight that EIF2α work

as the key effector of this interorganelle miscommunication. Remarkably, among the molecular biomarkers of ER-stress, the EIF2α was the unique to show a significant behavior as component of the PC1 analysis.

It has become a common sense that MAM contacts facilitate the transference of Ca^{2+} from the ER to mitochondria to stimulate oxidative metabolism. Based on this mechanistic relevance, it can be assumed that a synchronized MAM communication is a fundamental aspect behind the regulatory roles of mitochondria on bioenergetics and survival [47]. In our study, the energy necessary for the oxidative phosphorylation of ADP by the mitochondrial Complex V (ATP-Synthase) is dissipated even in the presence of saturated concentrations of ADP. This implies in less efficiency of ATP production probably due to specific Complex V problems or alterations in the mitochondrial membrane potential leading to uncoupling. Accordingly, we noticed an increased proton leakage coupled with mitochondrial elevated H_2O_2 production, a feasible biomarker of mitochondrial membrane potential alterations, and a prominent reactive oxygen specie (ROS) involved in the oxidative damage to the plasma and mitochondrial membranes that ultimately may prolong bioenergetics deficits [34,48]. Verfaillie et al(2012)[17] reported that PERK, a stress sensor of UPR, mediates mitochondrial apoptosis through the sustained elevations of CHOP and ROS, and further facilitating the transit of ROS between ER and mitochondria. As discussed earlier, we did not find differences in hippocampal PERK levels due to PP2A inhibition albeit the downstream PERK effectors like pEIF2α^{Ser51}, CHOP and H_2O_2 (ROS) behave similarly in both works, even considering they have used Phox-ER stress stimuli in murine embryonic fibroblast cell cultures. Therefore, our results suggest that PP2A-induced ER-stress mounts a composite of apoptotic signals, bioenergetics failure and redox disturbances via pEIF2α^{Ser51}/CHOP/ H_2O_2 without apparent need of increased PERK level. Alternatively, the inhibition of

PP2A belonging to the complex PP2A/AKT/IP3R settled directly at MAM junctions may cause an overload of Ca^{2+} from the ER to mitochondria, thus contributing to these outcomes [2].

Although cells tend to activate mechanisms to restore the functional homeostasis, a prolonged MAM dysfunction places the cells in an inevitable apoptotic path. Based on this principle we measured classic apoptotic markers linked to mitochondria and not surprisingly, the upregulation of pEIF2α^{Ser51}/ CHOP/ H_2O_2 signaling was implicated in the parallel increase of BAX/BCL2, cytochrome c, and cleaved caspase 3/caspase 3 implying that PP2A inhibition increases the apoptotic burden ultimately directing neural cells to death. Indeed, cell viability was decreased in OKA group and strongly correlated with both ER and mitochondrial components of the MAM dysfunction (see Figure 6). Surprisingly, pTau/Tau did not significantly correlate with ER-stress markers, H_2O_2 and MTT levels suggesting that short-term PP2A inhibition driven MAM dysfunction and detrimental molecular and memory outcomes precedes hyperphosphorylated Tau-induced abnormalities. Moreover, the higher expression levels of BAX/BCL2 after PP2A inhibition is coherent with the increased pEIF2α^{Ser51}/ CHOP effect on proapoptotic target genes [39]. Also, BAX upregulation and migration to the outer mitochondrial membrane causes prompting formation of pores associated with cytochrome c release, which is a master activator of proteolytic activity here represented by the cleaved caspase-3. The loss of mitochondrial energetic efficiency coupled with increased H_2O_2 demonstrated in this study agrees with the existence of membrane pores.

Through the HC analysis we confirmed the proximity of ER-stress, mitochondrial dysfunction and apoptotic markers implying they behave in complimentary abnormal manner when PP2A is “switch-off”. This principle suggests that ER stress and mitochondrial dysfunction may mutually reinforce each other, likely through ROS

production and calcium exchange [14,17]. However, considering that multiple components participating in the MAM interactions, some of them not known yet, it seems difficult to state precisely which is the highest detrimental effector of PP2A inhibition. Nevertheless, our PCA showed that H_2O_2 was ranked as the main contributor to the PC1 in the context of PP2A inhibition. Additionally, considering memory impairment as the worst neurological outcome of this study, we observed that the entire molecular and functional components used to create PC1 was able to explain the short- and long-term memory deficits after OKA-induced PP2A inhibition.

In summary, decreased PP2A activity upregulated the ER apoptotic signaling mechanistically associated with decreased mitochondrial ATP synthesis and increased H_2O_2 levels, implying that ER-stress propelled mitochondrial bioenergetics uncoupling. Also, the principal component analysis highlights the H_2O_2 as the higher effector of ER-mitochondria dysfunction leading to cells death and memory impairment.

Acknowledgements

This work was supported by the Brazilian grants of CNPq 426796/2016-0 and 141100/2013-3, CNPq-Instituto de Nacional de Neurociência Translacional-INNT #465346/2014-6, CAPES, FAPERGS-PPSUS and also by the FAPERGS/PRONEX 16/2551-0000499-4.

References

1. Giorgi C, Missiroli S, Patergnani S, Duszynski J, Wieckowski MR, Pinton P (2015) Mitochondria-associated membranes: composition, molecular mechanisms, and physiopathological implications. Antioxidants & redox signaling 22 (12):995-1019. doi:10.1089/ars.2014.6223
2. Tubbs E, Rieusset J (2017) Metabolic signaling functions of ER-mitochondria contact sites: role in metabolic diseases. Journal of molecular endocrinology 58 (2):R87-r106. doi:10.1530/jme-16-0189
3. Han J, Back SH, Hur J, Lin YH, Gildersleeve R, Shan J, Yuan CL, Krokowski D, Wang S, Hatzoglou M, Kilberg MS, Sartor MA, Kaufman RJ (2013) ER-stress-induced

transcriptional regulation increases protein synthesis leading to cell death. Nature cell biology 15 (5):481-490. doi:10.1038/ncb2738
4. Ueda M, Li S, Itoh M, Wang MX, Hayakawa M, Islam S, Tana, Nakagawa K, Chen H, Nakagawa T (2016) Expanded polyglutamine embedded in the endoplasmic reticulum causes membrane distortion and coincides with Bax insertion. Biochemical and biophysical research communications 474 (2):259-263. doi:10.1016/j.bbrc.2016.04.034
5. Zhao L, Ackerman SL (2006) Endoplasmic reticulum stress in health and disease. Current opinion in cell biology 18 (4):444-452. doi:10.1016/j.ceb.2006.06.005
6. Ron D, Walter P (2007) Signal integration in the endoplasmic reticulum unfolded protein response. Nature reviews Molecular cell biology 8 (7):519-529. doi:10.1038/nrm2199
7. Hoozemans JJ, Scheper W (2012) Endoplasmic reticulum: the unfolded protein response is tangled in neurodegeneration. The international journal of biochemistry & cell biology 44 (8):1295-1298. doi:10.1016/j.biocel.2012.04.023
8. Ferreiro E, Pereira CM (2012) Endoplasmic reticulum stress: a new playER in tauopathies. The Journal of pathology 226 (5):687-692. doi:10.1002/path.3977
9. Roussel BD, Kruppa AJ, Miranda E, Crowther DC, Lomas DA, Marciniak SJ (2013) Endoplasmic reticulum dysfunction in neurological disease. The Lancet Neurology 12 (1):105-118. doi:10.1016/s1474-4422(12)70238-7
10. Marciniak SJ, Yun CY, Oyadomari S, Novoa I, Zhang Y, Jungreis R, Nagata K, Harding HP, Ron D (2004) CHOP induces death by promoting protein synthesis and oxidation in the stressed endoplasmic reticulum. Genes & development 18 (24):3066-3077. doi:10.1101/gad.1250704
11. Paschen W, Mengesdorf T (2005) Endoplasmic reticulum stress response and neurodegeneration. Cell calcium 38 (3-4):409-415. doi:10.1016/j.ceca.2005.06.019
12. Hengartner MO (2000) The biochemistry of apoptosis. Nature 407 (6805):770-776. doi:10.1038/35037710
13. Lakhani SA, Masud A, Kuida K, Porter GA, Jr., Booth CJ, Mehal WZ, Inayat I, Flavell RA (2006) Caspases 3 and 7: key mediators of mitochondrial events of apoptosis. Science (New York, NY) 311 (5762):847-851. doi:10.1126/science.1115035
14. Malhotra JD, Kaufman RJ (2007) Endoplasmic reticulum stress and oxidative stress: a vicious cycle or a double-edged sword? Antioxidants & redox signaling 9 (12):2277-2293. doi:10.1089/ars.2007.1782
15. Pajak B, Kania E, Orzechowski A (2016) Killing Me Softly: Connotations to Unfolded Protein Response and Oxidative Stress in Alzheimer's Disease. Oxidative medicine and cellular longevity 2016:1805304. doi:10.1155/2016/1805304
16. Nakka VP, Prakash-Babu P, Vemuganti R (2016) Crosstalk Between Endoplasmic Reticulum Stress, Oxidative Stress, and Autophagy: Potential Therapeutic Targets for Acute CNS Injuries. Molecular neurobiology 53 (1):532-544. doi:10.1007/s12035-014-9029-6
17. Verfaillie T, Rubio N, Garg AD, Bultynck G, Rizzuto R, Decuypere JP, Piette J, Linehan C, Gupta S, Samali A, Agostinis P (2012) PERK is required at the ER-mitochondrial contact sites to convey apoptosis after ROS-based ER stress. Cell death and differentiation 19 (11):1880-1891. doi:10.1038/cdd.2012.74
18. Szegezdi E, Logue SE, Gorman AM, Samali A (2006) Mediators of endoplasmic reticulum stress-induced apoptosis. EMBO reports 7 (9):880-885. doi:10.1038/sj.embor.7400779
19. Kim I, Xu W, Reed JC (2008) Cell death and endoplasmic reticulum stress: disease relevance and therapeutic opportunities. Nature reviews Drug discovery 7 (12):1013-1030. doi:10.1038/nrd2755

20. Iqbal K, Alonso Adel C, Chen S, Chohan MO, El-Akkad E, Gong CX, Khatoon S, Li B, Liu F, Rahman A, Tanimukai H, Grundke-Iqbal I (2005) Tau pathology in Alzheimer disease and other tauopathies. Biochimica et biophysica acta 1739 (2-3):198-210. doi:10.1016/j.bbadis.2004.09.008
21. Nematullah M, Hoda MN, Khan F (2017) Protein Phosphatase 2A: a Double-Faced Phosphatase of Cellular System and Its Role in Neurodegenerative Disorders. Molecular neurobiology. doi:10.1007/s12035-017-0444-3
22. Lecca S, Pelosi A, Tchenio A, Moutkine I, Lujan R, Herve D, Mameli M (2016) Rescue of GABAB and GIRK function in the lateral habenula by protein phosphatase 2A inhibition ameliorates depression-like phenotypes in mice. Nature medicine 22 (3):254-261. doi:10.1038/nm.4037
23. Brush MH, Weiser DC, Shenolikar S (2003) Growth arrest and DNA damage-inducible protein GADD34 targets protein phosphatase 1 alpha to the endoplasmic reticulum and promotes dephosphorylation of the alpha subunit of eukaryotic translation initiation factor 2. Molecular and cellular biology 23 (4):1292-1303
24. Placido AI, Pereira CM, Correira SC, Carvalho C, Oliveira CR, Moreira PI (2017) Phosphatase 2A Inhibition Affects Endoplasmic Reticulum and Mitochondria Homeostasis Via Cytoskeletal Alterations in Brain Endothelial Cells. 54 (1):154-168. doi:10.1007/s12035-015-9640-1
25. Kim SM, Yoon SY, Choi JE, Park JS, Choi JM, Nguyen T, Kim DH (2010) Activation of eukaryotic initiation factor-2 alpha-kinases in okadaic acid-treated neurons. Neuroscience 169 (4):1831-1839. doi:10.1016/j.neuroscience.2010.06.016
26. Muller AP, Gnoatto J, Moreira JD, Zimmer ER, Haas CB, Lulhier F, Perry ML, Souza DO, Torres-Aleman I, Portela LV (2011) Exercise increases insulin signaling in the hippocampus: physiological effects and pharmacological impact of intracerebroventricular insulin administration in mice. Hippocampus 21 (10):1082-1092. doi:10.1002/hipo.20822
27. Kamat PK, Tota S, Rai S, Shukla R, Ali S, Najmi AK, Nath C (2012) Okadaic acid induced neurotoxicity leads to central cholinergic dysfunction in rats. European journal of pharmacology 690 (1-3):90-98. doi:10.1016/j.ejphar.2012.06.006
28. Arendt T, Holzer M, Fruth R, Bruckner MK, Gartner U (1995) Paired helical filament-like phosphorylation of tau, deposition of beta/A4-amyloid and memory impairment in rat induced by chronic inhibition of phosphatase 1 and 2A. Neuroscience 69 (3):691-698
29. Shenolikar S (1994) Protein serine/threonine phosphatases--new avenues for cell regulation. Annual review of cell biology 10:55-86. doi:10.1146/annurev.cb.10.110194.000415
30. Zimmer ER (2015) O envolvimento da proteína fosfatase 2A e do sistema glutamatérgico em processos neurodegenerativos relacionados à doença de Alzheimer: mecanismos e biomarcadores de imagem. Universidade Federal do Rio Grande do Sul Thesis
31. Evans DR, Myles T, Hofsteenge J, Hemmings BA (1999) Functional expression of human PP2Ac in yeast permits the identification of novel C-terminal and dominant-negative mutant forms. The Journal of biological chemistry 274 (34):24038-24046
32. Zimmer ER, Torrez VR, Kalinine E, Augustin MC, Zenki KC, Almeida RF, Hansel G, Muller AP, Souza DO, Machado-Vieira R, Portela LV (2015) Long-term NMDAR antagonism correlates reduced astrocytic glutamate uptake with anxiety-like phenotype. Frontiers in cellular neuroscience 9:219. doi:10.3389/fncel.2015.00219
33. Lueptow LM (2017) Novel Object Recognition Test for the Investigation of Learning and Memory in Mice. Journal of visualized experiments : JoVE (126). doi:10.3791/55718

34. Muller AP, Haas CB, Camacho-Pereira J, Brochier AW, Gnoatto J, Zimmer ER, de Souza DO, Galina A, Portela LV (2013) Insulin prevents mitochondrial generation of H(2)O(2) in rat brain. Experimental neurology 247:66-72. doi:10.1016/j.expneurol.2013.03.007
35. Preissler T, Bristot IJ, Costa BM, Fernandes EK, Rieger E, Bortoluzzi VT, de Franceschi ID, Dutra-Filho CS, Moreira JC, Wannmacher CM (2016) Phenylalanine induces oxidative stress and decreases the viability of rat astrocytes: possible relevance for the pathophysiology of neurodegeneration in phenylketonuria. Metabolic brain disease 31 (3):529-537. doi:10.1007/s11011-015-9763-0
36. Team RC (2015) R: A language and environment for statistical computing. R Foundation for Statistical Computing
37. Mundt AKaF (2017) Factoextra: Extract and Visualize the Results of Multivariate Data Analyses.
38. Le S (2008) FactoMineR: An R Package for Multivariate Analysis. Journal of Statistical Software
39. Pihan P, Carreras-Sureda A, Hetz C (2017) BCL-2 family: integrating stress responses at the ER to control cell demise. Cell death and differentiation 24 (9):1478-1487. doi:10.1038/cdd.2017.82
40. Wang J, Tung YC, Wang Y, Li XT, Iqbal K, Grundke-Iqbal I (2001) Hyperphosphorylation and accumulation of neurofilament proteins in Alzheimer disease brain and in okadaic acid-treated SY5Y cells. FEBS letters 507 (1):81-87
41. He J, Yamada K, Zou LB, Nabeshima T (2001) Spatial memory deficit and neurodegeneration induced by the direct injection of okadaic acid into the hippocampus in rats. Journal of neural transmission (Vienna, Austria : 1996) 108 (12):1435-1443. doi:10.1007/s007020100018
42. Kamat PK, Rai S, Swarnkar S, Shukla R, Nath C (2014) Molecular and cellular mechanism of okadaic acid (OKA)-induced neurotoxicity: a novel tool for Alzheimer's disease therapeutic application. Molecular neurobiology 50 (3):852-865. doi:10.1007/s12035-014-8699-4
43. Prostko CR, Brostrom MA, Brostrom CO (1993) Reversible phosphorylation of eukaryotic initiation factor 2 alpha in response to endoplasmic reticular signaling. Molecular and cellular biochemistry 127-128:255-265
44. Baleriola J, Walker CA, Jean YY, Crary JF, Troy CM, Nagy PL, Hengst U (2014) Axonally synthesized ATF4 transmits a neurodegenerative signal across brain regions. Cell 158 (5):1159-1172. doi:10.1016/j.cell.2014.07.001
45. Reddy RK, Mao C, Baumeister P, Austin RC, Kaufman RJ, Lee AS (2003) Endoplasmic reticulum chaperone protein GRP78 protects cells from apoptosis induced by topoisomerase inhibitors: role of ATP binding site in suppression of caspase-7 activation. The Journal of biological chemistry 278 (23):20915-20924. doi:10.1074/jbc.M212328200
46. Wang M, Wey S, Zhang Y, Ye R, Lee AS (2009) Role of the unfolded protein response regulator GRP78/BiP in development, cancer, and neurological disorders. Antioxidants & redox signaling 11 (9):2307-2316. doi:10.1089/ars.2009.2485
47. Hayashi T, Rizzuto R, Hajnoczky G, Su TP (2009) MAM: more than just a housekeeper. Trends in cell biology 19 (2):81-88. doi:10.1016/j.tcb.2008.12.002
48. Sies H (2017) Hydrogen peroxide as a central redox signaling molecule in physiological oxidative stress: Oxidative eustress. Redox biology 11:613-619. doi:10.1016/j.redox.2016.12.035

Legend to figures

Figure 1. Experimental design and model validation. The protocol comprises a single i.c.v injection of artificial cerebrospinal fluid (aCSF, vehicle) or okadaic acid (OKA, 100 ng) followed by behavioral tests, and brain hippocampus dissection at day 7 for neurochemical and molecular analysis. The activity of enzyme (at 24 h and 7 days) (A and B) and the expression levels of PP2A subunits A and C (at 7 days, B and C) were significantly decreased. Relative to CT the activity was inhibiting by 40 %. Compared to OKA, the CT group explored preferentially the novel object during short- and long-term memory test, and had higher scores at short- and long-term recognition object index (SROI and LROI, D and E). The immunocontent of Tau^{Ser396}/Tau total ratio was significantly increased in OKA relative to CT (F). *Refers to significant difference between CT and OKA ($p< 0.05$), (n = 6 mice per group) (Data are mean ± S.D).

Figure 2. PP2A inhibition increases the molecular markers of endoplasmic reticulum (ER) stress. Chaperone GRP78 (A), $pPERK^{thr981}$/PERK (B), $pEIF2\alpha^{Ser51}$/EIFα (C), CHOP (D), ATF6 (E) and IRE1α (F). *Denotes significant difference between CT and OKA ($p< 0.05$). The values are expressed as percentage of control (n = 6 mice per group) (Data are mean ± S.D).

Figure 3. PP2A inhibition impairs mitochondrial function. Evaluation of electron transport system through O_2 flux per mass displayed deficient phosphorylation of ADP in OKA group represented by decreased Respiratory Control Ratio (RCRa) (A). The mitochondrial membrane potential ($\Delta\Psi_m$) variation in the Succinate-Routine, and ADP-Succinate was significantly different in OKA group (B). The changes $\Delta\Psi_m$ leads to increased proton leakage (C), and impacted the mitochondrial H_2O_2 production (D).

Significant difference between CT and OKA (p< 0.05), (n = 6, mice per group) (Data are mean ± S.D).

Figure 4. OKA-induced PP2A inhibition of PP2A increases markers of apoptosis. The immunocontents of BAX/BCL2 ratio (A), cytochrome c (B), cleaved caspase 3/caspase 3 total ratio (C) increased, which was followed by decreased cell viability (MTT) (D). *Significant difference between CT and OKA. The values are expressed as percentage of control (*p< 0.05). (n = 6, mice per group) (Data are mean ± S.D).

Figure 5. The Pearson correlation analysis displays an ER-mitochondria dysfunction affecting cell viability. The immunocontent of the ER-stress marker pEIF2α^{Ser51}/EIFα significantly correlated with BAX/BCL2 (A), respiratory control ratio (RCRa) (B), H_2O_2 (C), and decreased cell viability (MTT) (D). The elevated mitochondrial H_2O_2 production significantly correlated with decreased cell viability (MTT) (E) and the immunocontent of Tau^{Ser396}/Tau did not significantly correlated with cell viability (MTT) (F). (*p< 0.05),(n = 6, mice per group) (Data are mean ± S.D).

Figure 6. Multivariate analysis of neurochemical, and bioenergetics data. Normalized experimental data was submitted to unsupervised hierarchical clustering (A) and principal components analysis (PCA). The percentage of variance explained by each PC (B) and the percentage of contribution of each inputted experimental variable to PC1 (C) were obtained, and the outcome association of the first component was evaluated (D) using Student t test (* *Denotes significance when p<0.05*). Moreover, *Pearson* correlation test showed a significant association between PC1 with PP2A activity, short- and long-term object recognition impairment, and cell viability (MTT) (E, F, G and G).

Supplementary Legends

Supplementary Figure 1. Okadaic acid (OKA)-induced PP2A inhibition does not impaired locomotor behavior but caused recognition memory deficits. In the open field task (OF), there was no significant difference between groups in the distance traveled (CT, circles and OKA, squares) ($p>0.724$, A). During training period of novel object recognition task both groups (CT and OKA) spent similar percentage of time exploring objects A and B (B). The CT group explored preferentially the novel object during short- and long-term memory test (both $p<0.0001$, C and D, repectively).

Supplementary Figure 2. Influence of PP2A inhibition on the PERK/EIF2α balance and mitochondrial responses to substrates. The (pEIF2αSer51/EIF2α) / (pPERKThr981/PERK) ratio was significantly elevated in OKA vs CT group ($p<0.016$, A). The oxygen consumption was estimated through respirometry analysis in hippocampal homogenates after the sequential addition of metabolic substrates to mitochondrial complexes (PMGS and ADP), inhibitors of mitochondrial complexes (oligomycin, rotenone, antimicyn A and KCN), and a membrane uncoupler (FCCP). The global variation in the oxygen consumption (B), the specific parameters associated to mitochondrial states (C), and the mitochondrial membrane potential (safranin dye) (D) in response to manipulations indicates how mitochondria manage the flux oxygen and membrane potential to sustain ATP synthesis. Basically, the oxygen flux in P(CII) is significantly impaired in OKA relative to CT group ($p< 0.0032$, C). Negative values refer to increase membrane potential meanwhile positive values refer to decrease membrane potential. * Denotes significant difference at $p<0.05$.

Supplementary Figure 3. Inhibition of PP2A activity correlates with parameters of ER-stress mitochondria dysfunction and apoptosis. The PP2A activity is strongly associated with biomarkers of mitochondrial function (RCRa and H_2O_2 - B and C), ER-stress (pEIF2αSer51/EIF2α - D), recognition memory (LROI and SROI - F and G), apoptotic neurodegeneration (BAX/BCL2, Cleaved Caspase3/Caspase, pTauSer396/Tau - A, E, H and I) cells viability (MTT - H). The significance and magnitude of correlations are shown in the correspondent figure.

Figure 1

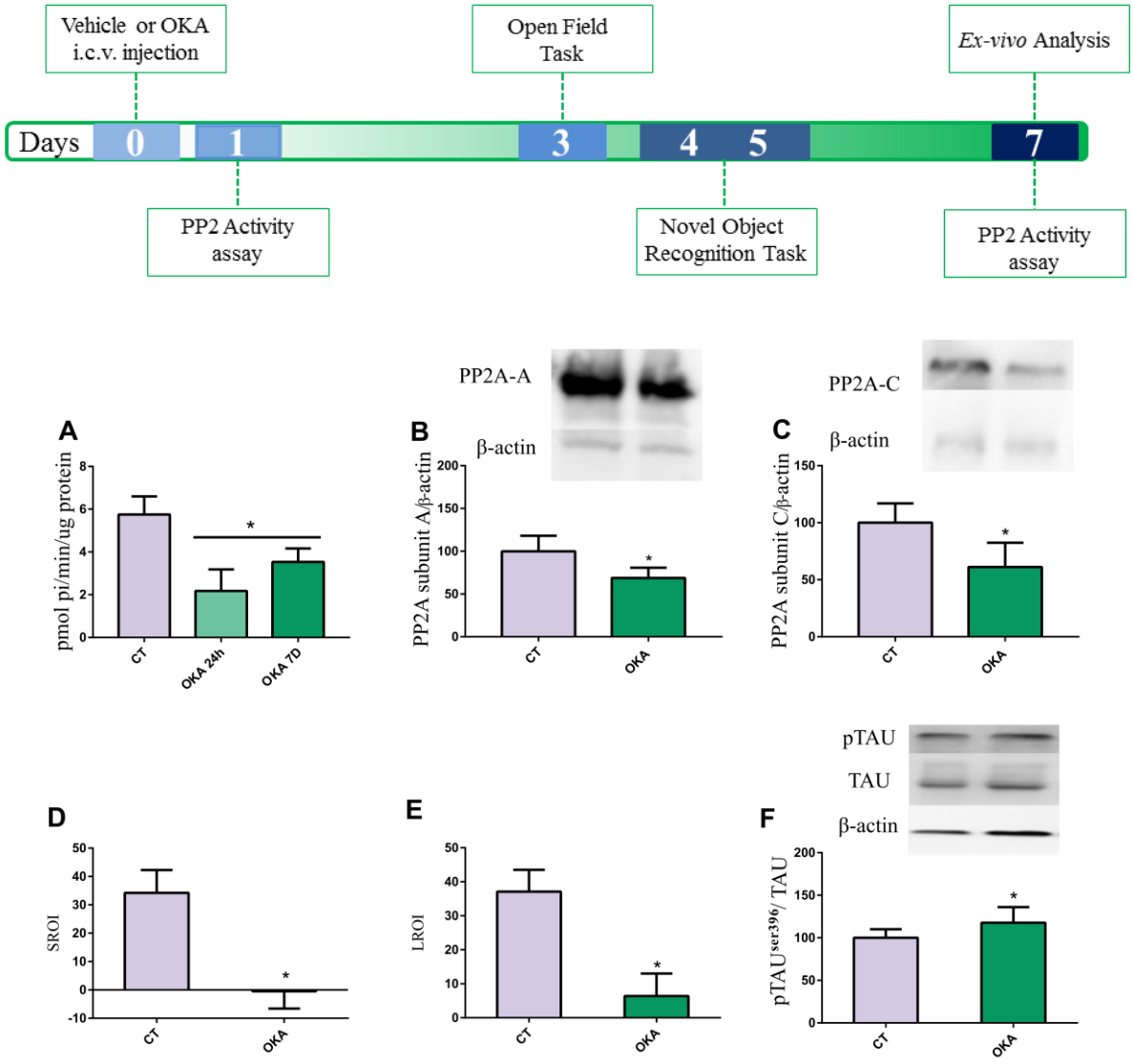
Vehicle or OKA i.c.v. injection
Open Field Task
Ex-vivo Analysis
Days
0
1
3
4
5
7
PP2 Activity assay
Novel Object Recognition Task
PP2 Activity assay
A
pmol pi/min/ug protein
CT
OKA 24h
OKA 7D
B
PP2A-A
β-actin
PP2A subunit A/β-actin
CT
OKA
C
PP2A-C
β-actin
PP2A subunit C/β-actin
CT
OKA
D
SROI
CT
OKA
E
LROI
CT
OKA
F
pTAU
TAU
β-actin
pTAUser396/TAU
CT
OKA

Figure 2

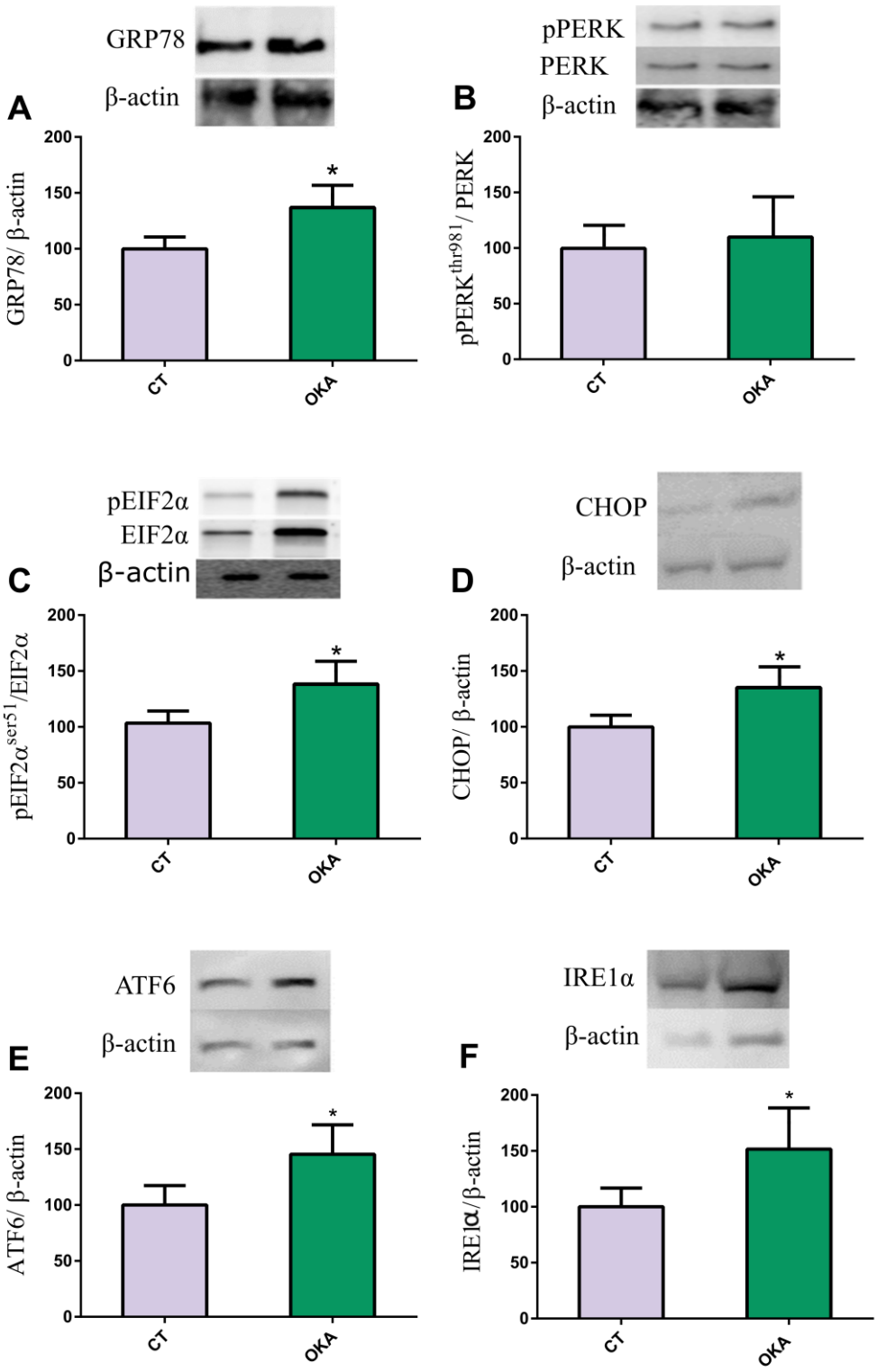
A
GRP78
β-actin
GRP78/ β-actin
200
150
100
50
0
*
CT
OKA
B
pPERK
PERK
β-actin
pPERK^thr981 / PERK
200
150
100
50
0
CT
OKA
C
pEIF2α
EIF2α
β-actin
pEIF2α^ser51/EIF2α
200
150
100
50
0
*
CT
OKA
D
CHOP
β-actin
CHOP/ β-actin
200
150
100
50
0
*
CT
OKA
E
ATF6
β-actin
ATF6/ β-actin
200
150
100
50
0
*
CT
OKA
F
IRE1α
β-actin
IRE1α/β-actin
200
150
100
50
0
*
CT
OKA

Figure 3

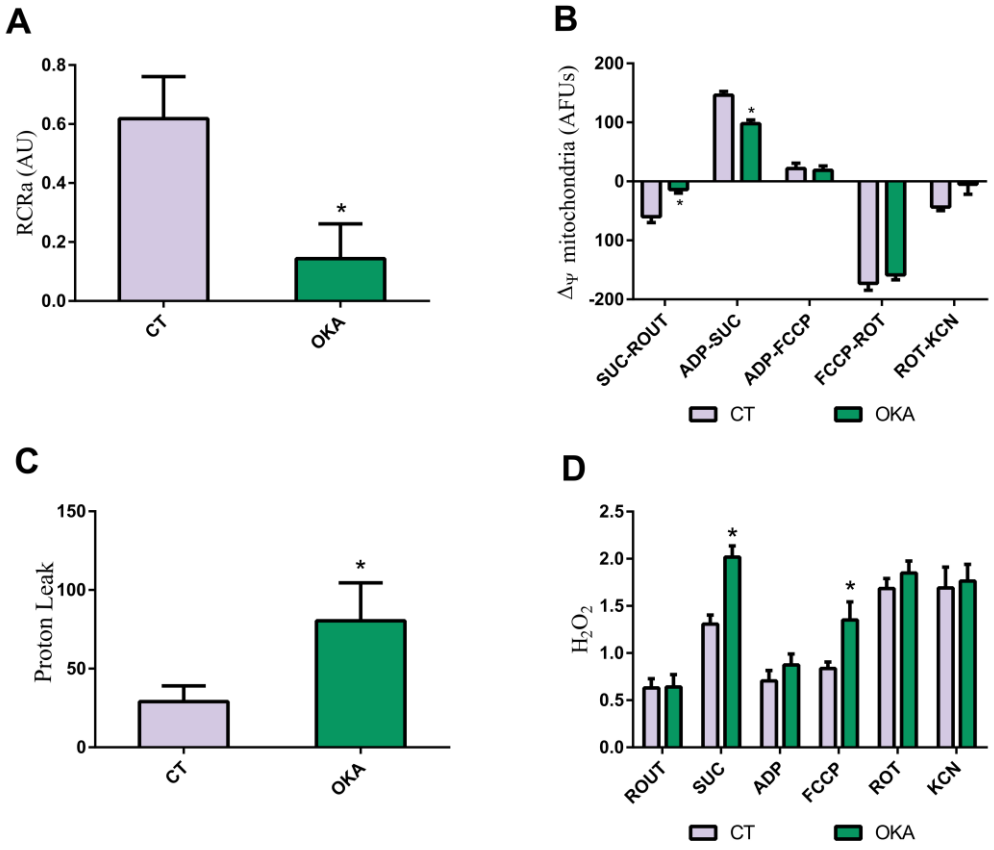
A
RCRa (AU)
0.8
0.6
0.4
0.2
0.0
*
CT
OKA
B
Δψ mitochondria (AFUs)
200
100
0
100
-200
*
*
SUC-ROUT
ADP-SUC
ADP-FCCP
FCCP-ROT
ROT-KCN
CT
OKA
C
Proton Leak
150
100
50
0
*
CT
OKA
D
H2O2
2.5
2.0
1.5
1.0
0.5
0.0
*
*
ROUT
SUC
ADP
FCCP
ROT
KCN
CT
OKA

Figure 4

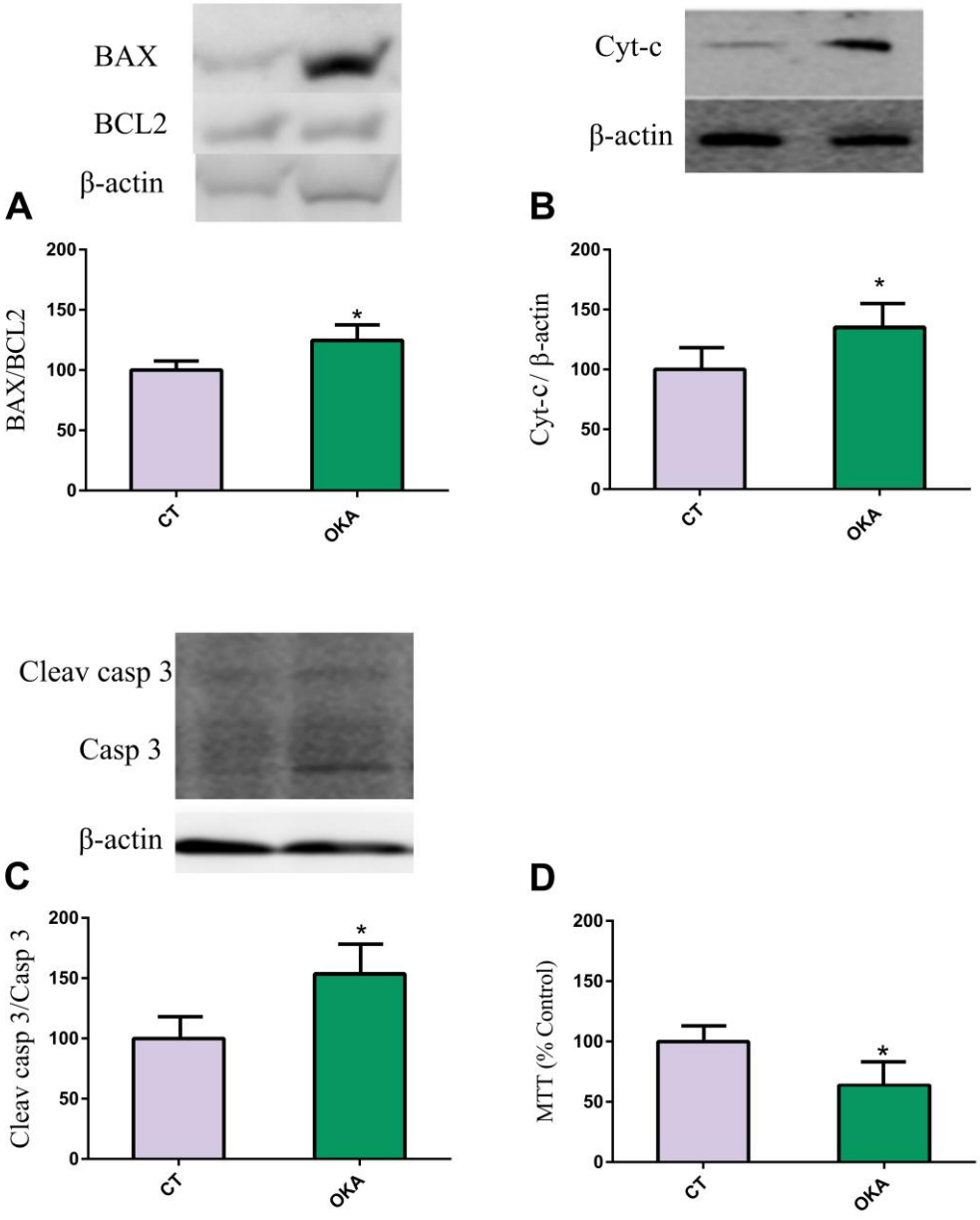
BAX
BCL2
β-actin
A
BAX/BCL2
200
150
100
50
0
*
CT
OKA
Cyt-c
β-actin
B
Cyt-c/ β-actin
200
150
100
50
0
*
CT
OKA
Cleav casp 3
Casp 3
β-actin
C
Cleav casp 3/Casp 3
200
150
100
50
0
*
CT
OKA
D
MTT (% Control)
200
150
100
50
0
*
CT
OKA

Figure 5

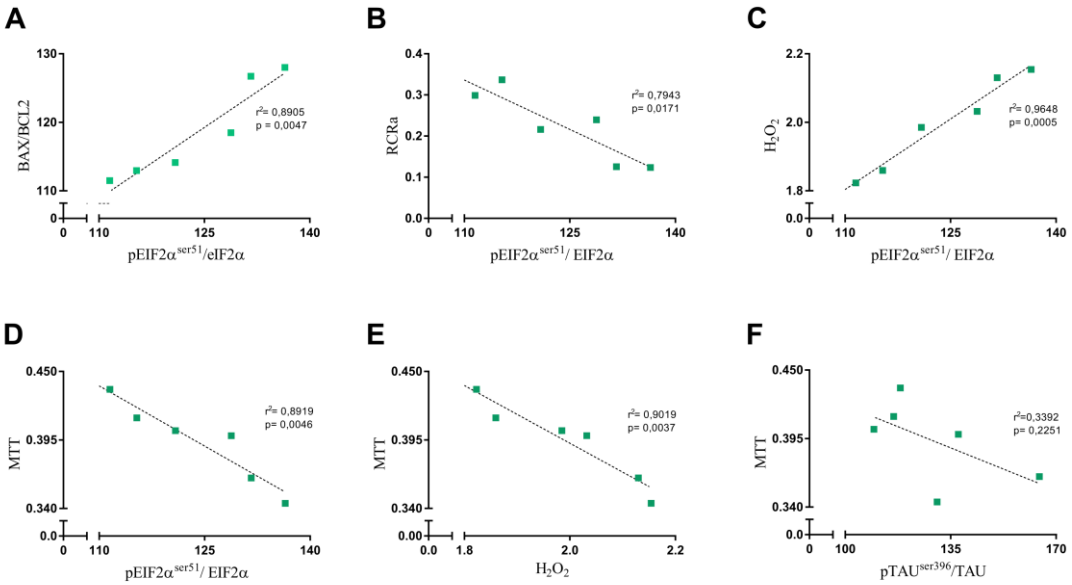
A
BAX/BCL2
r²= 0,8905
p = 0,0047
pEIF2α ser51/eIF2α
B
RCRa
r²= 0,7943
p= 0,0171
pEIF2α ser51/ EIF2α
C
H2O2
r²= 0,9648
p= 0,0005
pEIF2α ser51/ EIF2α
D
MTT
r²= 0,8919
p= 0,0046
pEIF2α ser51/ EIF2α
E
MTT
r²= 0,9019
p= 0,0037
H2O2
F
MTT
r²=0,3392
p= 0,2251
pTAU ser396/TAU

Figure 6

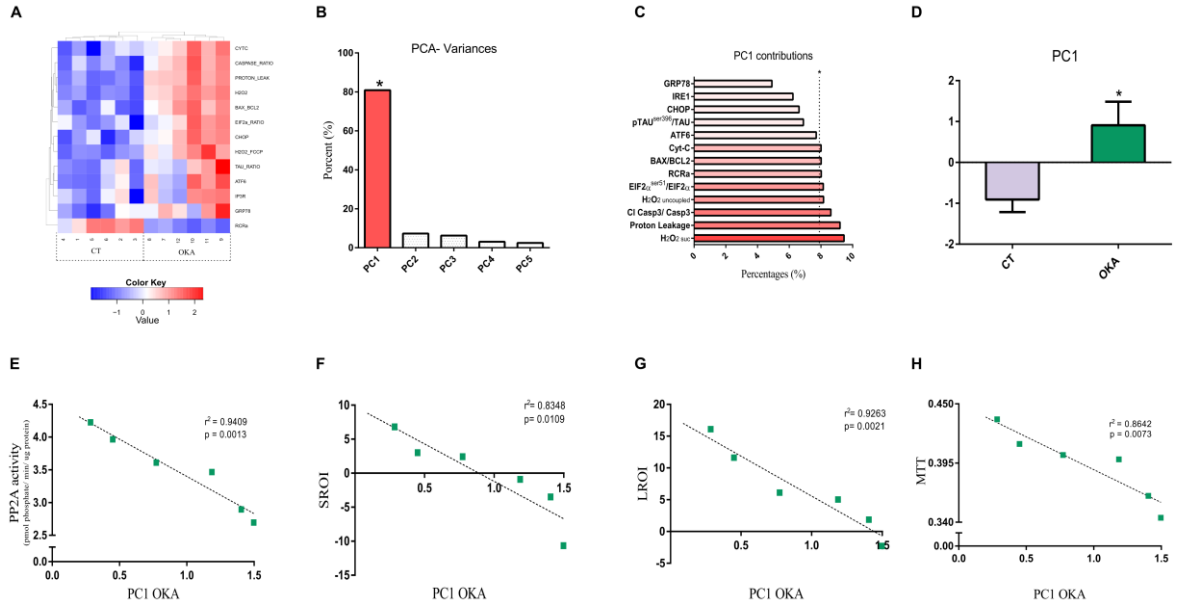
A
B
PCA- Variances
Percent (%)
PC1
PC2
PC3
PC4
PC5
C
PC1 contributions
GRP78
IRE1
CHOP
pTAU ser396/TAU
ATF6
Cyt-C
BAX/BCL2
RCRa
EIF2α ser51/EIF2α
H2O2 uncoupled
CI Casp3/ Casp3
Proton Leakage
H2O2 suc
Percentages (%)
D
PC1
CT
OKA
Color Key
Value
CT
OKA

E
PP2A activity
(pmol phosphate/ min/ ug protein)
r2 = 0.9409
p = 0.0013
PC1 OKA
F
r2= 0.8348
p= 0.0109
SROI
PC1 OKA
G
r2= 0.9263
p= 0.0021
LROI
PC1 OKA
H
r2 = 0.8642
p = 0.0073
MTT
PC1 OKA

Supplementary Figure 1

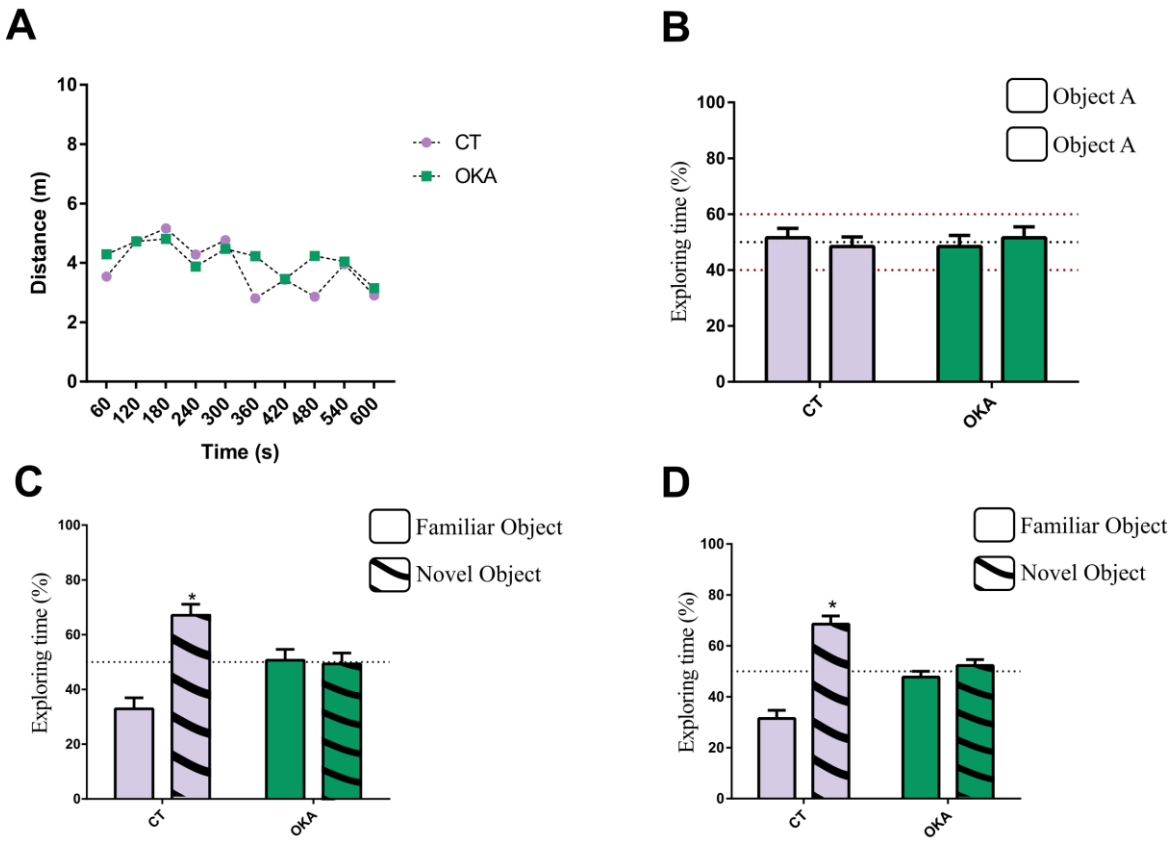

Supplementary Figure 2

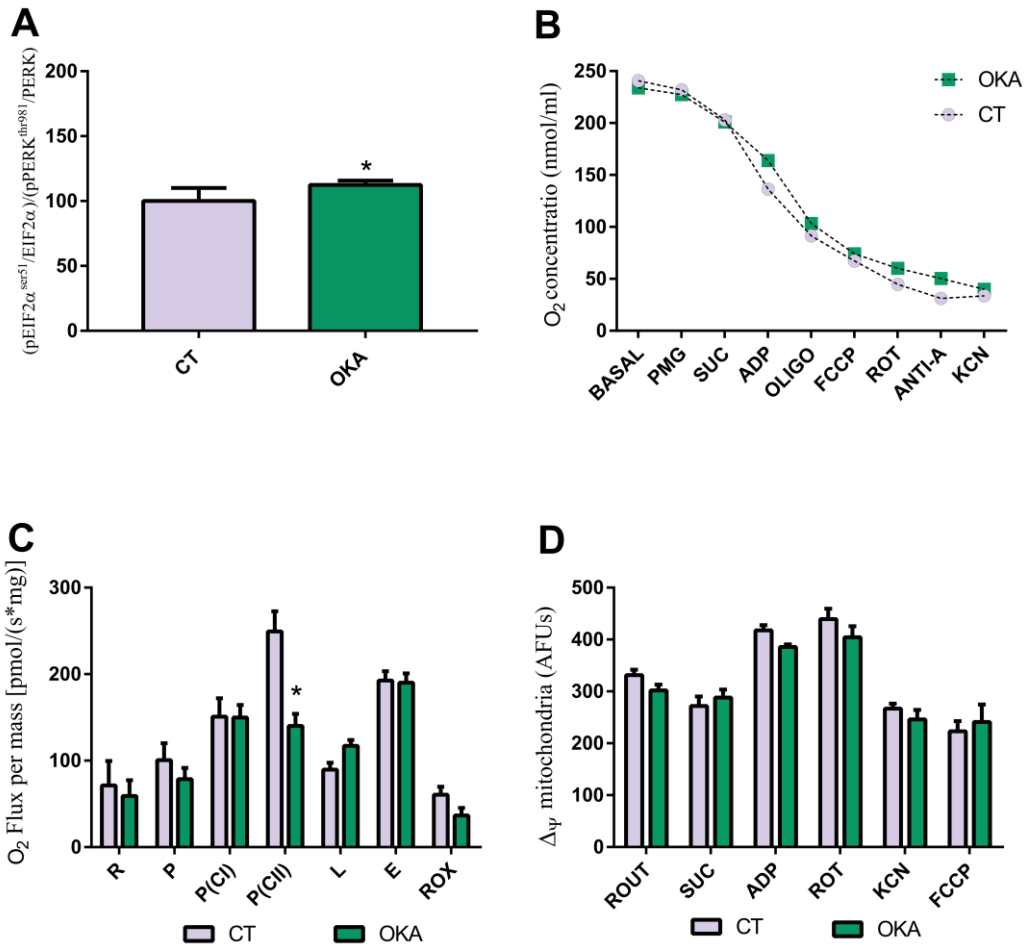

Supplementary Figure 3

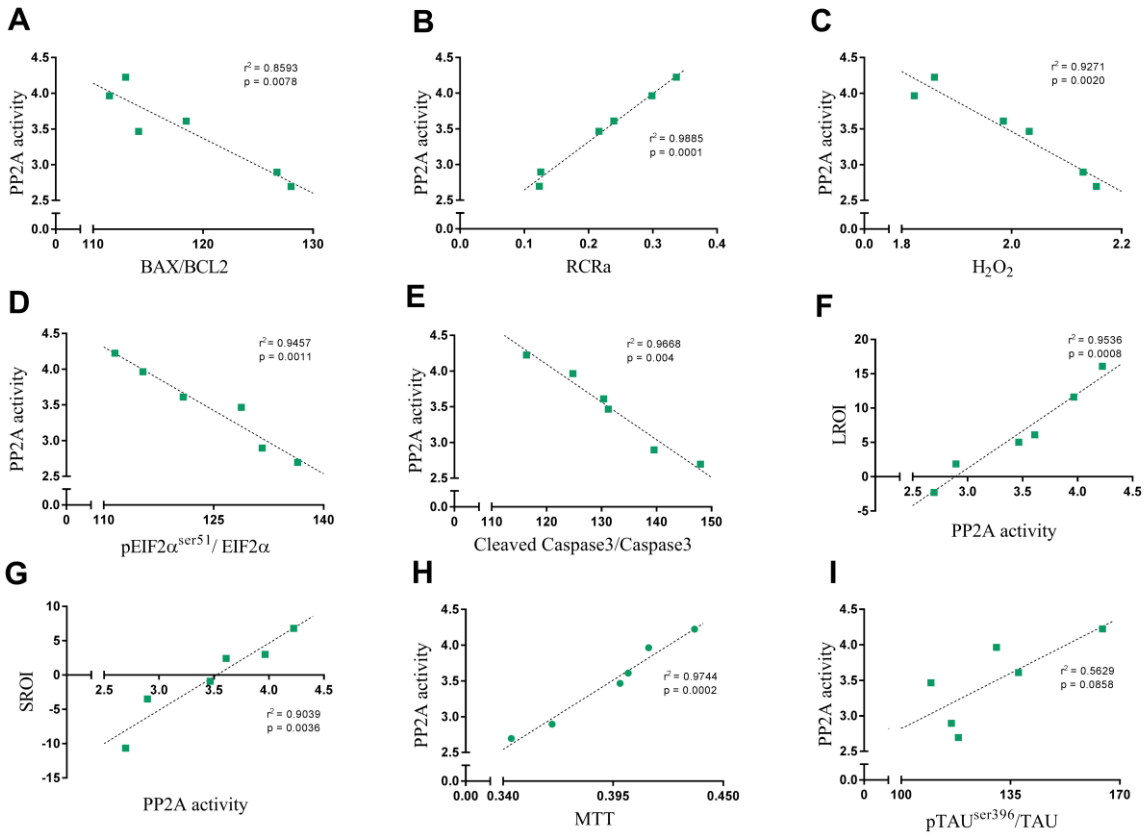

CAPÍTULO II – *Memantine mediates astrocytic activity in response to excitotoxicity induced by PP2A inhibition*

No capítulo II, apresentamos o artigo publicado no periódico *Neuroscience Letters*.

Neste artigo, queríamos explorar o envolvimento do sistema astrocitário em mecanismos de neuroproteção frente à inibição da PP2A, alteração comum em doenças neurodegenerativas. Para isso, utilizamos um modelo já conhecido por nosso grupo (ver Capítulo I e Anexo I-A), induzindo essa inibição com infusão intrahipocampal de OKA. Antes dessa infusão, os animais passaram por um pré-tratamento com MN, droga antagonista do receptor NMDA liberada pelo FDA no tratamento da DA em estágios moderado a grave. OKA levou a um aumento de reatividade astrocitária, demonstrada pelo aumento de GFAP, independentemente do pré-tratamento. O uso de MN induziu aumento na secreção de S100B e redução da captação hipocampal de glutamato somente frente à toxicidade induzida pelo OKA. Esses resultados reforçam a importância da interação neurônio-astrócito nos mecanismos de neuroproteção frente à redução da atividade de PP2A e corroboram a necessidade de novos estudos visando os astrócitos como possíveis alvos no tratamento de doenças neurodegenerativas que tenham como característica a redução dessa fosfatase.

Accepted Manuscript

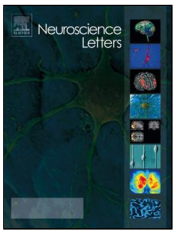

Title: Memantine mediates astrocytic activity in response to excitotoxicity induced by PP2A inhibition

Authors: Vitor Rocco Torrez, Eduardo R. Zimmer, Eduardo Kalinine, Clarissa Branco Haas, Kamila Cagliari Zenki, Alexandre Pastoris Muller, Diogo Onofre de Souza, Luis Valmor Portela

PII: S0304-3940(18)30885-1
DOI: https://doi.org/10.1016/j.neulet.2018.12.034
Reference: NSL 34011

To appear in: *Neuroscience Letters*

Received date: 13 September 2018
Revised date: 13 December 2018
Accepted date: 22 December 2018

Please cite this article as: Torrez VR, Zimmer ER, Kalinine E, Branco Haas C, Cagliari Zenki K, Pastoris Muller A, de Souza DO, Portela LV, Memantine mediates astrocytic activity in response to excitotoxicity induced by PP2A inhibition, *Neuroscience Letters* (2018), https://doi.org/10.1016/j.neulet.2018.12.034

Memantine mediates astrocytic activity in response to excitotoxicity induced by PP2A inhibition

Vitor Rocco Torrez[a#], Eduardo R. Zimmer[a,b,c#], Eduardo Kalinine[a,d], Clarissa Branco Haas[a], Kamila Cagliari Zenki[a], Alexandre Pastoris Muller[a,e], Diogo Onofre de Souza[a] and Luis Valmor Portela[a*].

[a] Department of Biochemistry, Posgraduate Program in Biological Sciences: Biochemistry, Federal University of Rio Grande do Sul (UFRGS), Porto Alegre, RS, Brazil;

[b] Department of Pharmacology, Posgraduate Program in Biological Sciences: Pharmacology and Therapeutics, Federal University of Rio Grande do Sul (UFRGS), Porto Alegre, RS, Brazil;

[c] Brain Institute of Rio Grande do Sul, Pontifícal Catholic University of Rio Grande do Sul (PUCRS), Porto Alegre, RS, Brazil;

[d] Department of Physical Education, Laboratory of Performance, Sport, Health and Paraympic Sports, Federal University of Sergipe (UFS); Sergipe, SE, Brazil

[e] Laboratory of Exercise, Biochemistry and Physiology, University of Southern Santa Catarina (UNESC), Criciuma, SC, Brazil

[#]Both authors contributed equally to this work

ACCEPTEDEmailaddresses:vitortorrez@gmail.com, eduardo.zimmer@ufrgs.br,

eduardokalinine@hotmail.com, clarissabhaas@gmail.com, kamizenki@yahoo.com.br,

alexandrep.muller@gmail.com, diogo@ufrgs.br, roskaportela@gmail.com.

*** Corresponding author:**

Luis Valmor Portela, Ph. .

Department of Biochemistry, ICBS, UFRGS

2600 Ramiro Barcelos street, 90035-003, Porto Alegre, RS, Brazil

E-mail address: roskaportela@gmail.com

Telephone: 55 51 33085558

Fax: 55 51 33085544

Highlights

- Memantine and okadaic acid (OKA) evoke astrocytic activation
- Memantine and OKA mediates astrocytic S100B secretion and Glutamate uptake
- Neuron-astrocyte interplay is necessary for this response

Abstract

Reduced activity of protein phosphatase 2A (PP2A) is a common feature in Alzheimer's disease (AD) and non-AD tauopathies. The administration of okadaic acid (OKA), a potent PP2A and PP1 inhibitor, is a common research tool for inducing AD-like alterations such as tau hyperphosphorylation and cognitive decline. ecently, we showed that OKA increases cerebrospinal fluid (CSF) glutamate levels, which was strongly correlated with cognitive decline. Also, we demonstrated that memantine (MN), a glutamatergic NMDAR channel blocker, was capable of preventing the increase in CSF glutamate levels and cognitive decline. Here, we aimed to analyze whether the protective effects of MN involve intrinsic astrocytic properties, particularly related to glutamate uptake and astrocytic reactivity – indexed by the expression of S100B and glial fibrillary acidic protein (GFAP). Rats received intraperitoneal injections of MN or saline over 3 consecutive days before receiving intrahippocampal infusion of OKA or saline. Afterward, they were submitted to behavioral tasks and then, euthanatized for neurochemical analysis. Here, we showed that the neuroprotective effects of MN in response to OKA neurotoxicity involve astrocytic activation. MN decreased glutamate uptake in the hippocampus and increased the release of S100B protein in the CSF in response to OKA neurotoxicity, which indicates a possible neurons-astrocyte coupling protective mechanism. These findings shed light on astrocytes as potential targets for treating neurological disorders associated with decreased PP2A activity.

Keywords: astrocytes, glutamate, memantine, tauopathies, neuroprotection.

Abbreviations: AD - Alzheimer's Disease; PP2A - protein phosphatase 2A; CSF - cerebrospinal fluid; OKA - okadaic acid; MN - memantine; GFAP - glial fibrillary acidic protein;

Declarations of interest: none

Author's contribution:

Vitor Rocco Torrez: study design, animal surgery, and data analysis;

Eduardo Kalinine: animal surgery, intrahipocampal infusions, and data analysis.

Clarissa Branco Haas: glutamate uptake assay in brain slices, immunostaining;

Kamila Cagliari Zenki: glutamate uptake assay in brain slices and immunostaining;

Eduardo Rigon Zimmer: statistical analysis, figures layout, and manuscript writing;

Alexandre Pastoris Muller: cerebrospinal fluid sampling, statistical analysis and immunostaing;

Diogo Onofre de Souza: manuscript writing, results discussions and financial support;

Luis Valmor Portela: study design, data analysis, and manuscript writing.

Introduction

Reduced activity of cerebral protein phosphatase 2A (PP2A) is a common feature in Alzheimer's disease (AD) and non-AD tauopathies [1-4]. In fact, PP2A compromised activity contributes to abnormal phosphorylation of tau protein, which then causes microtubule destabilization, neuronal death and cognitive impairment [5] . In this context, okadaic acid (OKA), an inhibitor of PP2A, has been used to mimic human tauopathy in rodent models (for review, see [6]).

In a recent study, we mimic PP2A reduced activity by injecting OKA, an inhibitor of PP2A activity, in the hippocampus of Wistar rats [7]. We showed that PP2A inhibition increases cerebrospinal fluid (CSF) glutamate levels, being this alteration correlated to cognitive decline. In addition, we demonstrated that memantine (MN), a glutamate N-methyl-D-aspartate receptor (NMDAR) channel blocker, was capable of

decreasing extracellular glutamate levels and preventing cognitive decline [7]. However, whether glutamate uptake by astrocytes is compromised by OKA, which potentially might explain the increased glutamate levels and the benefits of MN, remains unclear. Recently, Costa et al. [8] demonstrates that PP2A inhibition decreases hippocampal glutamine synthetase activity and glial excitatory amino acid transporter 2 (EAAT2) also known as GLT-1 but did not alter glutamate uptake. Interestingly, we have shown that OKA infusion increases glutamate levels in the CSF [7]. These findings highlight the influence of tripartite glutamatergic synapse dysfunction in the OKA-induced neurotoxicity [9].

Conceptually, persistently elevated glutamate levels in the synaptic cleft can cause hyperactivation of glutamatergic receptors and cell death, a pathophysiological process collectively referred to as excitotoxicity [10]. In physiological conditions, astrocytes are responsible for the first line of defense by releasing trophic substances like S100B protein, and predominantly, removing excess of glutamate from the synaptic cleft, in this manner maintaining the excitatory stimulation on glutamate receptors tightly controlled [11]. By contrast, reactive astrocytes release neuroinflammatory or trophic factors, which contributes to exacerbating neuronal death [12-14]. Considering this perspective, the S100B protein, which within the brain is secreted predominantly by astrocytes, exert both reparative and neurodegenerative effects, and it is tightly associated with changes in astrocytes morphology [15, 16]. Beyond this morphological change, astrocyte reactivity is characterized by the up-regulation of a broad-spectrum of neuroactive molecules that may determine life and death of adjacent neural cells. In clinical and experimental studies the assessment of S100B and glial fibrillary acidic protein (GFAP) in biological fluids are considered biomarkers of astrocyte reactivity [17, 18].

With this in mind, we aimed to investigate whether pretreatment with MN administration prevents OKA-induced neurotoxicity in specific components of the astrocytic machinery like the expression levels of S100B and GFAP and glutamate uptake activity.

Material and Methods

2.1 - Animals

Male Wistar rats (400-500 g), 4-5 months old, were obtained from the State Foundation for Health Science Research (FEPPS, Porto Alegre/RS, Brazil). Animals were placed into a controlled temperature room (22 °C) under a 12 h light/12 h dark cycle (lights on at 7 am) and had free access to food and water. Animals (n=24) were divided equally into four groups: control (CN), memantine (MN), okadaic acid (OKA) and memantine/okadaic acid (MN+OKA). To avoid social isolation, we kept 4 animals per cage [19]. All experiments were in agreement with the Committee on the Care and Use of Experimental Animal Resources, UFRGS, Brazil. Behavioral phenotype of these animals has been published previously (for additional information, please see [7]).

2.2 - Drugs

Memantine (Ref. M-9292, Sigma, USA) was dissolved in saline (NaCl, 0.9 %) at a concentration of 20 mg/ml; and okadaic acid (Ref. O8010, Sigma, USA) was dissolved in artificial CSF (aCSF) at concentration of 50 ng/µL.

2.3 – Treatment and surgical procedure

Animals received a daily intraperitoneal (i.p.) injection of MN (20 mg/kg) or saline (NaCl, 0.9%) over 3 consecutive days. On the third day of MN injections, animals were anesthetized by an i.p. injection of ketamine (Cetamin, Schering-Plough

Coopers, Brazil, 100 mg/kg body weight) and xylazine (Coopazine, Syntec, Brazil, 10 mg/kg body weight). An intrahippocampal (i.h.) infusion of 2uL okadaic acid (100 ng) or vehicle (saline 0,9%) was made into the right hemisphere in the CA1 region at the following coordinate location, with reference to bregma: A -3.6, L 2.0, and V 2.4 [20,21]. Eight days after surgery the animals (n= 6 per group) were anesthetized and the CSF was collected (40 to 80 µL) by direct puncture of the cisterna magna with an insulin syringe (27 gauge x 1/2-inch length) and stored at - 80 °C. Samples with blood contamination were discarded [22]. Immediately after, they were sacrificed and the hippocampus were dissected for neurochemical assessment. The ipsilateral hemispheres were used for glutamate uptake analysis (n = 6). Additional animals were used for verifying astrocyte reactivity through GFAP immunohistochemitry (n = 3) (see figure 1 for experimental design). The doses of MN and OKA, and the time regimen were chosen based on our previously published work [7].

[Insert Figure 1]

2.4 - Immunohistochemistry

The GFAP staining was performed as previously described [23]. Animals (n = 3 per group) were killed and the hippocampus were post-fixed in 4 % paraformaldehyde in 0.1 M phosphate buffer pH 7.4, then cryoprotected in a 30 % sucrose solution in PB at 4 °C. Coronal sections (50 µm) were obtained using a Vibratome (Leica, Germany). One-in-8 random series were collected for immunohistochemistry. They were then incubated with rabbit polyclonal GFAP (Dako, UK, 1:500) in PBS-Tx containing 2% BSA, for 48 h at 4 °C. After being washed several times with PBS, they were incubated with a 488 alexa-conjugated donkey anti-rabbit antibody for 2 h at room temperature.

Sections were analyzed and photographed with a confocal microscope (Olympus, Japan), to determine fluorescence insensitivity by Image J software.

2.5 - Measurement of CSF S100B levels

The concentration of S100B protein was measure by a commercially available S100 enzyme-linked immunoabsorbent assay (ELISA) kit (Diasorin, Saluggia, Italy). The assay is highly sensitive in detecting protein in biological fluids. After sequential incubations of samples and secondary antibody labeled with peroxidase in a microplate covered with anti-S100B antibody the reaction system produced a colored product read in a spectrophotometer (Molecular devices, USA). S100B level was expressed as ng/ml and the variation coefficient of duplicates in all range levels of standards and samples were within 5% [17].

2.6 - Glutamate Uptake assay in hippocampus

Animals (n=6, per group) were sacrificed and brain regions dissected. Thus, hippocampus was utilized to glutamate uptake assay. Glutamate uptake was performed according to Thomazi and colleagues [24]. Hippocampal slices (0.4 mm) were obtained through a McIlwain chopper and pre-incubated for 15 min at 37ºC in a Hank's balanced salt solution (HBSS) containing (mM): 137 mM NaCl; 0.63 mM Na_2HPO_4; 4.17 mM $NaHCO_3$; 5.36 mM KCl; 0.44 mM KH_2PO_4; 1.26 mM $CaCl_2$; 0.41 mM $MgSO_4$; 0.49 mM $MgCl_2$ and 1.11 mM glucose, in pH 7.2. Then, 0.66 and 0.33 Ci ml^{-1} L-[^{3}H]glutamate in a 100 M final concentration glutamate was added. Incubation was stopped after 5 minutes with two ice-cold washes of 1 ml HBSS, immediately followed by the addition of 0.5 N NaOH, which was then kept overnight. Unspecific uptake was measured using the same protocol described above, with differences in the temperature

(4 °C) and medium composition (N-methyl-D-glucamine instead of sodium chloride). Na^+-dependent uptake was considered as the difference between the total uptake and the unspecific uptake. Both uptakes were performed in triplicate. Incorporated radioactivity was measured using a liquid scintillation counter.

2.7 - Statistical Analysis

Results are presented as the means ± sem. Differences between groups were analyzed by analysis of variance (ANOVA) followed by Bonferroni's. Correlation between glutamate uptake and S100B levels was analyzed by Pearson's correlation. Differences between groups were considered statistically significant at $p<0.05$.

Results

3.1 - Okadaic acid increases GFAP fluorescence in the hippocampus

The One-way ANOVA revealed a significant group effect (figure 2, $F_{[3,8]} = 51.52$, $p = 0.0001$). Bonferroni's *post-hoc* demonstrated that OKA increased GFAP fluorescence in comparison to CN ($p = 0.0001$) and MN ($p = 0.0003$) groups. Additionally, MN+OKA group has increased GFAP fluorescence as well in comparison to CN ($p = 0.0001$) and MN ($p = 0.0002$) groups. However, MN group does not differ from CN group ($p = 0.3107$).

[Insert Figure 2]

3.2 – Memantine administration prior to okadaic acid increases CSF S100B levels

A significant group effect was revealed by One-way ANOVA (figure 3A, $F_{[3,20]} = 12.36$, $p = 0.0001$). Bonferroni's *post-hoc* demonstrated that MN and OKA groups did

not differ from CN group (p = 0.99 for both comparisons). However, MN+OKA group has increased CSF levels of S100B in comparison to CN, MN and OKA groups (p = 0.0012, p = 0.0001 and p = 0.001).

3.3 - Memantine administration prior to okadaic acid decreases glutamate uptake in hippocampal slices

Statistical analysis trough One-way ANOVA revealed a significant group effect (figure 3B, $F_{[3,20]} = 21.69$, p = 0.0001). Bonferroni's *post-hoc* indicated that MN and OKA groups did not differ from each other (p = 0.1425) and from CN group (p = 0.99 and p = 0.2345, respectively). By contrast, the MN+OKA group has decreased hippocampal glutamate uptake when compared to MN, OKA and CN groups (p = 0.0001, p = 0.0001 and p = 0.0009, respectively).

3.4 - Hippocampal glutamate uptake is inversely correlated with S100B CSF levels

Pearson's linear correlation revealed a significant negative correlation between hippocampal glutamate uptake and S100B CSF levels (figure 3C. Pearson's R = -0. 5502, $R^2 = 0.3028$, p = 0.0053).

Discussion

The present study revealed that the blockage of NMDAr, by memantine, remodels astrocytic activity in response to excitotoxicity induced by PP2A inhibition. In a previous report, we demonstrated that MN pretreatment prevents OKA-induced cognitive impairment [7]. Here, using the same protocol, OKA increased levels of GFAP. In addition, when OKA-induced neurotoxicity was preceded by 3 days of MN administration (MN+OKA group), the reactive gliosis, indexed by GFAP levels,

remained elevated as observed in the OKA group. Also, MN *per se* did not alter GFAP expression but when employed before OKA infusion it increased S100B protein levels in CSF and in parallel reduced glutamate uptake. In addition, we found a negative correlation between S100B and glutamate uptake, which suggests that these variables are somehow linked. Correlations among GFAP levels and other variables studied here (glutamate uptake and S100B) have not been statistically tested because of the reduced sample used for GFAP immunostaining. Further studies with increased sample, focusing on these aspects, should be conducted to better elucidate these aspects.

As stated before, the astrocytic cytoskeletal protein GFAP is a classic marker of astrocyte reactivity [15] and its upregulation is remarkably present in the AD brains [25,26]. Physiologically, PP2A is the main responsible for tau dephosphorylation but it is also important to note that this phosphatase has a relevant role in other essential cellular mechanisms such as apoptosis [27]. Its inhibition and a subsequent aggregation of tau hyperphosphorilated filaments may pave the way for astrocyte reactivity [7]. Here, our findings suggest that OKA was able to recapitulate a microenvironmental scenario of astrocyte reactivity commonly seen in AD and tauopathies [28]. Interestingly, MN is a FDA approved drug for the treatment of AD whose mechanisms implies in decreased glutamatergic excitotoxicity via NMDAR blockade. However, MN effects on astrocytic machinery remain elusive. It is important to emphasize that astrocyte reactivity could represent both protective or detrimental processes [29,30].

[Insert Figure 3]

Indeed, S100B protein released by astrocytes exerts both beneficial and detrimental effects to neurons [31]. Interestingly, we found that CSF levels of S100B

protein were increased only in the MN+OKA group. Based on the preventing role of MN against OKA-induced glutamate excitotoxicity and cognitive impairment [7], one could argue that S100B is playing a neuroprotective role in this scenario. In agreement with this, it is known that S100B acts as a neurotrophic repairing factor [16] and also protects hippocampal neurons from glutamate excitotoxicity [32, 33].

Remarkably, we have showed that MN prevented OKA-induced increase in the CSF glutamate levels [7]. However, by using hippocampal slices we found reduced glutamate uptake in the MN+OKA group, and a significant inverse correlation with S100B levels. Indeed, Tramontina and colleagues have previously showed an association between these variables. Their previous works using hippocampal astrocyte culture and C6 glioma cells showed that S100B stimulates glutamate uptake, which suggests that in the absence of neurons, S100B presents an opposite effect as we reported here [34, 35]. Also, it is important to emphasize that S100B levels was only altered in the combination of OKA and neuronal NMDAR antagonism by MN, which suggests that this phenomenon is dependent of neuron-to-astrocyte communication. Interestingly, Sakatani and colleagues already propose that neuronal activity is capable of modulating the release of S100B [36]. Alternatively, it has been showed that memantine depresses glutamate release by neurons [37], thus the reduced glutamate uptake associated with increased release of S100B by astrocytes could be interpreted as an adaptive response to reduced glutamate release by neurons. Moreover, Costa et al. [8] showed that OKA do not alter hippocampal glutamate uptake, which was replicated by the present work. Piecing together, one could claim that MN preventing OKA neurotoxicity involves astrocytic remodeling. For further elucidating this assumption, additional studies are needed.

Conclusion

In conclusion, increased astrocyte reactivity, S100B release and decreased hippocampal glutamate uptake are involved in MN neuropreventive effects against OKA-induced toxicity. These results reinforce the role of astrocytes as potential targets for treating PP2A related tauopathies.

Competing interest

The authors report no financial or personal conflicts of interest.

Author declaration

All authors have read and approved the final version of this manuscript. This work is original, was not published and is not under consideration for publication elsewhere.

Funding

This work was supported by the Brazilian grants of CNPq #426796/2016-0 and 141100/2013-3, CNPq-Instituto Nacional de Neurociência Translacional-INNT #465346/2014-6 and also by the FAPERGS/PRONEX #16/2551-0000499-4

References

1. Gong, C.X., et al., *Phosphatase activity toward abnormally phosphorylated tau: decrease in Alzheimer disease brain*. J Neurochem, 1995. **65**(2): p. 732-8.
2. Gong, C.X., et al., *Phosphoprotein phosphatase activities in Alzheimer disease brain*. J Neurochem, 1993. **61**(3): p. 921-7.
3. Arif, M., et al., *Tau pathology involves protein phosphatase 2A in parkinsonism-dementia of Guam*. Proc Natl Acad Sci U S A, 2014. **111**(3): p. 1144-9.
4. Vogelsberg-Ragaglia, V., et al., *PP2A mRNA expression is quantitatively decreased in Alzheimer's disease hippocampus*. Exp Neurol, 2001. **168**(2): p. 402-12.

5. Zimmer, E.R., et al., *In vivo tracking of tau pathology using positron emission tomography (PET) molecular imaging in small animals.* Transl Neurodegener, 2014. **3**(1): p. 6.
6. Kamat PK, Rai S, Nath C. *Okadaic acid induced neurotoxicity: an emerging tool to study Alzheimer's disease pathology*. Neurotoxicology. 2013; **37**:163-72
7. Zimmer, E.R., et al., *Pretreatment with memantine prevents Alzheimer-like alterations induced by intrahippocampal okadaic acid administration in rats.* Curr Alzheimer Res, 2012. **9**(10): p. 1182-90.
8. Costa, A.C., et al., *Neuroglial alterations in rats submitted to the okadaic acid-induced model of dementia.* Behav Brain Res, 2012. **226**(2): p. 420-7
9. Zimmer, E.R., et al., *Inhibition of protein phosphatase 2A: focus on the glutamatergic system.* Mol Neurobiol, 2016. 53(6): p. 3753-3755.
10. Meldrum, B.S., *Glutamate as a neurotransmitter in the brain: review of physiology and pathology.* J Nutr, 2000. **130**(4S Suppl): p. 1007S-15S.
11. Anderson, C.M. and R.A. Swanson, *Astrocyte glutamate transport: review of properties, regulation, and physiological functions.* Glia, 2000. **32**(1): p. 1-14.
12. Fernandez, A.M., et al., *Regulation of the phosphatase calcineurin by insulin-like growth factor I unveils a key role of astrocytes in Alzheimer's pathology.* Mol Psychiatry, 2012. **17**(7): p. 705-18.
13. Vangeison, G. and D.A. Rempe, *The Janus-faced effects of hypoxia on astrocyte function.* Neuroscientist, 2009. **15**(6): p. 579-88.
14. Mayhew, J., P.M. Beart, and F.R. Walker, *Astrocyte and microglial control of glutamatergic signaling: a primer on understanding the disruptive role of chronic stress.* J Neuroendocrinol, 2015.
15. Verkhratsky, A., et al., *Astrocytes in Alzheimer's disease.* Neurotherapeutics, 2010. **7**(4): p. 399-412.
16. Van Eldik, L.J. and M.S. Wainwright, *The Janus face of glial-derived S100B: beneficial and detrimental functions in the brain.* Restor Neurol Neurosci, 2003. **21**(3-4): p. 97-108.
17. Böhmer, A.E., et al., *Neuron-specific enolase, S100B, and glial fibrillary acidic protein levels as outcome predictors in patients with severe traumatic brain injury.* Neurosurgery, 2011. **68**(6): p. 1624-30.
18. Chaves, M.L., et al., *Serum levels of S100B and NSE proteins in Alzheimer's disease patients.* J Neuroinfammation, 2010. **7**: p. 6
19. Leasure, J.L. and L. Decker, *Social isolation prevents exercise-induced proliferation of hippocampal progenitor cells in female rats.* Hippocampus, 2009. **19**(10): p. 907-12.
20. Paxinos, G. and C. Watson, *The rat brain in stereotaxic coordinates*. 2nd ed. 1986, Sydney ; Orlando: Academic Press. xxvi, 237 p. of plates.
21. Arias, C., et al., *The protein phosphatase inhibitor okadaic acid induces heat shock protein expression and neurodegeneration in rat hippocampus in vivo.* Exp Neurol, 1998. **153**(2): p. 242-54.
22. Cruz Portela, L.V., *Guanine and adenine nucleotidase activities in rat cerebrospinal fluid.* Brain Res, 2002. **950**(1-2): p. 74-8
23. Moreira, J.D., et al., *Short-term alterations in hippocampal glutamate transport system caused by one-single neonatal seizure episode: implications on behavioral performance in adulthood.* Neurochem Int, 2011. **59**(2): p. 217-23.
24. Thomazi, A.P., et al., *Ontogenetic profile of glutamate uptake in brain structures slices from rats: sensitivity to guanosine.* Mech Ageing Dev, 2004. **125**(7): p. 475-81.

25. Kato, S., et al., *Confocal observation of senile plaques in Alzheimer's disease: senile plaque morphology and relationship between senile plaques and astrocytes*. Pathol Int, 1998. **48**(5): p. 332-40.
26. Ross, G.W., et al., *Quantification of regional glial fibrillary acidic protein levels in Alzheimer's disease*. Acta Neurol Scand, 2003. **107**(5): p. 318-23.
27. Kamat PK, Tota S, Shukla R, Ali S, Najmi AK, Nath C. Mitochondrial dysfunction: a crucial event in okadaic acid (ICV) induced memory impairment and apoptotic cell death in rat brain. Pharmacol Biochem Behav. 2011; **100**(2):311-9
28. Higuchi, M., et al., *Transgenic mouse model of tauopathies with glial pathology and nervous system degeneration*. Neuron, 2002. **35**(3): p. 433-46.
29. Middeldorp, J. and E.M. Hol, *GFAP in health and disease*. Prog Neurobiol, 2011. **93**(3): p. 421-43.
30. Abraham, C.R., *Reactive astrocytes and alpha1-antichymotrypsin in Alzheimer's disease*. Neurobiol Aging, 2001. **22**(6): p. 931-6.
31. Van Eldik, L.J. and Wainwright, M.S., *The Janus face of glial-derived S100B: beneficial and detrimental functions in the brain*. Restor Neurol Neurosci, 2003; **21**(3-4):97-108.
32. Ahlemeyer, B., et al., *S-100beta protects cultured neurons against glutamate- and staurosporine-induced damage and is involved in the antiapoptotic action of the 5 HT(1A)-receptor agonist, Bay x 3702*. Brain Res, 2000. **858**(1): p. 121-8.
33. Kogel, D., et al., *S100B potently activates p65/c-Rel transcriptional complexes in hippocampal neurons: Clinical implications for the role of S100B in excitotoxic brain injury*. Neuroscience, 2004. **127**(4): p. 913-20.
34. Tramontina, F., et al., *High glutamate decreases S100B secretion by a mechanism dependent on the glutamate transporter*. Neurochem Res, 2006. **31**(6): p. 815-20.
35. Tramontina F., et al., *Glutamate uptake is stimulated by extracellular S100B in hippocampal astrocytes*. Cell Moll Neurobiol, 2006; **26**(1): 81-6
36. Sakatani, S., et al., *Neural-activity-dependent release of S100B from astrocytes enhances kainate-induced gamma oscillations in vivo*. J Neurosci, 2008. **28**(43): p. 10928-36.
37. Lu, C.W., T.Y. Lin, and S.J. Wang, *Memantine depresses glutamate release through inhibition of voltage-dependent Ca2+ entry and protein kinase C in rat cerebral cortex nerve terminals: an NMDA receptor-independent mechanism*. Neurochem Int, 2010. **57**(2): p. 168-76.

Figure captions

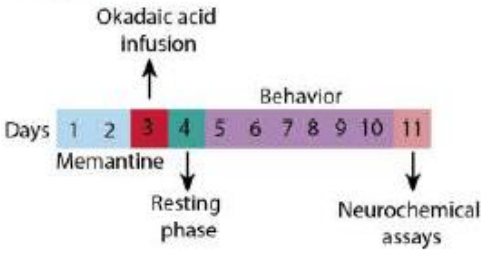

Figure 1. Timeline.

Schematic diagram of the experiments. Rats received an intrahipocampal (i.h.) injection of OKA or saline after three consecutive days of intraperitoneal (i.p.) saline or memantine (MN) injections.

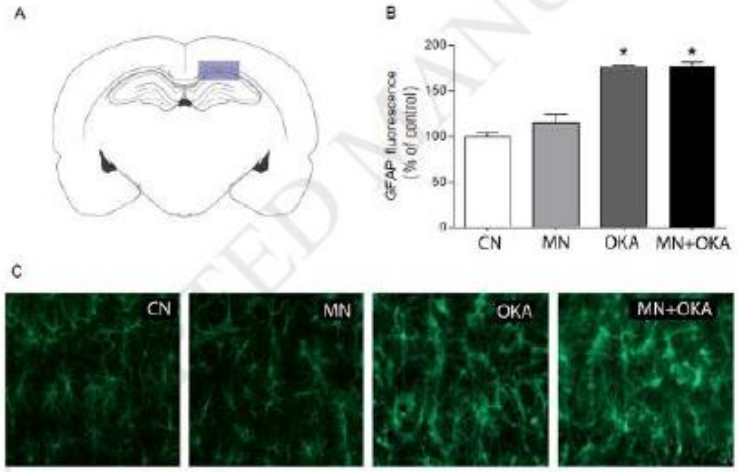

Figure 2. OKA increased GFAP fluorescence in hippocampus.

(A) Illustrative graphic of intrahippocampal infusion location (CA1 region) (B) Hippocampal slices of rats, which received intrahipocampal (i.h.) OKA infusion presented a significantly higher fluorescence of GFAP in hippocampal slices compared to control groups. This effect was not altered with intraperitoneal (i.p.) MN pretreatment

(C) Both OKA and MN+OKA groups increased GFAP fluorescence in comparison to CN or MN groups. OKA group do not differ from MN+OKA.

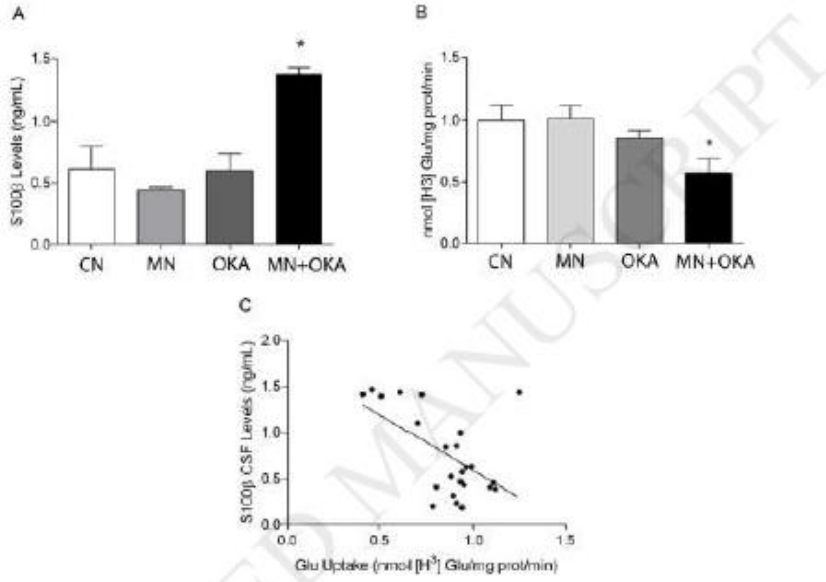

Figure 3. Correlation analysis between S100B and glutamate uptake.

(A) OKA increased CSF S100B levels only in rats pretreated with MN. There was no significant variation in the S100B levels among CN, MN and OKA groups. (B) MN+OKA group presented diminished hippocampal Glu-uptake in comparison to other groups. (C) CSF S100B level was inversely correlated with hippocampal glutamate uptake.

PARTE III

Discussão

Nessa tese, investigamos o envolvimento de diversos mecanismos na evolução da morte celular relacionada com a redução da atividade de PP2A, um marco comum entre a maioria das doenças neurodegenerativas. Nessa investigação, demos ênfase à disfunção da comunicação RE-mitocôndria nessas doenças e à importância da atividade astrocitária na neuroproteção frente a esses estímulos.

Diversos estudos demonstram um envolvimento crucial da redução da atividade da PP2A em diversos mecanismos que implicam no avanço de doenças neurodegenerativas (Nematullah et al, 2017). Com isso, o avanço na compreensão dessas relações parece essencial para aproximar-se do desenvolvimento de novos alvos terapêuticos para essas doenças. Nessa tese, buscamos investigar a associação da redução da atividade dessa fosfatase com outros achados comuns a essas patologias.

Devido a evidências de que o acúmulo de proteínas com alterações físico-químicas poderia estar relacionado com a atividade reduzida da PP2A (Magnaudeix et al, 2013) e à importante função do RE no controle da síntese e correção proteica, procuramos estudar as consequências dessa interação na patogênese e evolução de processos neurodegenerativos. De fato, diversas doenças neurodegenerativas, incluindo a Doença de Parkinson e a DA, têm envolvido em seu desenvolvimento o acúmulo de agregados proteicos associado a início de estresse do RE e ativação da UPR a fim de tentar reestabelecer a proteostase (Hoozemans et al, 2012).

Para isso, optamos por utilizar o modelo químico de inibição da PP2A pela infusão de OKA. O OKA é um conhecido inibidor de Ser/Tre fosfatases, com especificidade relativa para PP2A (Gong et al, 2000), já bastante estudado e consolidado como modelo animal de doenças neurodegenerativas (Kamat et al, 2014). A estratégia de utilizar um modelo químico parece ser a melhor forma de estudar as doenças

neurodegenerativas devido à grande diversidade de alterações genéticas possíveis de serem encontradas nessas patologias, restringindo assim a aplicabilidade do uso de modelos animais transgênicos para avaliar alterações comuns a esses distúrbios.

Inicialmente, encontramos alterações no processamento de memória de reconhecimento nos animais tratados com OKA. Essas alterações cognitivas vão de acordo com o encontrado em estudos prévios de nosso grupo (Zimmer et al, 2012) e corroboram a importância da redução da atividade da PP2A no desenvolvimento de distúrbios cognitivos.

Associadas a essas alterações, o OKA também levou a aumento da fosforilação do eIF2α no sítio da serina 51 e dos níveis de ATF6 e IRE1α, conhecidos marcadores de estresse do RE associado a UPR. A associação da inibição de PP2A com distúrbios na função do RE já havia sido mostrada previamente (Kim et al, 2010), entretanto, os mecanismos envolvidos nesses eventos ainda não foram bem elucidados. Reforçando a hipótese de que o OKA teria iniciado o estresse do RE, encontramos também em nosso estudo o aumento de CHOP, um fator de transcrição posterior na cascata da UPR, que leva a um aumento da síntese de proteínas pró-apoptóticas e estresse oxidativo (Marciniak et al, 2004). Em sentido oposto a essa upregulation de CHOP, observamos um aumento da GRP78, proteína essencial para o controle de qualidade proteico do RE e que coordena a UPR na tentativa de favorecer as sinalizações de sobrevivência celular (Wang et al, 2009). Esses resultados sugerem um papel regulatório da PP2A sobre fatores chave na homeostasia da UPR.

Em 2017, Plácido e seus colegas (Plácido et al, 2017) demonstraram que, além de iniciar estresse do RE, a inibição de PP2A levaria subsequentemente a um distúrbio na interação RE-mitocondrial. Em nosso trabalho, evidenciamos que a proteína eIF2α atua como principal efetor desse distúrbio na comunicação entre essas organelas. Indo de

encontro a esse achado, dentre os marcadores de estresse do RE, essa foi a única proteína a exercer papel importante como componente da análise de PC1, sendo, dessa forma, um dos principais fatores para o dano causado pela redução da atividade de PP2A.

É sabido que os pontos de contato entre o RE e a mitocôndria, conhecidos como MAM, facilitam o transporte de Ca^{2+} entre essas organelas e estimulam assim o metabolismo oxidativo (Giorgi et al, 2015). Dessa forma, manter uma regulação adequada dessa comunicação é fundamental para a estabilidade das funções mitocondriais bioenergéticas e de sobrevivência celular. Em nosso trabalho, procuramos testar a funcionalidade bioenergética mitocondrial frente a redução da atividade de PP2A. Encontramos uma redução da efetividade na produção de ATP nessas células relacionada a um distúrbio na fosforilação oxidativa de ADP no complexo V mitocondrial (ATP-sintase). Essa disfunção está possivelmente relacionada aos aumentos encontrados no vazamento de prótons, marcador de alterações no potencial de membrana das mitocôndrias, e na produção de H_2O_2, importante ROS vinculada a danos oxidativos nas membranas mitocondriais e que podem levar ao prolongamento de déficits energéticos (Sies, 2017). Verfaillie e seus colegas (Verfaillie et al, 2018) demonstraram que a PERK, um conhecido regulador da UPR, media o início da sinalização de apoptose mitocondrial via aumento prolongado de ROS e CHOP. Apesar de não termos encontrado aumento da PERK induzido pela redução da atividade de PP2A, encontramos uma amplificação dos principais efetores dessa cascata (pEIF2α, CHOP e H_2O_2), podendo levar ao à apoptose independente do aumento de PERK. Há também a hipótese alternativa de que essa ativação pró-apoptótica pode decorrer de uma sobrecarga de Ca2+ nas MAM devido ao distúrbio da cascata PP2A/AKT/IP3R (Tubbs et al, 2017).

A falha dos mecanismos de correção da homeostase e a consequente disfunção prolongada da comunicação RE-mitocôndria podem levar a célula à ativação da apoptose.

Baseado nisso, resolvemos testar marcadores da via mitocondrial apoptótica em nosso modelo de inibição da atividade de PP2A. Como esperado, o aumento da cascata de sinalização pEIF2α/CHOP/H_2O_2 estava associada ao aumento de BAX/BCL2, citocromo c e clivagem de caspase. O aumento de BAX/BCL-2 é compatível com a descrição encontrada na literatura do efeito em genes pro-apoptóticos da ativação prolongada da via pEIF2α/CHOP (Pihan et al, 2017). Ainda, o aumento de BAX pode levar a alterações na porosidade da membrana mitocondrial, com consequente vazamento de citocromo c e ativação de vias proteolíticas marcadas pela clivagem da caspase 3 (Rodriguez et al, 2011). Além disso, foi notória a redução da viabilidade celular, marcada por níceis de MTT.

De maneira surpreendente, a fosforilação da proteína tau induzida por essa alteração de inibição da atividade da PP2A induzida por OKA não teve correlação com os marcadores de estresse do RE, produção de H_2O_2 e níveis de MTT. Disso, concluímos que as alterações no controle da proteostase pelo RE, a disfunção da MAM, a ativação apoptótica e o consequente déficit cognitivo causado pela redução da atividade da PP2A podem preceder as alterações de fosforilação da proteína tau, ou pelo menos ocorrer de forma paralela e independente destas, o que ajuda a compreender a importância da PP2A na neuroprogressão das não-taupatias. Esse achado é corroborado por estudos que apontaram a ativação da UPR como um evento inicial do processo de formação de NFTs (van der Harg et al, 2014; Hoozemans et al, 2009). É interessante acrescentar que essa hiperfosforilação da proteína tau decorrente do processo neurodegenerativo e da disfunção de fosfatases leva, por sua vez, também a maior estresse do RE e ativação da UPR (Ferreiro e Pereira, 2012). Ademais, com o prolongamento desse processo, acrescentam-se à retroalimentação positiva desse ciclo, ações diretas da proteína tau hiperfosforilada sobre a função mitocondrial, prejudicando o transporte e a respiração

mitocondrial e aumentando o estresse oxidativo através de maior produção de ROS (Pajak et al, 2016; Reddy, 2011).

Dessa forma, estresse do RE, disfunção mitocondrial e estresse oxidativo parecem formar um círculo vicioso regulado pela diminuição da atividade da PP2A e potencialmente decisivo no avanço de diversas doenças neurodegenerativas, e que pode, em alguns casos, ter a presença da proteína tau em sua forma hiperfosforilada atuando como uma espécie de catalisadora desse circuito de morte neuronal. Neste sentido, tendo a presença de proteínas com alterações fisíco-químicas como um dos achados patológicos mais frequentes em doenças neurodegenerativas, pode-se pensar que outras dessas proteínas (e.g. β-amiloide, proteína priônica e α-sinucleína) podem atuar de forma similar nesse círculo vicioso. De fato, diversos estudos já têm apontado nessa direção (Wu et al, 2012; Lee et al, 2010a; Lou et al, 2010), porém novos estudos ainda são necessários para maiores conclusões.

Na tentativa de aumentar a confiabilidade de nossa análise da similaridade entre essas variáveis, realizamos a análise por agrupamento hierárquico (HC – do inglês, *hierarchical clustering*). Dessa forma, confirmamos a proximidade do estresse do RE, da disfunção mitocondrial e da ativação da apoptose, demonstrando que esses processos acontecem de forma complementar frente à inibição da atividade da PP2A. Neste sentido, sabe-se que pode ocorrer uma retroalimentação entre essas respostas via troca de cálcio e produção de ROS (Malhotra et al, 2007). Entretanto, visto tantas variáveis envolvidas nos efeitos deletérios da redução de atividade dessa fosfatase, torna-se difícil afirmar qual delas seria mais prejudicial para a viabilidade celular e, portanto, mais envolvida no processo neurodegenerativo. A fim de melhor elucidar este ponto, foi feita a análise estatística de PCA, considerando-se o déficit de memória como o pior desfecho neurológico encontrado em nosso estudo. Nossos resultados demonstraram que H_2O_2 era

o maior contribuinte para a formação do PC1, entretanto todos os componentes funcionais e moleculares usados na criação do PC1 demonstraram correlação com e poderiam explicar os déficits de memória de curto e longo prazo decorrentes da inibição da atividade de PP2A pelo OKA.

As conclusões desse primeiro estudo favorecem uma melhor compreensão desses complexos processos, tornando-os possíveis alvos para evolução de estudos que visem biomarcadores para um diagnóstico precoce para essas doenças ou ainda desenvolvimento de tratamentos através da intervenção em um desses circuitos de sinalização.

Nessa busca por novas opções de alvos para tratamento, procuramos melhor elucidar outros possíveis mecanismos neuroprotetores ativados nas doenças neurodegenerativas. Em um estudo prévio de nosso grupo (Zimmer et al, 2012), mostramos que o modelo de redução da atividade da PP2A induzido pelo OKA leva a um aumento de níveis de glutamato no CSF, e que esses níveis são associados linearmente ao grau de declínio cognitivo encontrado. Mostramos também que o pré-tratamento com memantina (MN), um bloqueador do canal glutamatérgico NMDA, foi capaz de prevenir todas essas alterações moleculares e comportamentais. É sabido que potencialmente todo processo neurodegenerativo leva a um aumento agudo ou crônico na liberação de glutamato na fenda sináptica e no espaço extracelular (Lewerenz e Maher, 2015). Os mecanismos que levaram a essa proteção encontrada após o tratamento com MN permaneceram incertos, e pensamos que buscar um melhor entendimento do que pode ter evitado a neuroprogressão subsequente à inibição da atividade da PP2A pode ser promissor para o desenvolvimento de intervenções terapêuticas nas doenças neurodegenerativas.

Como descrito previamente, o aumento da concentração glutamatérgica leva a um processo de hiperativação neuronal conhecido como excitotoxicidade, que, em última instância, leva a disfunção sináptica e morte celular, contribuindo para o avanço da doença neurodegenerativa. A primeira linha de defesa para este tipo de dano é feita pelos astrócitos, aumentando a recaptação glutamatérgica e liberando substâncias tróficas como a S100B (Anderson e Swanson, 2000). Apesar da ação já conhecida da MN sobre a ativação do receptor NMDA, a ação dessa droga sobre a atividade astrocitária é desconhecida. Visto a importância dessa linha de defesa no processo neurodegenerativo e a notável prevenção dos danos causados pela inibição da PP2A demonstrada após o uso da MN, resolvemos investigar a influência desse mecanismo em nossos resultados.

No estudo apresentado no capítulo II dessa tese, a ativação da resposta astrocitária parece ocorrer em nosso modelo e, de fato, ser modulada pelo uso da MN. O aumento da reatividade astrocitária, marcado pelos níveis da proteína citoesquelética GFAP, encontrado após a infusão de OKA, tanto nos animais tratados com MN quanto nos que não receberam qualquer tratamento, mimetiza um achado comum da DA e outras taupatias (Ross et al, 2003; Higuchi et al, 2002).

Curiosamente, a MN levou a um aumento nos níveis de S100B apenas frente ao estímulo nocivo do OKA. Apesar da ação da S100B poder ser tanto deletéria quanto benéfica aos neurônios, dependendo de sua concentração (Van Eldik e Wainwright, 2003), o papel preventivo dela contra a excitotoxicidade e o dano cognitivo nos animais submetidos ao nosso modelo levam a crer que nesse cenário ela está agindo de forma neuroprotetora.

Em nosso estudo, de maneira inicialmente inesperada, o aumento de S100B modulado pela MN demonstrou correlação com uma diminuição da recaptação glutamatérgica hipocampal. De fato, Tramontina e seus colaboradores já haviam

demonstrado uma relação entre essas duas variáveis (Tramontina et al, 2006). Entretanto, em seu experimento parece haver um efeito contrário ao que encontramos da S100B sobre a recaptação de glutamato. Como seus testes foram realizados em culturas de gliomas, pode-se propor que essa interação ocorre de forma diferente na presença de neurônios. Recentemente, a presença de receptores NMDA também em astrócitos foi descoberta e caracterizada (Lee et al, 2010b), o que poderia levar a crer em uma ação direta da MN sobre os astrócitos. Entretanto, o aumento de S100B e a redução da recaptação de glutamato encontrados em nosso estudo ocorreram apenas frente à combinação do antagonismo neuronal do NMDA exercido pela MN com a neurotoxicidade do OKA, não sendo induzidas por nenhuma dessas intervenções isoladamente.

Juntos, os achados descritos acima reforçam a ideia da dependência de uma interação astrócito-neurônio para o desenvolvimento de tais mecanismos neuroprotetores. Corroborando nossa hipótese, Sakatani e colaboradores propuseram que a atividade neuronal é capaz de modular a liberação astrocitária de S100B (Sakatani et al, 2008). Ademais, foi demonstrado que a MN reduz a liberação neuronal de glutamato (Lu et al, 2010), o que pode também levar a uma interpretação de que o aumento da liberação de S100B e a redução da recaptação glutamatérgica pelos astrócitos pode ser uma resposta adaptativa à diminuição da liberação neuronal de glutamato. Estudos prévios já haviam demonstrado que, isoladamente, OKA não altera a recaptação glutamatérgica (Costa et al, 2012), o que foi replicado por nosso experimento. Unindo essas informações, podemos crer que a ação neuroprotetora da MN frente à neurotoxicidade do OKA depende de uma modulação complexa da resposta astrocitária, o que reforça a importância de incluir os astrócitos em futuros estudos visando tratamento e possivelmente prevenção de doenças neurodegenerativas.

O estudo da influência dos astrócitos em tratamentos ainda é relativamente recente (Escartin e Bonvento, 2008). Inclusive, diversas drogas já em uso clínico e com alvos neuronais surgem também hoje como possíveis moduladores da atividade astrocitária (Haim et al, 2015). De fato, neurônios e astrócitos compartilham de diversos recepetores e transportadores de membrana, além de possuírem diversas vias de sinalização em comum. As estratégias terapêuticas testadas até agora para as doenças neurodegenerativas têm, em sua maioria, se concentrado majoritariamente nos neurônios e não têm obtido os resultados esperados (Huang e Mucke, 2012; Wild e Tabrizi, 2014). Em muitos casos, os tratamentos oferecidos aos pacientes são apenas sintomáticos e sua eficácia pode ainda diminuir com a progressão da doença (por exemplo, inibidores da acetilcolinesterase para DA, suplementação com L-DOPA para DP). Nenhum tratamento atual realmente impede que os neurônios se degenerem. À luz de suas muitas ações sobre os neurônios, as estratégias que visam os astrócitos reativos podem ser a chave para efetivamente sustentar a função neuronal e, consequentemente, a sobrevivência durante as doenças neurodegenerativas (Haim et al, 2015). De qualquer forma, como em parte descrito nessa tese, essa regulação não é simples, pois estimular a reatividade astrocitária pode também iniciar efeitos nocivos aos neurônios. Para nos aproximarmos de um tratamento mais completo, será importante buscar compreender, com novos estudos, a complexidade dessas relações e amplificar a nossa visão de cérebro para além dos neurônios.

Conclusão

Nesta tese, procuramos avançar o conhecimento acerca de importantes vias de sinalização que impactam negativamente na patogênese e na evolução de diversas doenças neurodegenerativas associadas à diminuição da atividade da PP2A. Demonstramos que a alteração do funcionamento dessa fosfatase está envolvida com um aumento do estresse do RE associado com disfunção mitocondrial, levando a declínio da síntese de ATP e aumento na produção de ROS, com subsequente ativação apoptótica e morte neuronal. Demonstramos que o principal fator ligado à manutenção dessa disfunção RE-mitocondrial é a produção de H_2O_2 e que esses processos estão fortemente vinculados à progressão da neurodegeneração e aparecimento de déficits de memória.

Além disso, demonstramos que a ação neuroprotetora da MN frente à inibição da atividade da PP2A induzida pelo OKA envolve aumento da reatividade astrocitária e da liberação de S100B e diminuição da recaptação de glutamato, reforçando a importância de levar-se em conta a interação neurônio-astrócito para o desenvolvimento de tratamentos cada vez mais efetivos para as doenças neurodegenerativas.

Em resumo, tentamos aqui ampliar o entendimento sobre os processos de neurodegeneração e, com isso, contribuir para a busca de novos métodos diagnósticos e possíveis alvos terapêuticos para essas patologias.

Referências Bibliográficas

Anderson CM and Swanson RA "Astrocyte glutamate transport: review of properties, regulation, and physiological functions". *Glia* 2000, 32, 1–14

Anderson, MA, Ao Y., and Sofroniew MV "Heterogeneity of reactive astrocytes". *Neurosci. Lett.* 2014, 565, 23–29.

Chen W, Wang Z, Jiang C, Ding Y "PP2A-Mediated Anticancer Therapy", *Gastroenterology Research and Practice*, 2013, 2013:675429

Costa, AC, Tramontina AC, Biasibetti R, Batassini C, Lopes MW, Wartchow KM, Bernardi C, Tortorelli LS, Real RB, Gonçalves CA, "Neuroglial alterations in rats submitted to the okadaic acid-induced model of dementia". *Behav Brain Res*, 2012. 226(2): p. 420-7

Dong X, Wang Y, Qin Z "Molecular mechanisms of excitotoxicity and their relevance to pathogenesis of neurodegenerative diseases". *Acta Pharmacol Sin* 2009, 30 (4): 379–387

Duran-Aniotz C, Martinez G, Hetz C "Memory loss in Alzheimer's disease: are the alterations in the UPR network involved in the cognitive impairment?" *Frontiers in Aging Neuroscience*, 2014, 6: 8

Escartin, C., and Bonvento, G. "Targeted activation of astrocytes: a potential neuroprotective strategy". *Mol. Neurobiol.* 2008 38, 231–241

Ferreiro E, Pereira CM “Endoplasmic reticulum stress: a new playER in tauopathies”. *J Pathol* 2012, 226(5):687–692

Giorgi C, Missiroli S, Patergnani S, Duszynski J, Wieckowski MR, Pinton P “Mitochondria-associated membranes: composition, molecular mechanisms, and physiopathological implications”. *Antioxidants & redox signaling* 2015 22 (12):995-1019

Greenamyre JT, Maragos WF, Albin RL, Penney JB, Young AB “Glutamate transmission and toxicity in Alzheimer's disease”. *Prog Neuropsychopharmacol Biol Psychiatry* 1988, 12:421–430.

Haim BL, Carrillo-de Sauvage M-A, Ceyzériat K, Escartin C “Elusive roles for reactive astrocytes in neurodegenerative diseases”. *Front. Cell. Neurosci*. 2015, 9:278.

Harg JM van der, Nolle A, Zwart R et al “The unfolded protein response mediates reversible tau phosphorylation induced by metabolic stress” *Cell Death and Disease* 2012, 5: e1393

Heemels M.: "Neurodegenerative diseases." *Nature*, vol. 539, no. 7628, 2016, p. 179

Hetz C, Bernasconi P, Fisher J et al. “Proapoptotic BAX and BAK Modulate the Unfolded Protein Response by a Direct Interaction with IRE1a” *Science* 2006: 312, (5773), pp. 572-576

Higuchi, M, Ishihara T, Zhang B, Hong M, Andreadis A, Trojanowski J, Lee VM "Transgenic mouse model of tauopathies with glial pathology and nervous system degeneration". *Neuron*, 2002. **35**(3): p. 433-46

Ho YS, Yang X, Lau JC, Hung CH, Wuwongse S, Zhang Q, Wang J, Baum L, So KF, Chang RC "Endoplasmic reticulum stress induces tau pathology and forms a vicious cycle: implication in Alzheimer's disease pathogenesis". *J Alzheimers Dis* 2012, 28: 839-854

Hoozemans JJ, van Haastert ES, Nijholt DAT, Rozemuller AJM, Eikelenboom P, Scheper W. "The unfolded protein response is activated in pretangle neurons in Alzheimer's disease hippocampus". *Am J Pathol.* 2009;174:1241–51

Hoozemans JJ, Scheper W: "Endoplasmic reticulum: the unfolded protein response is tangled in neurodegeneration", *The international journal of biochemistry & cell biology*, 2012, 44, 1295-1298

Hu NW, Ondrejcak T, Rowan MJ "Glutamate receptors in preclinical research on Alzheimer's disease: Update on recent advances" *Pharmacology, Biochemistry and Behavior* 2012, 100, 855–862

Huang Y and Mucke L "Alzheimer mechanisms and therapeutic strategies." *Cell* 2012, 148, 1204–1222.

Kamat PK, Tota S, Shukla R, Ali S, Najmi AK, Nath C "Mitochondrial dysfunction: a crucial event in okadaic acid (ICV) induced memoryimpairment and apoptotic cell deat h in rat brain." *Pharmacology, Biochemistry and Behavior*, 2011, 110: 311–319

Kamat PK, Rai S, Swarnkar S, Shukla R, Nath C "Molecular and cellular mechanism of okadaic acid (OKA)-induced neurotoxicity: a novel tool for Alzheimer's disease therapeutic application". *Molecular neurobiology*, 2014, 50 (3):852-865

Kim AJ, Shi Y, Austin RC, Werstuck GH "Valproate protects cells from ER stress-induced lipid accumulation and apoptosis by inhibiting glycogen synthase kinase-3." *J Cell Sci* 2005, 118:89–99

Kim SM, Yoon SY, Choi JE, Park JS, Choi JM, Nguyen T, Kim DH "Activation of eukaryotic initiation factor-2 alpha-kinases in okadaic acid-treated neurons". *Neuroscience* 2010, 169 (4):1831-1839

Kovacs GG: "Concepts and classification of neurodegenerative diseases" *Neuropathology – Handbook of Clinical Neurology,* 2017, 145(3), p.301-307

Lee DY, Lee K-S, Lee HJ, Kim DH, Noh YH, et al. "Activation of PERK Signaling Attenuates Ab-Mediated ER Stress". *PLoS ONE* 2010a, 5(5): e10489.

Lee M-C, Ting KK, Adams S, Brew BJ, Chung R, et al. "Characterisation of the Expression of NMDA Receptors in Human Astrocytes". *PLoS ONE* 2010b 5(11): e14123.

Lewerenz J and Maher P "Chronic Glutamate Toxicity in Neurodegenerative Diseases—What is the Evidence?" *Front. Neurosci*. 2015, 9:469

Li JQ, Yu JT, Jiang T, Tan L "Endoplasmic reticulum dysfunction in Alzheimer's Disease". *Mol. Neurobiol*, 2014, 51: 383-395

Lin MT, Beal MF "Mitochondrial dysfunction and oxidative stress in neurodegenerative diseases" *Nature*, 2006, 443: 787-795

Lin SS, Bassik MC, Suh H, Nishino M, Arroyo JD, Hahn WC, Korsmeyer SJ, Roberts TM, "PP2A Regulates BCL-2 Phosphorylation and Proteasome-mediated Degradation at the Endoplasmic Reticulum", *J Biol Chem*, 2006; 281(32):23003-12

Lou H, Montoya SE, Alerte TN, Wang J, Wu J, Peng X, Hong CS, Friedrich EE "Serine 129 phosphorylation reduces the ability of alpha-synuclein to regulate tyrosine hydroxylase and protein phosphatase 2A in vitro and in vivo". *J Biol Chem* 2010, 285(23):17648–17661

Lu, C.W., T.Y. Lin, and S.J. Wang, "Memantine depresses glutamate release through inhibition of voltage-dependent Ca2+ entry and protein kinase C in rat cerebral cortex nerve terminals: an NMDA receptor-independent mechanism*"*. *Neurochem Int*, 2010. 57(2): p. 168-76

Magnaudeix A, Wilson CM, Page G, Bauvy C, Codogno P, Levegue P, Labrousse F, Corre-Delage M, Yardin C, Terro F "PP2A blockade inhibits autophagy and causes intraneuronal accumulation of ubiquitinated proteins" *Neurobiology of Aging* 2013, 34, 770 –790

Malhotra JD, Kaufman RJ "Endoplasmic reticulum stress and oxidative stress: a vicious cycle or a double-edged sword?" *Antioxidants & redox signaling*, 2007, 9 (12):2277-2293

Marciniak SJ, Yun CY, Oyadomari S, Novoa I, Zhang Y, Jungreis R, Nagata K, Harding HP, Ron D "CHOP induces death by promoting protein synthesis and oxidation in the stressed endoplasmic reticulum." *Genes & development* 2004, 18 (24):3066-3077

Meldrum BS, "Glutamate as a neurotransmitter in the brain: review of physiology and pathology". *J Nutr*, 2000. 130(4): p. 1007S-15S

Nematullah, M., Hoda, M.N. & Khan, F. "Protein Phosphatase 2A: a Double-Faced Phosphatase of Cellular System and Its Role in Neurodegenerative Disorders". *Mol Neurobiol,* 2018, 55(2): 1750-61

Pajak B, Kania E, Orzechowski A "Killing Me Softly: Connotations to Unfolded Protein Response and Oxidative Stress in Alzheimer's Disease". *Oxidative medicine and cellular longevity* 2016, 2016:1805304

Paschen W, Mengesdorf T "Endoplasmic reticulum stress response and neurodegeneration". *Cell Calcium,* 2005, 38, 409–415.

Pihan P, Carreras-Sureda A, Hetz C "BCL-2 family: integrating stress responses at the ER to control cell demise". *Cell death and differentiation* 2017, 24 (9):1478-1487

Placido AI, Pereira CM, Correira SC, Carvalho C, Oliveira CR, Moreira PI "Phosphatase 2A Inhibition Affects Endoplasmic Reticulum and Mitochondria Homeostasis Via Cytoskeletal Alterations in Brain Endothelial Cells". 2017, 54 (1):154-168

Reddy PH "Abnormal tau, mitochondrial dysfunction, impaired axonal transport of mitochondria, and synaptic deprivation in Alzheimer's disease" *Brain Research* 2011, 1415; 136-148

Rodriguez D, Rojas-Rivera D, Hetz C "Integrating stress signals at the endoplasmic reticulum: The BCL-2 protein family rheostat" *Biochimica et Biophysica Acta* 2011, 1813: 564–574

Ross, G.W., et al., "Quantification of regional glial fibrillary acidic protein levels in Alzheimer's disease". *Acta Neurol Scand*, 2003. 107(5): p. 318-23

Roussel BD, Kruppa AJ, Miranda E, Crowther DC, Lomas DA, Marciniak SJ, "Endoplasmic reticulum dysfunction in neurological disease", *The Lancet Neurology*, 2013, 12, 105-118.

Saito T, Konno T, Hosokawa T, Asada A, Ishiguro K, Hisanaga I "p25/cyclin-dependent kinase 5 promotes the progression of cell death in nucleus of endoplasmic reticulum-stressed neurons". *J Neurochem,* 2007, 102:133–140

Sakatani, S., et al., "Neural-activity-dependent release of S100B from astrocytes enhances kainate-induced gamma oscillations in vivo". *J Neurosci*, 2008. 28(43): p. 10928-36

Sies H "Hydrogen peroxide as a central redox signaling molecule in physiological oxidative stress: Oxidative eustress". *Redox biology* 2017, 11:613-619

Shi Y "Serine/Threonine Phosphatases: Mechanism through Structure**"** *Cell,* 2009, 139, 468-484

Song L, Sarno P, Jope RS "Central Role of Glycogen Synthase Kinase-3 in Endoplasmic Reticulum Stress-induced Caspase-3 Activation**"** *The Journal of Biological Chemistry*, 2002, 277 (47): 44701-44708

Sontag JM, Sontag E "Protein phosphatase 2A dysfunction in Alzheimer's disease". *Front Mol Neurosci*, 2014, 7:16

Szegezdi E, Logue SE, Gorman AM, Samali A, "Mediators of endoplasmic reticulum stress-induced apoptosis", *EMBO reports*, 2006, 7, 880-885.

Taleski G, Sontag E "Protein phosphatase 2A and tau: an orchestrated 'Pas de Deux'" *FEBS Letters*, 2018, 592(7):1079-1095.

Tramontina, F., Leite MC, Gonçalves D, Tramontina AC, Souza DF, Frizzo JK, Nardin P, Gottfried C, Woffchuk ST, Goncalves CA "High glutamate decreases S100B secretion by a mechanism dependent on the glutamate transporter". *Neurochem Res*, 2006. **31**(6): p. 815-20

Tubbs E, Rieusset J "Metabolic signaling functions of ER-mitochondria contact sites: role in metabolic diseases". *Journal of molecular endocrinology*, 2012, 58 (2):R87-r106

Van Eldik LJ and Wainwright MS, "The Janus face of glial-derived S100B: beneficial and detrimental functions in the brain". *Restor Neurol Neurosci*, 2003; 21(3-4):97-108

Verfaillie T, Rubio N, Garg AD, Bultynck G, Rizzuto R, Decuypere JP, Piette J, Linehan C, Gupta S, Samali A, Agostinis P, "PERK is required at the ER-mitochondrial contact sites to convey apoptosis after ROS-based ER stress", *Cell death and differentiation*, 2012, 19, 1880-1891

Walter P and Ron D "The unfolded protein response: from stress pathway to homeostatic regulation". *Science* 2011, 334, 1081–1086

Wang M, Wey S, Zhang Y, Ye R, Lee AS "Role of the unfolded protein response regulator GRP78/BiP in development, cancer, and neurological disorders." *Antioxidants & redox signaling* 2009, 11 (9):2307-2316

Wild EJ and Tabrizi SJ “Targets for future clinical trials in Huntington’s disease: what’s in the pipeline?” *Mov. Disord.* 2014, 29, 1434–1445

Wu J, Lou H, Alerte TN, Stachowski EK, Chen J, Singleton AB, Hamilton RL, Perez RG “Lewy-like aggregation of α-synuclein reduces protein phosphatase 2A activity in vitro and in vivo”. *Neuroscience*, 2012 207:288–297

Zimmer ER, Kalinine E, Haas CB, Torrez VR, Souza DO, Muller AP, Portela LV “Pretreatment with memantine prevents Alzheimer-like alterations induced by intrahippocampal okadaic acid administration in rats.” *Curr Alzheimer Res* 2012, 9(10):1182–1190

Zimmer ER, Torrez VR, Kalinine E, Augustin MC, Zenki KC, Almeida RF, Hansel G, Muller AP, Souza DO, Machado-Vieira R, Portela LV “Long-term NMDAR antagonism correlates reduced astrocytic glutamate uptake with anxiety-like phenotype”. *Frontiers in cellular neuroscience* , 2015, 9:219

Anexos

ANEXO I: Artigos publicados durante o período de doutoramento cujos temas se relacionam a esta tese, mas não foram incluídos no corpo principal da tese.

ANEXO I-A. *Long-term NMDAR antagonism correlates reduced astrocytic glutamate uptake with anxiety-like phenotype*

No ANEXO I-A apresentamos o artigo publicado no periódico *Frontiers in Cellular Neuroscience*

frontiers in Cellular Neuroscience

ORIGINAL RESEARCH
published: 03 June 2015
doi: 10.3389/fncel.2015.00219

Long-term NMDAR antagonism correlates reduced astrocytic glutamate uptake with anxiety-like phenotype

*Eduardo R. Zimmer[1], Vitor R. Torrez[1], Eduardo Kalinine[1,2], Marina C. Augustin[1], Kamila C. Zenki[1], Roberto F. Almeida[1], Gisele Hansel[1], Alexandre P. Muller[1,3], Diogo O. Souza[1], Rodrigo Machado-Vieira[4,5,6] and Luis V. Portela[1]**

[1] Department of Biochemistry, Universidade Federal do Rio Grande do Sul, Porto Alegre, Brazil, [2] Department of Physiology, Universidade Federal de Sergipe, São Cristovão, Brazil, [3] Laboratory of Exercise, Biochemistry and Physiology, Universidade do Extremo Sul Catarinense, Criciúma, Brazil, [4] Laboratory of Neuroscience, LIM-27, Institute and Department of Psychiatry, Universidade de São Paulo, São Paulo, Brazil, [5] Center for Interdisciplinary Research on Applied Neurosciences (NAPNA), Universidade de São Paulo, São Paulo, Brazil, [6] Experimental Therapeutics and Pathophysiology Branch, National Institute of Mental Health, National Institutes of Health, Bethesda, MD, USA

OPEN ACCESS

Edited by:
Johann Steiner, Otto-von-Guericke University Magdeburg, Germany

Reviewed by:
Francisco Ciruela, Universitat de Barcelona, Spain
Paul Guest, University of Cambridge, UK

**Correspondence:*
Luis V. Portela, Department of Biochemistry, Universidade Federal do Rio Grande do Sul, 2600 Ramiro Barcelos Street, 90035-003, Porto Alegre, Rio Grande do Sul, Brazil
roskaportela@gmail.com

Received: 14 April 2015
Accepted: 22 May 2015
Published: 03 June 2015

Citation:
Zimmer ER, Torrez VR, Kalinine E, Augustin MC, Zenki KC, Almeida RF, Hansel G, Muller AP, Souza DO, Machado-Vieira R and Portela LV (2015) Long-term NMDAR antagonism correlates reduced astrocytic glutamate uptake with anxiety-like phenotype. Front. Cell. Neurosci. 9:219. doi: 10.3389/fncel.2015.00219

The role of glutamate *N*-methyl-D-aspartate receptor (NMDAR) hypofunction has been extensively studied in schizophrenia; however, less is known about its role in anxiety disorders. Recently, it was demonstrated that astrocytic GLT-1 blockade leads to an anxiety-like phenotype. Although astrocytes are capable of modulating NMDAR activity through glutamate uptake transporters, the relationship between astrocytic glutamate uptake and the development of an anxiety phenotype remains poorly explored. Here, we aimed to investigative whether long-term antagonism of NMDAR impacts anxiety-related behaviors and astrocytic glutamate uptake. Memantine, an NMDAR antagonist, was administered daily for 24 days to healthy adult CF-1 mice by oral gavage at doses of 5, 10, or 20 mg/kg. The mice were submitted to a sequential battery of behavioral tests (open field, light–dark box and elevated plus-maze tests). We then evaluated glutamate uptake activity and the immunocontents of glutamate transporters in the frontoparietal cortex and hippocampus. Our results demonstrated that long-term administration of memantine induces anxiety-like behavior in mice in the light–dark box and elevated plus-maze paradigms. Additionally, the administration of memantine decreased glutamate uptake activity in both the frontoparietal cortex and hippocampus without altering the immunocontent of either GLT-1 or GLAST. Remarkably, the memantine-induced reduction in glutamate uptake was correlated with enhancement of an anxiety-like phenotype. In conclusion, long-term NMDAR antagonism with memantine induces anxiety-like behavior that is associated with reduced glutamate uptake activity but that is not dependent on GLT-1 or GLAST protein expression. Our study suggests that NMDAR and glutamate uptake hypofunction may contribute to the development of conditions that fall within the category of anxiety disorders.

Keywords: anxiety, astrocytes, behavior, glutamate, memantine

Introduction

Anxiety disorders are among the most prevalent psychiatric conditions worldwide. These disorders have been associated with social isolation, alcoholism, and increased suicide attempts and are also considered to be risk factors for the development of additional psychiatric disorders (Gross and Hen, 2004). Hence, it is imperative to understand the neurobiological mechanisms that are associated with anxiety disorders. It has recently been proposed that a functional imbalance of the tripartite glutamatergic synapse plays a role in anxiety disorders (Clement and Chapouthier, 1998; Nutt and Malizia, 2001; Nemeroff, 2003; Machado-Vieira et al., 2009, 2012). Indeed, glutamatergic neurotransmission offers multiple potential pharmacological targets for treating anxiety-related disorders, such as postsynaptic receptor signaling, presynaptic glutamate release, and astrocytic glutamate uptake (Szabo et al., 2009; Zarate et al., 2010; Riaza Bermudo-Soriano et al., 2012; Pilc et al., 2013).

Currently, antagonism of *N*-methyl-D-aspartate receptor (NMDAR) has been proposed as a feasible strategy for reducing the major symptoms that are linked to anxiety-like behavior (Cortese and Phan, 2005). Indeed, when memantine, an NMDAR antagonist, is administered to patients presenting with depression, anxiety or obsessive-compulsive disorder, their neuropsychiatric symptoms appear to be relieved (Tariot et al., 2004; Sani et al., 2012). By contrast, a recent work demonstrated that chronic antagonism of NMDAR induces elevated anxiety in healthy mice (Hanson et al., 2014). Overall, the current data that are available regarding the association between the use of NMDAR antagonists and the presentation of anxiety-related behaviors refute a simple model of dose-effect and instead seem to be closely related to the regimen, type of drug, or route of administration (Silvestre et al., 1997; Riaza Bermudo-Soriano et al., 2012; Schwartz et al., 2012). Additionally, it is prudent to consider that glutamatergic neurotransmission involves not only neuronal receptors (ionotropic and metabotropic) but also astroglial transporters that participate in neuron-astrocyte coupling.

Two major astroglial Na^+-dependent glutamate transporters, glutamate transporter 1 (GLT-1, also known as EAAT2) and glutamate aspartate transporter (GLAST, also known as EAAT1), take up glutamate from synapses to maintain the homeostasis that is necessary to orchestrate the physiological activity of receptors (Danbolt, 2001). Remarkably, cerebral GLT-1 and GLAST are predominately localized in astrocytes, with very low expression in other cell types (Zhou and Danbolt, 2014). Moreover, astrocytes account for 95% of the glutamate uptake activity in the brain (Danbolt et al., 1992; Lehre and Danbolt, 1998). Importantly, a recent work demonstrated that cerebral microinjection of the GLT-1 inhibitor, dihydrokainic acid (DHK), induced anhedonia and anxiety in rats (John et al., 2015). Thus, one could claim that astrocytic dysfunction may have a considerable impact on the expression of anxiety-like phenotypes (Bechtholt-Gompf et al., 2010; Schroeter et al., 2010; Lee et al., 2013). Based on the principles of neuron-astrocyte coupling, we hypothesized that long-term antagonism of NMDAR would impact astrocytic function and that this would likely affect anxiety phenotype.

In this study, we aimed to investigate the impact of long-term NMDAR antagonism by memantine on anxiety-related paradigms and their potential association with astrocytic glutamate transport.

Materials and Methods

Animals

Three-month-old CF-1 mice were housed in standard cages (48 cm × 26 cm). The animals were kept in a room with controlled temperature (22° C) under a 12 h light/12 h dark cycle (lights on at 7 am) and had free access to food and water. The mice (n = 40) were randomized into four groups: control (CO), memantine 5 mg (MN5), memantine 10 mg (MN10), and memantine 20 mg (MN20). To avoid social isolation, we maintained two animals per cage (Leasure and Decker, 2009). All behavioral tests were performed between 1:00 pm and 5:00 pm. All experiments were conducted in accordance with official governmental guidelines in compliance with the Federation of Brazilian Societies for Experimental Biology and were approved by the Ethical Committee of the Federal University of Rio Grande do Sul, Brazil.

Drug Administration

Memantine (Sigma, USA) was dissolved in distilled water at three different concentrations (0.5, 1.0, and 2.0 mg/mL) to standardize the volume used for oral administration and reach the desired dose. For 24 days, the animals received daily administration of either 5, 10, or 20 mg/kg of memantine, or an equivalent volume of distilled water, via oral gavage. Body weight and food intake were monitored. All groups received oral gavage at 1 h after each behavioral task.

Open Field Test

On the 22nd day, the animals were submitted to an open field task to evaluate spontaneous locomotion and exploratory activity. The apparatus was made of a black-painted box measuring 50 cm × 50 cm and was surrounded by 50 cm high walls. The experiments were conducted in a quiet room under low-intensity light (12 lx). Each mouse (n = 10 per group) was placed in the center of the arena, and the distance traveled (total and central zone), time spent in the central zone, and mean speed were measured over a course of 10 min (Muller et al., 2012). The experiment was recorded with a video camera that was positioned above the arena. The analysis was performed using a computer-operated tracking system (Any-maze, Stoelting, Woods Dale, IL, USA).

Light–Dark Task

On the 23rd day, the light–dark task was performed as previously described (Crawley and Goodwin, 1980) with some modifications to analyze anxiety profiles. The light–dark apparatus consisted of a wood rectangular box with two separated chambers. One chamber had black walls and floor (50 cm × 50 cm × 50 cm)

and was not illuminated. The other side had white walls and floor (50 cm × 50 cm × 50 cm) and was illuminated by a 100 W white lamp that was placed overhead. The two compartments were separated by a wall, which had a small opening at floor level. For each experiment, an animal (n = 10 per group) was initially placed in the white chamber and then allowed to explore the two-chamber area for a duration of 5 min. The following parameters were recorded by a trained and blinded-to-treatment observer: number of transitions between the two chambers, time spent in the light chamber, and risk assessment behavior. After each experiment, the apparatus was cleaned with 70% alcohol and dried before being used with the next animal.

Elevated Plus-Maze Task

On the 24th day, the animals were submitted to an elevated plus-maze task to evaluate further signs of anxiety-like behavior. The elevated plus-maze was performed as previously described (Pellow, 1986). The elevated plus-maze apparatus consisted of two open arms (30 cm × 5 cm) and two enclosed arms (30 cm × 5 cm × 10 cm), which were separated by a central platform (5 cm × 5 cm) with the two identical arms of each type being placed opposite to each other. The height of the maze was 70 cm, and the experiments were conducted under dim red light in a quiet room. Each mouse (n = 10 per group) was individually placed onto the central platform of the plus-maze, facing one of the open arms, and was observed/recorded for 5 min by a trained and blinded-to-treatment observer. The time spent in the open arms and the total distance traveled were used for further analysis. After each session, the maze was cleaned with 70% ethanol. Data analysis was performed using a computer-operated tracking system (Any-maze, Stoelting, Woods Dale, IL, USA).

Glutamate Uptake Assay

On the 25th day, the animals (n = 6 per group) were sacrificed/dissected and left hippocampal and left frontoparietal cortical brain slices were taken for use in a glutamate uptake assay. The glutamate uptake assay was performed according to Thomazi et al. (2004). Brain hippocampal and frontoparietal cortical slices (0.4 mm) were obtained using a McIlwain tissue chopper and were pre-incubated for 15 min at 37° C in Hank's balanced salt solution (HBSS), containing 137 mM NaCl, 0.63 mM Na_2HPO_4, 4.17 mM $NaHCO_3$, 5.36 mM KCl, 0.44 mM KH_2PO_4, 1.26 mM $CaCl_2$, 0.41 mM $MgSO_4$, 0.49 mM $MgCl_2$, and 1.11 mM glucose, at pH 7.2. Afterward, 0.66 and 0.33 Ci ml^{-1} L-[^{3}H]glutamate were added to a final 100 M concentration of glutamate for incubation with hippocampal and cortical samples, respectively. The incubations were stopped after 5 and 7 min for the hippocampal and cortical samples, respectively, with two ice-cold washes of 1 ml HBSS, which were immediately followed by the addition of 0.5 N NaOH. The samples were kept in this solution overnight. Nonspecific uptake was measured using the same protocol as described above, with differences in temperature (4° C) and medium composition (*N*-methyl-D-glucamine instead of sodium chloride). Na^+-dependent uptake was considered as the difference between the total uptake and the non-specific uptake. Note that astrocytic transport mediated by GLAST and GLT-1 is responsible for the Na^+-dependent glutamate uptake (Anderson and Swanson, 2000). Both uptakes were performed in triplicate. Any radioactivity that was incorporated into the slices was measured using a liquid scintillation counter.

Western Blotting

For western blot analysis, right hippocampal and right frontoparietal cortical homogenates (n = 6, per group) were prepared in PIK buffer (1% NP-40, 150 mM NaCl, 20 mM Tris, pH 7.4, 10% glycerol, 1 mM $CaCl_2$, 1 mM $MgCl_2$, 400 µM sodium vanadate, 0.2 mM PMSF, 1 µg/ml leupeptin, 1 µg/ml aprotinin, and 0.1% phosphatase inhibitor cocktails I and II from Sigma–Aldrich) and centrifuged (Zimmer et al., 2012). Supernatants were collected and total protein was measured using Peterson's method (Peterson, 1977). Samples containing 20 µg of protein from the hippocampal homogenate were separated by electrophoresis on a polyacrylamide gel and electrotransferred to PVDF membranes. Protein bands within each sample lane were compared to standard molecular weight markers (Precision Plus Protein™ Dual Color Standards, Bio-Rad), which were used to identify the molecular weights of proteins of interest. Non-specific binding sites were blocked using Tween–Tris buffered saline (TTBS, 100 mM Tris–HCl, pH 7.5) with 5% albumin for 2 h. Samples were incubated overnight at 4° C with primary antibodies against GLT-1 (Abcam, 1:1000), GLAST (Abcam, 1:1000), and β-actin (Sigma, 1:5000). Following primary antibody incubation, the membranes were incubated with secondary antibodies (anti-rabbit, GE life sciences, 1:3000; anti-mouse, GE life sciences, 1:5000) for 2 h at room temperature. Films were scanned, and band intensity was analyzed using ImageJ software (Abramoff et al., 2004).

Statistical Analysis

Differences between groups were analyzed with analysis of variance (ANOVA) followed by Tukey's *post hoc* test. Correlations between behavioral assessments and glutamate uptake were analyzed by Pearson's correlation coefficient. The results are presented as mean values ± SEM. Differences were considered significant at $p < 0.05$.

Results

Long-Term NMDAR Antagonism does not Alter Spontaneous Locomotion but Induces Anxiety-Like Behavior

Administration of memantine did not cause significant changes in either distance traveled [**Figure 1A**; $F_{(3,36)} = 1.642$, $p = 0.1967$] or time spent in the central zone [**Figure 1B**; $F_{(3,36)} = 0.1697$, $p = 0.9162$] in the open field. Occupancy plots are used to illustrate the similarities between groups in the open field test (**Figure 1C**).

Long-Term NMDAR Antagonism Reduced Time Spent in the Light Compartment of the Light–Dark Box

In the light–dark box (**Figure 1G**), all of the doses of memantine that were tested significantly reduced the time spent in the light

compartment by the memantine-administered mice compared to the CO group [**Figure 1D**; $F_{(3,36)} = 7.364$, MN5: $p = 0.03$, MN10: $p = 0.002$, MN20: $p = 0.01$]. However, transition numbers (light to dark) were unrelated to memantine administration [**Figure 1E**; $F_{(3,36)} = 0.8257$, $p = 0.4884$]. Additionally, there were no differences among groups in risk assessment index [**Figure 1F**; $F_{(3,36)} = 1.129$, $p = 0.3519$].

Long-Term NMDAR Antagonism Decreased Time Spent in the Open Arms of the Elevated Plus-Maze

The administration of memantine reduced the time spent by mice in the open arms of the elevated plus-maze (**Figure 1J**) when compared to the CO group [**Figure 1H**; $F_{(3,36)} = 6.974$, MN5: $p = 0.007$, MN10: $p = 0.002$, MN20: $p = 0.004$]; however, there were no changes in total distance traveled [**Figure 1I**; $F_{(3,36)} = 2.227$, $p = 0.1018$].

Long-Term NMDAR Antagonism Decreased Glutamate Uptake in the Frontoparietal Cortex and Hippocampus without Affecting the Immunocontents of GLAST and GLT-1

The administration of memantine significantly decreased glutamate uptake in slices of frontoparietal cortex [**Figure 2A**; $F_{(3,20)} = 11.458$, MN5: $p = 0.026$, MN10: $p < 0.001$, MN20: $p < 0.001$] and hippocampus [**Figure 2D**; $F_{(3,20)} = 15.008$, MN5: $p = 0.015$, MN10: $p < 0.001$, MN20: $p < 0.001$]. However, memantine did not alter the immunocontent of GLAST in either the frontoparietal cortex [**Figure 2B**; $F_{(3,20)} = 1.300$, $p = 0.3020$] or the hippocampus [**Figure 2E**; $F_{(3,20)} = 0.6174$, $p = 0.6118$]. Additionally, no alterations were found in the immunocontent of GLT-1 in either the frontoparietal cortex [**Figure 2C**; $F_{(3,20)} = 2.225$, $p = 0.1167$] or the hippocampus [**Figure 2F**; $F_{(3,20)} = 0.1520$, $p = 0.9272$].

Correlation Between Anxiety-Like Behavior and Glutamate Uptake

A positive correlation was found between time spent in the light compartment of the light dark-box and glutamate uptake in the frontoparietal cortex (**Figure 3A**; $p < 0.0001$, $R = 0.7289$) and hippocampus (**Figure 3C**; $p = 0.03$, $R = 0.4337$). Time spent in the open arms of the elevated plus-maze test was also correlated with glutamate uptake in the frontoparietal cortex (**Figure 3B**; $p = 0.03$, $R = 0.4313$) and hippocampus (**Figure 3D**; $p = 0.01$, $R = 0.4815$).

Discussion

Our results demonstrated that long-term antagonism of NMDAR by memantine induces anxiety-like behavior in healthy CF-1 mice. Additionally, memantine decreased glutamate uptake activity in the frontoparietal cortex and in the hippocampus

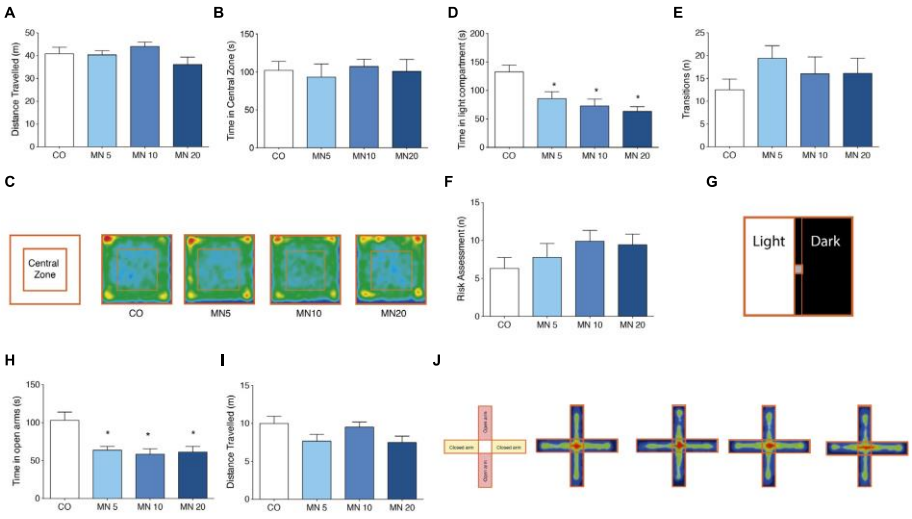

FIGURE 1 | Long-term NMDAR antagonism does not alter spontaneous locomotor and exploratory behavior, but induces anxiety-like behavior. (A) Total distance traveled in the open field. (B) Time in central zone in the open field. (C) Open field apparatus and occupancy plots. (D) Time in light compartment in the light–dark box. (E) Number of transitions in the light–dark box. (F) Risk assessment index in the light–dark box. (G) Light–dark box apparatus. (H) Time in open arms in the elevated plus-maze. (I) Distance traveled in the elevated plus-maze. (J) Elevated plus-maze apparatus and occupancy plots. Groups: control (CO), memantine 5 mg (MN 5), memantine 10 mg (MN 10), and memantine 20 mg (MN 20); $n = 10$ per group. Data are presented as mean values ± SEM.

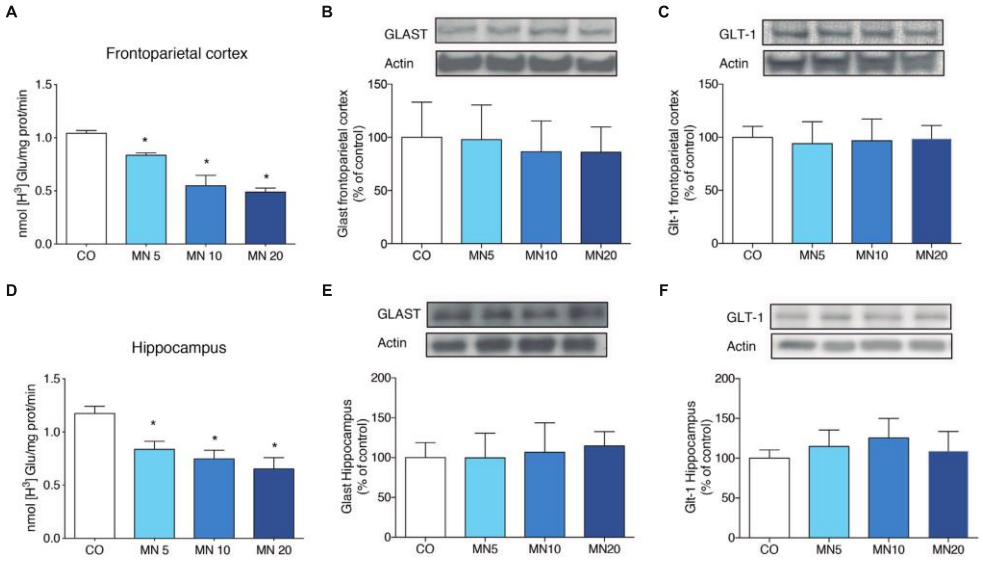

FIGURE 2 | Long-term NMDAR antagonism decreases glutamate uptake in the frontoparietal cortex and hippocampus, but does not alter astroglial transporter immunocontent. (A) Glutamate uptake in slices of frontoparietal cortex. (B) Immunocontent of GLAST in the frontoparietal cortex. (C) Immunocontent of GLT-1 in the frontoparietal cortex. (D) Glutamate uptake in slices of hippocampus. (E) Immunocontent of GLAST in the frontoparietal cortex. (F) Immunocontent of GLT-1T in the frontoparietal cortex. Groups: CO, memantine 5 mg (MN 5), memantine 10 mg (MN 10), and memantine 20 mg (MN 20); $n = 6$ per group. Data are presented as mean values ± SEM. $^*p < 0.05$ among groups.

with this phenomenon correlating with anxiety-like behavior. By contrast, the immunocontents of the astroglial glutamate transporters GLT-1 and GLAST were not affected.

Long-term administration of memantine did not induce significant changes in the spontaneous locomotion and exploratory activity of mice in the open field test. These findings imply that neither the dose nor the regimen of memantine that was used in our work led to non-specific effects such as sedation, which can potentially impair performance in anxiety-like tasks. This finding is in agreement with previous reports that have demonstrated that memantine administration does not alter locomotion or exploratory profiles (Reus et al., 2010). Conversely, we also showed that long-term memantine administration at doses of 5, 10, or 20 mg/kg leads to an anxiogenic phenotype that is manifested by decreased time spent in the light compartment (light–dark box) and reduced time spent in open arms (elevated plus-maze). Interestingly, a previous work showed that the administration of MK801, another non-competitive NMDAR antagonist, to rats induced an anxiety-like phenotype in the elevated plus-maze (Solati, 2011). In contrast to MK801, high doses of memantine (100 mg/kg) increased time spent in open arms, implying an anxiolytic effect. However, doses ranging from 10 to 30 mg/kg decreased time spent in open arms (~40%), without reaching statistical significance, which suggests a trend representative of an anxiogenic-like effect (Minkeviciene et al., 2008). Additionally, chronic antagonism of NMDAR with piperine18 exacerbated anxiogenic symptoms in C57BL/6 mice (Hanson et al., 2014). Indeed, it would appear that the antagonism of NMDAR does not follow a linear dose-response effect in terms of modulating anxiety-like behavior.

It has also been shown that memantine plays a role in controlling synaptic glutamate release. In fact, Lu et al. (2010) have shown that memantine suppresses glutamate release in cortical synaptosomes. In this study, however, we showed that long-term administration of memantine reduces glutamate uptake without affecting the glutamate transporters expression, GLT-1 and GLAST, in the frontoparietal cortex and hippocampus. Based on these findings, one could argue that memantine-induced reduction of glutamate uptake by astrocytes is a direct adaptive response to the reduced release of glutamate by neurons. This assumption reinforces a theoretical framework in which neurons and astrocytes are capable of sensing each other while regulating tripartite glutamatergic synapses (Wade et al., 2013; Karus et al., 2015). However, further studies using additional methodologies, such as immunostaining and electron microscopy, are necessary to better understand neuron-astrocyte coupling in the context of anxiety-like phenotypes.

Interestingly, a recent work demonstrated that blockade of GLT-1 in the central amygdala was also capable of inducing anxiety-like behavior, which reinforces the association between

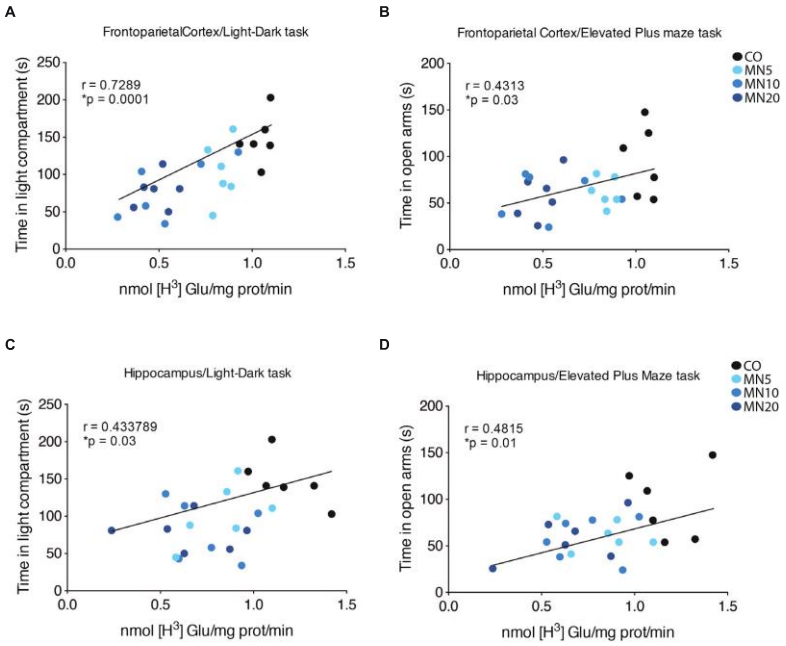

FIGURE 3 | Anxiety-like behavior correlates with glutamate uptake. (A) Linear correlation between time spent in light compartment during the light/dark task and glutamate uptake in slices of frontoparietal cortex. (B) Linear correlation between time spent in open arms and glutamate uptake in slices of frontoparietal cortex. (C) Linear correlation between time spent in light compartment during light/dark task and glutamate uptake in slices of hippocampus. (D) Linear correlation between time spent in open arms in elevated plus-maze test and glutamate uptake in slices of hippocampus. Groups: CO, memantine 5 mg (MN 5), memantine 10 mg (MN 10), and memantine 20 mg (MN 20); $n = 24$. Data presented by one animal per point. $^{*}p < 0.05$.

astrocytic glutamate uptake activity and the development of an anxiety phenotype (John et al., 2015). Remarkably, we were able to show through linear correlation that decreased glutamate uptake activity in the hippocampus and frontoparietal cortex was significantly correlated with an increased anxiety-like response.

Conclusion

Long-term NMDAR antagonism by memantine induces an anxiety phenotype that is associated with reduced glutamate uptake activity in healthy CF-1 mice, which suggests that interactions between neurons and astrocytes can shape anxiety-related behavior.

Author Contributions

EZ was responsible for the design, acquisition, analysis, interpretation, drafting, and approval of the final version of the manuscript. VT, EK, MA, KZ, RA, and GH were responsible for acquisition, analysis, interpretation, and approval of the final version of the manuscript. AM, DS, and RV were responsible for interpretation, drafting, critical revision, and approval of the final version of the manuscript. LV was responsible for the design, interpretation, drafting, critical revision, and approval of the final version of the manuscript.

Acknowledgments

This work was supported by the following Brazilian agencies and grants: National Counsel of Technological and Scientific Development (CNPq), CAPES, FAPERGS, Brazilian Institute of Neuroscience (IBNnet), FINEP, and National Institute of Science and Technology (INCT) – Excitotoxicity and Neuroprotection.

Supplementary Material

The Supplementary Material for this article can be found online at: http://journal.frontiersin.org/article/10.3389/fncel.2015.00219/abstract

References

Abramoff, M. D., Magalhaes, P. J., and Ram, S. J. (2004). Processing with ImageJ. *Biophotonics Intern.* 11, 36–42.

Anderson, C. M., and Swanson, R. A. (2000). Astrocyte glutamate transport: review of properties, regulation, and physiological functions. *Glia* 32, 1–14. doi: 10.1002/1098-1136(200010)32:1<1::AID-GLIA10>3.0.CO;2-W

Bechtholt-Gompf, A. J., Walther, H. V., Adams, M. A., Carlezon, W. A. Jr., Ongur, D., and Cohen, B. M. (2010). Blockade of astrocytic glutamate uptake in rats induces signs of anhedonia and impaired spatial memory. *Neuropsychopharmacology* 35, 2049–2059. doi: 10.1038/npp.2010.74

Clement, Y., and Chapouthier, G. (1998). Biological bases of anxiety. *Neurosci. Biobehav. Rev.* 22, 623–633. doi: 10.1016/S0149-7634(97)00058-4

Cortese, B. M., and Phan, K. L. (2005). The role of glutamate in anxiety and related disorders. *CNS Spectr.* 10, 820–830.

Crawley, J., and Goodwin, F. K. (1980). Preliminary report of a simple animal behavior model for the anxiolytic effects of benzodiazepines. *Pharmacol. Biochem. Behav.* 13, 167–170. doi: 10.1016/0091-3057(80)90067-2

Danbolt, N. C. (2001). Glutamate uptake. *Prog. Neurobiol.* 65, 1–105. doi: 10.1016/S0301-0082(00)00067-8

Danbolt, N. C., Storm-Mathisen, J., and Kanner, B. I. (1992). An [Na+ + K+]coupled L-glutamate transporter purified from rat brain is located in glial cell processes. *Neuroscience* 51, 295–310. doi: 10.1016/0306-4522(92)90316-T

Gross, C., and Hen, R. (2004). The developmental origins of anxiety. *Nat. Rev. Neurosci.* 5, 545–552. doi: 10.1038/nrn1429

Hanson, J. E., Meilandt, W. J., Gogineni, A., Reynen, P., Herrington, J., Weimer, R. M., et al. (2014). Chronic GluN2B antagonism disrupts behavior in wild-type mice without protecting against synapse loss or memory impairment in Alzheimer's disease mouse models. *J. Neurosci.* 34, 8277–8288. doi: 10.1523/JNEUROSCI.5106-13.2014

John, C. S., Sypek, E. I., Carlezon, W. A., Cohen, B. M., Ongur, D., and Bechtholt, A. J. (2015). Blockade of the GLT-1 transporter in the central nucleus of the amygdala induces both anxiety and depressive-like symptoms. *Neuropsychopharmacology* 40, 1700–1708. doi: 10.1038/npp.2015.16

Karus, C., Mondragao, M. A., Ziemens, D., and Rose, C. R. (2015). Astrocytes restrict discharge duration and neuronal sodium loads during recurrent network activity. *Glia* 63, 936–957. doi: 10.1002/glia.22793

Leasure, J. L., and Decker, L. (2009). Social isolation prevents exercise-induced proliferation of hippocampal progenitor cells in female rats. *Hippocampus* 19, 907–912. doi: 10.1002/hipo.20563

Lee, Y., Son, H., Kim, G., Kim, S., Lee, D. H., Roh, G. S., et al. (2013). Glutamine deficiency in the prefrontal cortex increases depressive-like behaviours in male mice. *J. Psychiatry Neurosci.* 38, 183–191. doi: 10.1503/jpn.120024

Lehre, K. P., and Danbolt, N. C. (1998). The number of glutamate transporter subtype molecules at glutamatergic synapses: chemical and stereological quantification in young adult rat brain. *J. Neurosci.* 18, 8751–8757.

Lu, C. W., Lin, T. Y., and Wang, S. J. (2010). Memantine depresses glutamate release through inhibition of voltage-dependent $Ca2^{+}$ entry and protein kinase C in rat cerebral cortex nerve terminals: an NMDA receptor-independent mechanism. *Neurochem. Int.* 57, 168–176. doi: 10.1016/j.neuint.2010.05.010

Machado-Vieira, R., Ibrahim, L., Henter, I. D., and Zarate, C. A. Jr. (2012). Novel glutamatergic agents for major depressive disorder and bipolar disorder. *Pharmacol. Biochem. Behav.* 100, 678–687. doi: 10.1016/j.pbb.2011.09.010

Machado-Vieira, R., Manji, H. K., and Zarate, C. A. (2009). The role of the tripartite glutamatergic synapse in the pathophysiology and therapeutics of mood disorders. *Neuroscientist* 15, 525–539. doi: 10.1177/1073858409336093

Minkeviciene, R., Banerjee, P., and Tanila, H. (2008). Cognition-enhancing and anxiolytic effects of memantine. *Neuropharmacology* 54, 1079–1085. doi: 10.1016/j.neuropharm.2008.02.014

Muller, A. P., Zimmer, E. R., Kalinine, E., Haas, C. B., Oses, J. P., Martimbianco De Assis, A., et al. (2012). Physical exercise exacerbates memory deficits induced by intracerebroventricular STZ but improves insulin regulation of H2O2 production in mice synaptosomes. *J. Alzheimers Dis.* 30, 889–898. doi: 10.3233/JAD-2012-112066

Nemeroff, C. B. (2003). The role of GABA in the pathophysiology and treatment of anxiety disorders. *Psychopharmacol. Bull.* 37, 133–146.

Nutt, D. J., and Malizia, A. L. (2001). New insights into the role of the GABA(A)-benzodiazepine receptor in psychiatric disorder. *Br. J. Psychiatry* 179, 390–396. doi: 10.1192/bjp.179.5.390

Pellow, S. (1986). Anxiolytic and anxiogenic drug effects in a novel test of anxiety: are exploratory models of anxiety in rodents valid? *Methods Find Exp. Clin. Pharmacol.* 8, 557–565.

Peterson, G. L. (1977). A simplification of the protein assay method of Lowry et al. which is more generally applicable. *Anal. Biochem.* 83, 346–356. doi: 10.1016/0003-2697(77)90043-4

Pilc, A., Wierońska, J. M., and Skolnick, P. (2013). Glutamate-based antidepressants: preclinical psychopharmacology. *Biol. Psychiatry* 73, 1125–1132. doi: 10.1016/j.biopsych.2013.01.021

Reus, G. Z., Stringari, R. B., Kirsch, T. R., Fries, G. R., Kapczinski, F., Roesler, R., et al. (2010). Neurochemical and behavioural effects of acute and chronic memantine administration in rats: further support for NMDA as a new pharmacological target for the treatment of depression? *Brain Res. Bull.* 81, 585–589. doi: 10.1016/j.brainresbull.2009.11.013

Riaza Bermudo-Soriano, C., Perez-Rodriguez, M. M., Vaquero-Lorenzo, C., and Baca-Garcia, E. (2012). New perspectives in glutamate and anxiety. *Pharmacol. Biochem. Behav.* 100, 752–774. doi: 10.1016/j.pbb.2011.04.010

Sani, G., Serra, G., Kotzalidis, G. D., Romano, S., Tamorri, S. M., Manfredi, G., et al. (2012). The role of memantine in the treatment of psychiatric disorders other than the dementias: a review of current preclinical and clinical evidence. *CNS Drugs* 26, 663–690. doi: 10.2165/11634390-000000000-00000

Schroeter, M. L., Abdul-Khaliq, H., Sacher, J., Steiner, J., Blasig, I. E., and Mueller, K. (2010). Mood disorders are glial disorders: evidence from in vivo studies. *Cardiovasc. Psychiatry Neurol.* 2010:780645. doi: 10.1155/2010/780645

Schwartz, T. L., Siddiqui, U. A., and Raza, S. (2012). Memantine as an augmentation therapy for anxiety disorders. *Case Rep. Psychiatry* 2012:749796. doi: 10.1155/2012/749796

Silvestre, J. S., Nadal, R., Pallares, M., and Ferre, N. (1997). Acute effects of ketamine in the holeboard, the elevated-plus maze, and the social interaction test in Wistar rats. *Depress. Anxiety* 5, 29–33. doi: 10.1002/(SICI)1520-6394(1997)5:1<29::AID-DA5>3.0.CO;2-0

Solati, J. (2011). Dorsal hippocampal N-methyl-d-aspartate glutamatergic and delta-opioidergic systems modulate anxiety behaviors in rats in a noninteractive manner. *Kaohsiung J. Med. Sci.* 27, 485–493. doi: 10.1016/j.kjms.2011.06.011

Szabo, S. T., Machado-Vieira, R., Yuan, P., Wang, Y., Wei, Y., Falke, C., et al. (2009). Glutamate receptors as targets of protein kinase C in the pathophysiology and treatment of animal models of mania. *Neuropharmacology* 56, 47–55. doi: 10.1016/j.neuropharm.2008.08.015

Tariot, P. N., Farlow, M. R., Grossberg, G. T., Graham, S. M., Mcdonald, S., and Gergel, I. (2004). Memantine treatment in patients with moderate to severe Alzheimer disease already receiving donepezil: a randomized controlled trial. *JAMA* 291, 317–324. doi: 10.1001/jama.291.3.317

Thomazi, A. P., Godinho, G. F., Rodrigues, J. M., Schwalm, F. D., Frizzo, M. E., Moriguchi, E., et al. (2004). Ontogenetic profile of glutamate uptake in brain structures slices from rats: sensitivity to guanosine. *Mech. Ageing Dev.* 125, 475–481. doi: 10.1016/j.mad.2004.04.005

Wade, J., Mcdaid, L., Harkin, J., Crunelli, V., and Kelso, S. (2013). Biophysically based computational models of astrocyte ~ neuron coupling and their functional significance. *Front. Comput. Neurosci.* 7:44. doi: 10.3389/fncom.2013.00044

Zarate, C. Jr., Machado-Vieira, R., Henter, I., Ibrahim, L., Diazgranados, N., and Salvadore, G. (2010). Glutamatergic modulators: the future of treating mood disorders? *Harv. Rev. Psychiatry* 18, 293–303. doi: 10.3109/10673229.2010.511059

Zhou, Y., and Danbolt, N. C. (2014). Glutamate as a neurotransmitter in the healthy brain. *J. Neural. Transm.* 121, 799–817. doi: 10.1007/s00702-014-1180-8

Zimmer, E. R., Kalinine, E., Haas, C. B., Torrez, V. R., Souza, D. O., Muller, A. P., et al. (2012). Pretreatment with memantine prevents Alzheimer-like alterations induced by intrahippocampal okadaic acid administration in rats. *Curr. Alzheimer Res.* 9, 1182–1190. doi: 10.2174/156720512804142877

Conflict of Interest Statement: The authors declare that the research was conducted in the absence of any commercial or financial relationships that could be construed as a potential conflict of interest.

X

ANEXO II: Artigos publicados durante o período de doutoramento cujos temas não se relacionam diretamente a esta tese.

ANEXO II-A. *Peripheral Oxidative Stress Biomarkers in Spinocerebellar Ataxia Type 3/Machado-Joseph Disease*

No ANEXO II-A apresentamos o artigo publicado no periódico *Metabolic Brain Disease*

Metab Brain Dis (2015) 30:1279–1284
DOI 10.1007/s11011-015-9672-2

SHORT COMMUNICATION

Progression rate of myelopathy in X-linked adrenoleukodystrophy heterozygotes

Clarissa Troller Habekost[1,12] · Fernanda Santos Pereira[9] · Carmen Regla Vargas[2,4,7] · Daniella Moura Coelho[7] · Vitor Torrez[2] · Jean Pierre Oses[11] · Luis Valmor Portela[2,3] · Pedro Schestatsky[5,8] · Vitor Torres Felix[8] · Ursula Matte[1,10,12] · Vanessa Leotti Torman[6] · Laura Bannach Jardim[1,5,7,9,12]

Received: 2 January 2015 / Accepted: 17 April 2015 / Published online: 30 April 2015

Abstract X-linked adrenoleukodystrophy heterozygote women can present adult onset myeloneuropathy and little is known about its natural history. We aimed to describe the progression rate of the neurological impairment in the prospective follow-up of our cohort and to look for prognostic factors. The neurological scales Japanese Orthopaedic Association (JOA) and Severity Score System for Progressive Myelopathy (SSPROM) were applied at baseline in 29 symptomatic carriers and in follow-up visits. Age at onset, disease duration, X inactivation pattern, determination of the allele expressed, plasma levels of the very long chain fatty acids and of the neuron-specific enolase, and somatosensory evoked potentials, were taken at baseline. The slope of the linear regression of both JOA and SSPROM versus disease duration since the first symptom was estimated using mixed modeling. JOA and SSPROM decreased 0.42 and 1.87 points per year, respectively ($p<0.001$). None of the parameters under study influenced these rates. We estimated that the number of carriers per arm needed in a future 12 month trial with 80 % power and a 50 % reduction in disease progression would be 225 women for JOA and 750 for SSPROM. The progression rates of the studied neurological scales were small, did not depend on any modifier factor known, and reflected the characteristically slow worsening of symptoms in X-ALD heterozygotes. Better biomarkers are still necessary for future studies.

Clarissa Troller Habekost and Fernanda Santos Pereira contributed equally to this work.

Electronic supplementary material The online version of this article (doi:10.1007/s11011-015-9672-2) contains supplementary material, which is available to authorized users.

✉ Laura Bannach Jardim
ljardim@hcpa.ufrgs.br

[1] Post-Graduation Programs in Genetics and Molecular Biology, Porto Alegre, Brazil

[2] Post-Graduation Programs in Genetics and Biochemistry, Porto Alegre, Brazil

[3] Department of Biochemistry, Porto Alegre, Brazil

[4] Department of Analysis, Porto Alegre, Brazil

[5] Department of Internal Medicine, Porto Alegre, Brazil

[6] Department of Statistics, Universidade Federal do Rio Grande do Sul (UFRGS), Porto Alegre, Brazil

[7] Medical Genetics Service, Hospital de Clinicas de Porto Alegre, Rua Ramiro Barcelos 2350, 90.035-903 Porto Alegre, Brazil

[8] Neurology Service, Hospital de Clinicas de Porto Alegre, Porto Alegre, RS, Brazil

[9] Laboratory of Genetic Identification, Hospital de Clinicas de Porto Alegre, Porto Alegre, Brazil

[10] Laboratory of Gene Therapy, Hospital de Clínicas de Porto Alegre, Rio Grande do Sul, Brazil

[11] Laboratório de Neurociências Clínicas, Centro de Ciências da Vida e da Saúde, Universidade Católica de Pelotas, Centro, Brazil

[12] Instituto Nacional de Genética Médica Populacional (INAGEMP), Porto Alegre, Brazil

Keywords Female carrier · JOA · Natural History · SSPROM · X chromosome inactivation · X-linked Adrenoleukodystrophy

Abbreviations

ABCD1	Gene for the adenosine triphosphate (ATP)-binding cassette protein, subfamily D
cDNA	Complementary DNA
HUMARA	Human androgen-receptor locus
JOA	Japanese Orthopaedic Association
NH	Natural history
NSE	Neuron-specific enolase
OMIM	Online Mendelian Inheritance in Man
SSEP	Somato-sensory evoked potentials
SSPROM	Severity Score System for Progressive Myelopathy
VLCFA	Very long chain fatty acids
X-ALD	X-linked adrenoleukodystrophy

Introduction

X-linked adrenoleukodystrophy (X-ALD, OMIM #300100) is a peroxisomal disorder caused by defects in the gene for the adenosine triphosphate (ATP)-binding cassette protein, subfamily D (*ABCD1*) (Moser et al. 2001; Jangouk et al. 2012; Engelen et al. 2012; Horn et al. 2013), leading to accumulation of unbranched saturated very long chain fatty acids (VLCFA) in plasma and tissues and to diverse clinical presentations in males and females.

Heterozygote women might be asymptomatic or present with mild/moderate myeloneuropathy (Moser et al. 2001; Jangouk et al. 2012; Engelen et al. 2012; Mosser et al. 1994; Garg et al. 1983; Restuccia et al. 1997; Schmidt et al. 2001). We and others have recently reported results from cross-sectional studies, where there was a higher than expected proportion of symptomatic women (63 to 87 %), disability was mild, and symptoms were clearly related to ageing (Horn et al. 2013; Habekost et al. 2014; Engelen et al. 2014). As symptomatic individuals are very common among female heterozygotes, pharmacological management of heterozygotes will be needed, and clinical trials are expected.

Clinical evaluations have been efficient to detect neurological impairment in females (Habekost et al. 2014; Engelen et al. 2014). The myelopathy scales Japanese Orthopaedic Association (JOA) (Yonenobu et al. 2001) and Severity Score System for Progressive Myelopathy (SSPROM) (Castilhos et al. 2012) differentiated symptomatic from asymptomatic heterozygote women, and were correlated with age and with disease duration(DD) (Habekost et al. 2014). Since there is a lack of longitudinal or natural history (NH) of X-ALD females, we aimed to describe the progression rate of JOA and SSPROM scales in this prospective follow-up of our cohort and to relate it to factors such as age at onset, X inactivation pattern, plasma levels of VLCFA, neuron-specific enolase (NSE), and somato-sensory evoked potentials (SSEP), obtained at baseline.

Methods

Population

This is a prospective follow-up cohort of X-ALD of women whose cross-sectional findings have already been described (Habekost et al. 2014). All symptomatic heterozygotes diagnosed by our center in South Brazil were invited to be screened for other causes of myeloneuropathy. The heterozygotes whose symptoms were only attributed to X-ALD were invited to come for follow-up visits, when new neurological assessments were performed. Detailed information about population of origin was presented by Jardim et al. (Jardim et al. 2010). Exclusion criteria and baseline findings have been previously described (Habekost et al. 2014). This study was approved by the Institutional Bioethics Commission (GPPG-HCPA-110308) and all subjects gave written consent to participate.

Neurological assessments

At the baseline, heterozygote women were classified as symptomatic if complaints of neuropathic pain, paresthesia, sphincter dysfunction or paresis were present or as asymptomatic if these complaints were absent. To describe the NH of JOA and SSPROM scales, new assessments for the symptomatic females were planned at 6 month intervals. JOA and SSPROM scores varies from −2 to 17 and from 0 to 100 points, respectively; the higher scores correspond to the asymptomatic state. Developed to evaluate patients with degenerative cervical compression, JOA includes questions about motor disability of upper and lower limbs, about sensory losses and about sphincter function. SSPROM includes questions about these same domains, plus questions about motor strength and tonus/reflexes (Supplemental File 1). All examinations were carried out by the same examiner (CTH).

Neurophysiological testing and biochemical studies

At baseline, SSEP of the posterior tibial nerves produced the potentials P40 (for details, see (Habekost et al. 2014). Blood collections to measure plasma levels of the VLCFA C22:0, C24:0 and C26:0, and NSE, were obtained under fasting conditions (at least 3 h). VLCFA values of C26:0, of C26:0/C22:0, and of discriminant factor 3.805(C24:0/C22:0) +

5.296(C26:0/C22:0) + 5.15(C26:0) (Moser and Moser 1991; Moser et al. 1999), were studied. Details of all these methods were described in (Habekost et al. 2014).

X chromosome inactivation and cDNA studies

At baseline, peripheral blood was collected to assess the pattern of X chromosome inactivation. Genomic DNA was obtained by the salting out procedure (Miller et al. 1988) and X-inactivation patterns were assessed with the human androgen-receptor locus (HUMARA) methylation assay (Habekost et al. 2014; Allen et al. 1992).

Complementary DNA (cDNA) was obtained from women with skewed inactivation patterns (equal or larger than 75:25), in order to determine which allele was being preferably expressed. Peripheral blood was collected in PAXgene Blood RNA tubes (PreAnalytix, BD) and mRNA was extracted using PAXgene Blood RNA Kit (Qiagen). Then, 5 μg of RNA were converted to cDNA using *SuperScript II Reverse Transcriptase* and RNaseOUT (Invitrogen). Primers for exons 3, 6, 7 and 8, where the mutations carried by those with skewed inactivation patterns - p.Arg401Trp, p.Arg518Gln, p.Glu577X and p.Arg617His - are located, were used to amplify the cDNA. Amplified fragments were purified with Exo I-SAP (GE Healthcare) and submitted to automate sequencing on ABI 3100 using BigDye v3.1 (Applied Biosystems). Peak height at the site of heterozigosity was used to infer which allele was predominant (Wang et al. 2013).

Statistical analysis and determination of the progression rate of disease

To assess the disease progression rate, JOA and SSPROM scores of symptomatic women were studied. The slope of the linear regression of JOA and SSPROM versus disease duration since the start of the first symptom was estimated using mixed modeling, adjusting for repeated measurements.

Random coefficient models were adjusted to fit the growth curves. Some advantages of this model are that it dispenses equal intervals between assessments and that it incorporates patients with single measures - although it is not possible to estimate a slope for these patients, they contribute to estimate the intercept of the curves. This model fits curves for each subject, and the parameters of the individual curves are used to estimate group curves. Models were adjusted to the following explanatory variables: age at onset, VLCFA, NSE, SSEP and X inactivation pattern, at baseline.

Each model resulted in a mean adjusted line, represented by a graphic, showing JOA and/or SSPROM progression. Adjusted lines represented the whole group or its subgroups produced in accordance to prognostic variables. Where prognostic variables were continuous, percentiles were calculated, and a line for each value was produced in order to see the changes in JOA and/or SSPROM progression.

Estimates obtained from growth curves without covariates were used to calculate sample size needed in a future 12 month trial with 80 % power, expecting to reduce the progression to 50 %. The Zhang and Wang SAS macro were used (Zhang and Wang 2009).

All tests were two-sided and $p<0.05$ was considered significant. The statistical analyses were done using the Statistical Analysis Software SAS version 9.3.

Results

Twenty-nine out of 33 heterozygote women were symptomatic. General characteristics of the study population are depicted in Table 1. Only the symptomatic women were analyzed. None of them were on chronic management such as drugs for spasticity, or bladder dysfunctions.

The 29 baseline evaluations were obtained before May, 2013. Several subjects did not come back in 6 months, as planned; some of them came back 3–4 years later. A total of 21 follow up evaluations of JOA and SSPROM were obtained in a mean (range) interval of 9±3 (6 to 48) months. Fourteen women were evaluated once, nine were evaluated twice, and six women were evaluated three times. To assess disease progression, we used these 50 JOA and SSPROM scores (29 baseline plus 21 follow up evaluations). Individual raw data were presented in Supplemental File 2.

From the 29 symptomatic women, 17 were identified as informative women by HUMARA locus and capillary electrophoresis, at baseline. The median ratio of X-inactivation was 66:33. The five women with less skewing (percentile 25) had ratios lower than 60.25:39.75; the five more skewed women (percentile 75) had ratios higher than 72.5:27.5 (Table 1). Among these five women, four showed ratios greater than 75:25, but none showed highly skewed patterns (of more than 90:10). The results for cDNA sequencing for these four women can be seen on Supplemental Figure 3, which shows preferential pattern of expression, consistent with HUMARA results.

Disease progression and sample size estimations

Age at onset, VLCFA, skewed patterns of inactivation, NSE and SSEP at baseline were not related to different JOA or SSPROM progression rates (Supplemental Figures 1, 2 and 3).

With the obtained growth curves, the estimated value of JOA score at the disease onset was of 16.6 points, and the mean (SE) annual decrease (worsening) of JOA was of 0.42 points (0.048) ($p<0.001$, Fig. 1a). The estimated value of SSPROM score at the disease onset was of 96.5 points, and

Table 1 Clinical, biochemical and molecular characteristics of the X-ALD women, at baseline

	Values obtained in symptomatic women	Values obtained in asymptomatic carriers
Number of subjects	29	4
Age at onset of the first symptom mean±sd (range)	39.4±10 (21–59)	
Age (years) at examination mean±sd (range)	43.9±10.2 (24–61)	
Disease duration (years) mean±sd (range)	4.5±3.3 (1–15)	
JOA mean±sd (range: −2 to 17)	14.5±1.7	16.6±0.2
SSPROM mean±sd (range: 0 to 100)	86.6±7.9	98.4±1.1
SSPROM Motor Disability (range: 0 to 30 – normal) *based on the "overall disability sum score", ODSS* (Merkies et al. 2002)	27.3±2.6	30±0
SSPROM Motor Strength (0 to 20 – normal) *based on The Medical Research Council scale – 0 to 5 – for each limb* (Medical Research Council 1976)	17.5±5	19.1±1.3
SSPROM sensory losses (0 to 20 – normal)	16.1±2.3	18.5±9
SSPROM spasticity/hyperreflexia (0 to 10 – normal) *Adapted from Ashworth scale in a descending order* (Bohannon and Smith 1987).	5.7±1.8	9.4±1.2
SSPROM sphincter control (0 to 30 – normal) *Based on Kurtzke scale* (Kurtzke 1983)	17.8±2.3	27.6±2.6
SSEP N20 (ms) Mean±sd (normal: up to 20.5) [a]	20.1±4.2	18±0.9
SSEP P40 (ms) mean±sd (normal: up to 41.5) [a]	55.3±32.8	38.9±3.8
VLCFA C26:0 (um/L) mean±sd (normal: 0.78–1.54) [a]	1.93±0.42	
VLCFA C26:0/C22:0 mean±sd (normal: 0.01–0.03) [a]	0.076±0.028	
VLCFA discriminant factor [b] mean±sd (normal: up to 10.86)[a]	14.28±2.55	
NSE (ng/mL) mean±sd	12.95±7.3	7.2±7
Inactivation pattern of X chromosome in leukocytes: median (range)	66:34 (50:50 to 85:15)	
Skewed inactivation (>75:25)	4 carriers	

[a] Reference range in normal females

[b] Discriminant factor = 3.805(C24:0/C22:0) + 5.296(C26:0/C22:0) + 5.15(C26:0), as described by (Moser and Moser 1991; Moser et al. 1999)

the mean (SE) annual decrease (worsening) of SSPROM was of 1.87 points (0.22) ($p<0.001$, Fig. 1b).

The number of patients needed per arm in a future 12 months trial with 80 % power and that expects to reduce the neurological progression to 50 % in comparison to NH, would be 225 per arm for JOA, and 750 per arm for SSPROM.

Discussion

We were able to give a comprehensive quantitative account of the neurologic deterioration in X-ALD heterozygote women. Progression rate of JOA and SSPROMM was slow as expected, presented small variances, and no modifier factors were identified.

We have chosen to follow the NH of JOA and SSPROM because these scales cover both pyramidal, sphincter and sensory manifestations of a myelopathy, and because they correlated with age and with disease duration in the cross-sectional segment of this study (Habekost et al. 2014). Although we did not obtain follow-up evaluations from all women – some of them live in remote regions and were lost -, the range of the disease duration covered by the present cohort allowed a statistical model for disease progression. The study design produced a linear progression of neurologic disability. A non linear progression could not be detected by this study: although possible, however, there is no reason to anticipate different progression rates for different phases of this disease. Due to these findings, we believe that the present data is the best evidence on the NH of X-ALD heterozygote women.

The slow progression of the neurological impairments in X-ALD women is in agreement with its under recognition in general (Jangouk et al. 2012), and with the mild disabilities detected in recent studies (Habekost et al. 2014; Engelen et al. 2014). These progression rates might raise some doubt on the applicability of these scales in future clinical trials due to the large number of patients or the long follow up duration necessary for a measurable effect. Therefore, biomarkers that make future clinical trials feasible are needed.

Age at onset, the amount of the neurological damage (measured by SSEP of lower limbs and by NSE, at baseline), and the X inactivation patterns (directly measured by the proportion of active alleles; but also roughly estimated by the serum VLCFA levels) were our first candidates as modifier factors for the progression rate of this disease. All gave negative results.

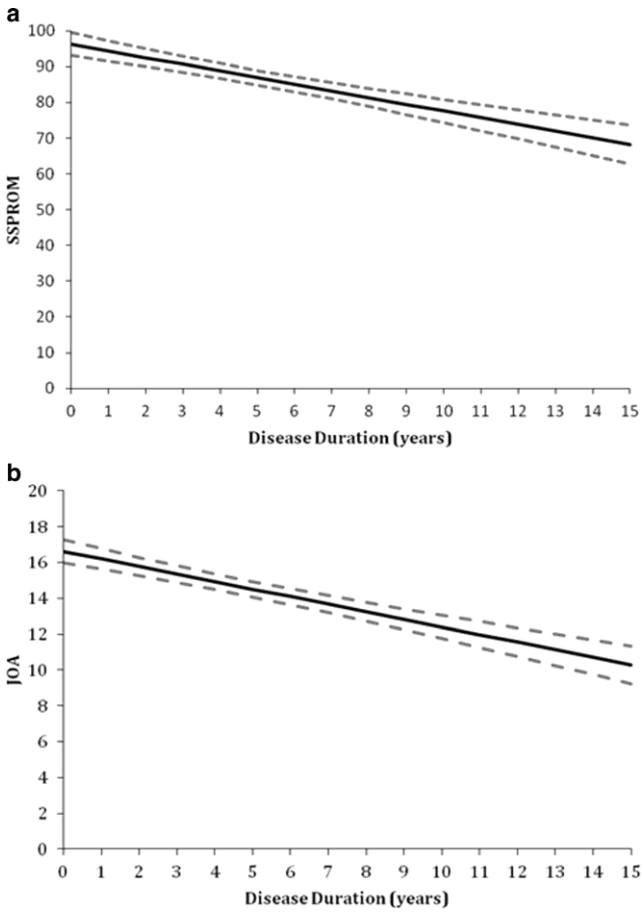

Fig. 1 The progression rate of (1A) JOA and (2) SSPROM scores of symptomatic women heterozygote for X-ALD, according to disease duration, in years. General growth curves (linear model)

We did not identify a factor that affects disease progression in females, but this should not discourage the search for better biomarkers in this rare disease, especially when facing the slow rate of neurologic progression. A traceable substance or biological variable that would change together with the neurological impairment, and whose responsiveness to disease progression and to a potential drug would be measurable, should be one of the important targets in the study of female carriers of X-ALD.

Acknowledgments We would like to thank the patients and their families for taking part in this study. We would also like to thank Raphael M. Castilhos and Deborah Blank for their technical assistance and contribution in early stages of this project; Karina C. Donis, André dos Anjos and Jonas Alex Saute for their contribution in recruiting some patients; and Ana Louzada for her technical assistance in the neurophysiological studies. This work was supported by Fundo de Incentivo à Pesquisa do Hospital de Clínicas de Porto Alegre (FIPE-HCPA), Project 110308; and by Instituto Nacional de Ciência e Tecnologia em Excitotoxicidade e Neuroproteção (INCTEN), Porto Alegre, Brazil. Habekost CT and Pereira FS were funded by Instituto Nacional de Genética Médica Populacional (INAGEMP). Pereira FS, Matte U, Portela LV, Vargas CR and Jardim LB are funded by Conselho Nacional de Desenvolvimento Científico e Tecnológico (CNPq).

Compliance with ethical standards All the authors report no disclosures. The names of funding organizations were presented in the acknowledgements section. This study was approved by the Institutional Bioethics Commission (GPPG-HCPA-110308) and all subjects gave written consent to participate.

Authors' contributions CTH participated in the design of the study, carried out the recruitment, interviews and clinical studies, and helped to draft the manuscript. FSP carried out the molecular genetic studies, participated in the analysis, and helped to draft the manuscript. PS carried out

the SSEP studies and participated in the analysis. PS and VTF carried out peripheral neurophysiology studies and participated in the analysis of the data. DMC performed VLCFA analyses and helped in the coordination of data. CRV performed VLCFA analyses and helped in the acquisition of funding. VT performed NSE analyses and participated in the analysis of data. LVP performed NSE studies and helped in the acquisition of funding. UM participated in the molecular analysis and in the coordination of data, and helped to draft the manuscript. VLT performed the statistical analyses, and helped to draft the manuscript. LBJ conceived the study, participated in the design and coordination of the study, helped to perform the statistical analysis, and drafted the manuscript. All authors read and approved the final manuscript.

References

Allen RC, Zoghbi HY, Moseley AB et al (1992) Methylation of HpaII and HhaI sites near the polymorphic CAG repeat in the human androgen-receptor gene correlates with X chromosome inactivation. Am J Hum Genet 51(6):1229–1239

Bohannon RW, Smith MB (1987) Interrater reliabiity of a modified Ashworth scale of muscle spasticity. Phys Ther 67:206–207

Castilhos RM, Blank D, Netto CB et al (2012) Severity score system for progressive myelopathy: development and validation of a new clinical scale. Braz J Med Biol Res 45(7):565–572

Engelen M, Kemp S, de Visser M, van Geel BM, Wanders RJ, Aubourg P, Poll-The BT (2012) X-linked adrenoleukodystrophy (X-ALD): clinical presentation and guidelines for diagnosis, follow-up and management. Orphanet J Rare Dis 7:51

Engelen M, Barbier M, Dijkstra IM et al (2014) X-linked adrenoleukodystrophy in women: a cross-sectional cohort study. Brain 137(Pt 3): 693–706. doi:10.1093/brain/awt361

Garg BP, Markand ON, DeMyer WE et al (1983) Evoked response studies in patients with adrenoleukodystrophy and heterozygous relatives. Arch Neurol 40:356–359

Habekost CT, Schestatsky P, Torres VF et al (2014) Neurological impairment among heterozygote women for X-linked Adrenoleukodystrophy: a case control study on a clinical, neurophysiological and biochemical characteristics. Orphanet J Rare Dis 9(1):6. doi:10.1186/1750-1172-9-6

Horn MA, Retterstol L, Abdelnoor M, Skjeldal OH, Tallaksen CM (2013) Adrenoleukodystrophy in Norway: high rate of de novo mutations and age-dependent penetrance. Pediatr Neurol 48:212–219

Jangouk P, Zackowski KM, Naidu S, Raymond GV (2012) Adrenoleukodystrophy in female heterozygotes: underrecognized and undertreated. Mol Genet Metab 105(2):180–185

Jardim LB, da Silva AC, Blank D, Villanueva MM, Renck L, Costa ML, Vargas CR, Deon M, Coelho D, Vedolin L, de Castro CG Jr, Gregianin L, Bonfim C, Giugliani R (2010) X-linked adrenoleukodystrophy: clinical course and minimal incidence in South Brazil. Brain Dev 32(3):180–190

Kurtzke JF (1983) Rating neurologic impairment in multiple sclerosis: an expanded disability status scale (EDSS). Neurology 33:1444–1452

Medical Research Council (1976) Aids to the examination of the peripheral nervous system. Memorandum No 45. Her Majesty's Stationery Office, London

Merkies ISJ, Schmitz PIM, van der Meché FGA et al (2002) Clinimetric evaluation of a new overall disability scale in immune mediated polyneuropathies. J Neurol Neurosurg Psychiatry 72:596–601

Miller SA, Dykes DD, Polesky HF (1988) A simple salting out procedure for extracting DNA from human nucleated cells. Nucleic Acids Res 16(3):1215

Moser HW, Moser AB (1991) Measurement of saturated very long chain fatty acid in plasma. In: Hommes FA (ed) Techniques of diagnostic human biochemical genetics. Wiley, New York

Moser AB, Kreiter N, Bezman L et al (1999) Plasma very long chain fatty acids in 3,000 peroxisome disease patients and 29,000 controls. Ann Neurol 45(1):100–110

Moser H, Smith K, Watkins P et al (2001) X-linked adrenoleukodystrophy. In: Scriver C, Beaudet A, Sly W, Valle D (eds) The metabolic and molecular bases of inherited disease. McGraw-Hill, New York, pp 3257–3301

Mosser J, Lutz Y, Stoeckel ME et al (1994) The gene responsible for adrenoleukodystrophy encodes a peroxisomal membrane protein. Hum Mol Genet 3(2):265–271

Restuccia D, Di Lazzaro V, Valeriani M et al (1997) Neurophysiological abnormalities in adrenoleukodystrophy carriers. Evidence of different degrees of central nervous system involvement. Brain 120(Pt 7): 1139–1148

Schmidt S, Träber F, Block W et al (2001) Phenotype assignment in symptomatic female carriers of X-linked adrenoleukodystrophy. J Neurol 248(1):36–44

Wang Z, Yan A, Lin Y et al (2013) Familial skewed x chromosome inactivation in adrenoleukodystrophy manifesting heterozygotes from a Chinese pedigree. PLoS One 8(3), e57977

Yonenobu K, Abumi K, Negata K et al (2001) Interobserver and intraobserver reliability of the Japanese orthopaedic association scoring system for evaluation of cervical compression myelopathy. Spine 26:1890–1895

Zhang Z, Wang L (2009) Statistical power analysis for growth curve models using SAS. Behav Res Methods 41(4):1083–1094

ANEXO II-B. *Progression rate of myelopathy in X-linked adrenoleukodystrophy heterozygotes*

No ANEXO II-B apresentamos o artigo publicado no periódico *Frontiers in Neurology*

frontiers in Neurology

ORIGINAL RESEARCH
published: 20 September 2017
doi: 10.3389/fneur.2017.00485

Peripheral Oxidative Stress Biomarkers in Spinocerebellar Ataxia Type 3/Machado–Joseph Disease

Adriano M. de Assis[1,2†], Jonas Alex Morales Saute[3,4,5,6,7†], Aline Longoni[1], Clarissa Branco Haas[1], Vitor Rocco Torrez[1], Andressa Wigner Brochier[1], Gabriele Nunes Souza[4], Gabriel Vasata Furtado[6,8], Tailise Conte Gheno[6,8], Aline Russo[4], Thais Lampert Monte[3,5], Raphael Machado Castilhos[8], Artur Schumacher-Schuh[5,8], Rui D'Avila[4], Karina Carvalho Donis[4], Carlos Roberto de Mello Rieder[3,5,9], Diogo Onofre Souza[1,10], Suzi Camey[11,12], Vanessa Bielefeldt Leotti[11,12], Laura Bannach Jardim[3,4,6,7,8] and Luis Valmor Portela[1,10]*

[1] Programa de Pós-Graduação em Ciências Biológicas: Bioquímica, Universidade Federal do Rio Grande do Sul (UFRGS), Porto Alegre, Brazil, [2] Programa de Pós-Graduação em Saúde e Comportamento, Centro de Ciências da Vida e da Saúde, Universidade Católica de Pelotas (UCPel), Pelotas, Brazil, [3] Programa de Pós-Graduação em Medicina: Ciências Médicas, Universidade Federal do Rio Grande do Sul (UFRGS), Porto Alegre, Brazil, [4] Serviço de Genética Médica, Hospital de Clínicas de Porto Alegre (HCPA), Porto Alegre, Brazil, [5] Serviço de Neurologia, Hospital de Clínicas de Porto Alegre (HCPA), Porto Alegre, Brazil, [6] Laboratório de Identificação Genética, Hospital de Clínicas de Porto Alegre (HCPA), Porto Alegre, Brazil, [7] Departamento de Medicina Interna, Universidade Federal do Rio Grande do Sul (UFRGS), Porto Alegre, Brazil, [8] Programa de Pós-Graduação em Genética e Biologia Molecular, Universidade Federal do Rio Grande do Sul (UFRGS), Porto Alegre, Brazil, [9] Departamento de Neurologia, Universidade Federal de Ciências da Saúde de Porto Alegre (UFCSPA), Porto Alegre, Brazil, [10] Departamento de Bioquímica, Instituto de Ciências Básicas da Saúde (ICBS), Universidade Federal do Rio Grande do Sul (UFRGS), Porto Alegre, Brazil, [11] Programa de Pós-Graduação em Epidemiologia, Universidade Federal do Rio Grande do Sul (UFRGS), Porto Alegre, Brazil, [12] Departamento de Estatística, Universidade Federal do Rio Grande do Sul (UFRGS), Porto Alegre, Brazil

OPEN ACCESS

Edited by:
Mark Mapstone,
University of California, Irvine,
United States

Reviewed by:
Pedro Ribeiro,
Federal University of
Rio de Janeiro, Brazil
Silmar Teixeira,
Federal University of
Piauí, Brazil
E. Lezi,
Duke University,
United States

***Correspondence:**
Jonas Alex Morales Saute
jsaute@hcpa.edu.br

[†]These authors have contributed equally to this work.

Specialty section:
This article was submitted to Movement Disorders, a section of the journal Frontiers in Neurology

Received: 10 March 2017
Accepted: 31 August 2017
Published: 20 September 2017

Citation:
de Assis AM, Saute JAM, Longoni A, Haas CB, Torrez VR, Brochier AW, Souza GN, Furtado GV, Gheno TC, Russo A, Monte TL, Castilhos RM, Schumacher-Schuh A, D'Avila R, Donis KC, de Mello Rieder CR, Souza DO, Camey S, Leotti VB, Jardim LB and Portela LV (2017) Peripheral Oxidative Stress Biomarkers in Spinocerebellar Ataxia Type 3/Machado–Joseph Disease. Front. Neurol. 8:485. doi: 10.3389/fneur.2017.00485

Objectives: Spinocerebellar ataxia type 3/Machado–Joseph disease (SCA3/MJD) is a polyglutamine disorder with no current disease-modifying treatment. Conformational changes in mutant ataxin-3 trigger different pathogenic cascades, including reactive oxygen species (ROS) generation; however, the clinical relevance of oxidative stress elements as peripheral biomarkers of SCA3/MJD remains unknown. We aimed to evaluate ROS production and antioxidant defense capacity in symptomatic and presymptomatic SCA3/MJD individuals and correlate these markers with clinical and molecular data with the goal of assessing their properties as disease biomarkers.

Methods: Molecularly confirmed SCA3/MJD carriers and controls were included in an exploratory case–control study. Serum ROS, measured by 2′,7′-dichlorofluorescein diacetate (DCFH-DA) as well as superoxide dismutase (SOD) and glutathione peroxidase (GSH-Px) antioxidant enzyme activities, levels were assessed.

Results: Fifty-eight early/moderate stage symptomatic SCA3/MJD, 12 presymptomatic SCA3/MJD, and 47 control individuals were assessed. The DCFH-DA levels in the symptomatic group were 152.82 nmol/mg of protein [95% confidence interval (CI), 82.57–223.08, $p < 0.001$] higher than in the control and 243.80 nmol/mg of protein (95% CI, 130.64–356.96, $p < 0.001$) higher than in the presymptomatic group. The SOD activity in the symptomatic group was 3 U/mg of protein (95% CI, 0.015–6.00, $p = 0.048$)

lower than in the presymptomatic group. The GSH-Px activity in the symptomatic group was 13.96 U/mg of protein (95% CI, 5.90–22.03, $p < 0.001$) lower than in the control group and 20.52 U/mg of protein (95% CI, 6.79–34.24, $p < 0.001$) lower than in the presymptomatic group and was inversely correlated with the neurological examination score for spinocerebellar ataxias ($R = -0.309$, $p = 0.049$).

Conclusion: Early/moderate stage SCA3/MJD patients presented a decreased antioxidant capacity and increased ROS generation. GSH-Px activity was the most promising oxidative stress disease biomarker in SCA3/MJD. Further longitudinal studies are necessary to identify both the roles of redox parameters in SCA3/MJD pathophysiology and as surrogate outcomes for clinical trials.

Keywords: spinocerebellar ataxia type 3, Machado–Joseph disease, oxidative stress, reactive oxygen species, polyglutamine disorders

INTRODUCTION

Machado–Joseph disease (MJD), also referred to as spinocerebellar ataxia type 3 (SCA3/MJD), is an autosomal dominant neurodegenerative disorder caused by a CAG repeat expansion (CAGexp) at *ATXN3*, the gene that codes for ataxin-3. SCA3/MJD is part of the so-called group of polyglutamine (PolyQ) disorders (1); it is the most common form of SCA worldwide (2), with a minimal prevalence of 6:100,000 in Rio Grande do Sul, Brazil (3, 4).

Spinocerebellar ataxia type 3/Machado–Joseph disease onset typically occurs at approximately 32–40 years of age (2, 3, 5, 6). Gait ataxia is the main neurological sign; however, ataxia subsequently affects speech, swallowing, and limb coordination. Pyramidal, extrapyramidal, and peripheral nerve findings also occur during the disease course (1). The median survival time after onset is 21 years (7).

Expansion of the polyQ tract induces conformational changes in ataxin-3, which affects many properties of the protein, including stability and degradation (8), subcellular localization (9), molecular interactions with other proteins (10–12), and propensity to aggregate (9).

Aggregates of mutant polyQ proteins may be taken up by neuronal mitochondria, which leads to disturbances in the membrane potential and a subsequent increase in reactive oxygen species (ROS) production (13). Recent studies have demonstrated an imbalance between the ROS production and antioxidant defense capacity in patients and cellular models of SCA3/MJD, linking these abnormalities to the neurodegenerative process of the disease (12–15). In addition, oxidative stress increases ataxin-3 nuclear localization (16), a crucial step for SCA3/MJD *in vivo* phenotypic manifestation (17).

Natural history (NH) studies with well-validated SCA scales have indicated a very slow progression of ataxic and non-ataxic signs in SCA3/MJD (18–20) and have stressed the need for large sample sizes to test disease-modifying therapies in future randomized clinical trials (RCTs) (18–24). Surrogate biomarkers may hasten RCT and drug discoveries for SCA3/MJD, a disorder with no modifying treatment to date. The potential clinical relevance of oxidative stress elements as peripheral biomarkers of SCA3/MJD in patients has rarely been addressed (12, 15).

Considering the hypothesis of an oxidative stress imbalance in SCA3/MJD that may precede disease onset, we aimed to evaluate the peripheral ROS production and antioxidant defense capacity in symptomatic and presymptomatic SCA3/MJD individuals and a control population. We also evaluated the relationship of these markers with clinical and molecular data, with the goal to assess their properties as disease biomarkers.

MATERIALS AND METHODS

Population, Design, and Eligibility Criteria

Symptomatic patients with a molecular diagnosis of SCA3/MJD or asymptomatic individuals with a normal neurological examination at 50% risk of SCA3/MJD on the basis of an affected first-degree relative who were seeking presymptomatic testing were recruited for this single-site, exploratory, case–control study at the Neurogenetics outpatients clinic, Hospital de Clinicas de Porto Alegre, from May 2011 to July 2013.

The data for symptomatic patients were collected during the baseline assessments of a RCT, in which a disease duration of more than 10 years and an inability to walk independently (canes, sticks, or walkers were allowed) were exclusion criteria (23). The control group consisted of previously at-risk individuals who did not carry CAG_{exp} at *ATXN3* plus healthy unrelated individuals with age, gender, and environmental characteristics similar to symptomatic individuals. Thyroid, renal, or hepatic disorders or a history of other significant neurological or systemic medical disorders were also exclusion criteria.

Molecular and Clinical Evaluations

The *ATXN3* expanded region was analyzed as previously described (25). The Neurological Examination Score for Spinocerebellar Ataxias (NESSCA) (26) and the Scale for the Assessment and Rating of Ataxia (SARA) (27) were performed in all symptomatic individuals. The disease duration and age at disease onset of first symptom were provided by the patients and/or relatives. The median estimated age at onset of the presymptomatic group was calculated with the individuals' current age and CAG_{exp} length in *ATXN3*, as previously reported (28).

Sample Collection

Biological material collection was performed between 8 a.m. and 4 p.m. under fasting conditions. Serum was obtained *via* blood centrifugation at 6,000 × *g* for 5 min, frozen immediately, and stored at −80°C until analysis.

Redox Assays

All samples and standards were measured in triplicate with variation coefficients <10%.

ROS Levels

To assess the ROS levels, 2′,7′-dichlorofluorescein diacetate (DCFH-DA) (Sigma-Aldrich, St. Louis, MO, USA) was used as a probe (29). An aliquot of the serum sample (60 µl) was incubated with DCFH-DA (final concentration 100 µM) at 37°C, in the dark, for 30 min. DCFH oxidation was measured fluorimetrically, using 488 nm excitation and 525 nm emission wave lengths. A standard curve using standard DCF (Sigma-Aldrich, St. Louis, MO, USA) (0.25–10 mM) was performed in parallel with the samples, and the results were expressed as nanomoles per milligram protein.

Antioxidant Enzyme Activities

The superoxide dismutase (SOD) (EC 1.15.1.1) activity was assessed by quantifying the inhibition of superoxide-dependent auto-oxidation of epinephrine and analyzing the absorbance of the samples at 480 nm. In microplate wells that contained serum samples (30 µl–60 µg of protein), 140 µl of glycine buffer (final concentration 50 mM; pH 10.2) and 10 µl of catalase (Sigma-Aldrich, St. Louis, MO, USA) (EC 1.11.1.6) (final concentration 10 µM) were added. In standard wells, only 180 µl of glycine buffer (final concentration 50 mM; pH 10.2) and 10 µl of catalase were added (final concentration 10 µM). The reaction was initiated by the addition of 10 µl of epinephrine (Sigma-Aldrich, St. Louis, MO, USA) (final concentration 60 mM) in all wells. The zero time absorbance was obtained at 480 nm, followed by recording the absorbance after 10 min at 32°C. The SOD activity unit was defined as the required enzyme amount to inhibit epinephrine oxidation by 50%. Data were expressed as units per milligram protein (29).

The glutathione peroxidase (GSH-Px, EC 1.11.1.9) activity was measured in a 96-well plate according to the method described by Wendel (30) using tert-butyl hydroperoxide as the substrate (Sigma-Aldrich, St. Louis, MO, USA). Nicotinamide adenine dinucleotide phosphate (NADPH) disappearance was monitored spectrophotometrically at 340 nm in a medium that contained (final concentrations): 2 mM of reduced glutathione (GSH), 0.15 U/ml glutathione reductase (GR) (EC 1.8.1.7), 0.4 mM azide, 0.5 mM tert-butyl hydroperoxide, and 0.1 mM NADPH plus serum sample (40 µl–80 µg of protein). One GSH-Px unit was defined as 1 µmol of NADPH consumed per minute, and the specific activity is represented as units per milligram of protein.

Statistical Analysis

All investigated variables showed a normal distribution *via* a one-sample Kolmogorov–Smirnov test. The baseline characteristics among the groups were compared with ANOVA, independent samples *t*-test or chi-square test. The ROS levels and antioxidant enzyme activities among the groups were compared using the Generalized Linear Model (GLM) corrected for age. Differences between the specific groups in the GLM were assessed using Wald chi-square with Bonferroni correction for multiple comparisons. Correlations were performed with the Pearson correlation test, followed by a linear regression model when required. Statistical significance was defined as $p < 0.05$.

The *Z*-score was calculated using the following formula:

$$Z = \frac{x - \mu}{\sigma}$$

where x is the sample value (raw score), μ is the population mean, and σ is the standard deviation of the population. The absolute value of *Z* represents the distance between the raw score and the population mean in units of SD (31).

Ethics

The study was approved by the Ethics in Research Committee of our institution (register number 10-513). Written informed consent was obtained from all subjects prior to participation.

RESULTS

Fifty-eight individuals comprised the early/moderate stage symptomatic SCA3/MJD group, 12 individuals comprised the asymptomatic SCA3/MJD group, and 47 individuals comprised the healthy control group (9 related and 38 unrelated to the SCA3/MJD individuals). The clinical and demographic characteristics are described in **Table 1**.

The serum DCFH-DA levels ($p < 0.001$) and the SOD ($p = 0.026$) and GSH-Px ($p < 0.001$) activities were different among some of the groups (**Figures 1** and **2**, Table S1 in Supplementary Material).

The levels of the ROS marker DCFH-DA in the symptomatic group were 152.82 nmol/mg of protein [95% confidence interval (CI), 82.57–223.08, $p < 0.001$] higher than in the control and

TABLE 1 | Demographics of the enrolled individuals.

	Healthy controls	Symptomatic SCA3/MJD	Presymptomatic	
	Mean (SD)	Mean (SD)	Mean (SD)	*p*
N	47	58	12	
Age (years)	40.7 (13.3)	40.6 (9.6)	32.4 (8.1)	0.053[a]
Female sex (*n*, %)	27 (57.4)	29 (48.3)	7 (58.3)	0.596[b]
Age at onset (years)	–	34.5 (9.1)	–	
Disease duration (years)	–	5.3 (2.5)	–	
CAG_{exp} length	–	75.4 (3.2)	73.5 (3.0)	0.071[c]
NESSCA	–	14.2 (4.8)	–	
SARA	–	9.7 (4.1)	–	
Predicted disease onset (years)	–	–	5.5 (2.1)	

[a]*ANOVA.*
[b]*Chi-square.*
[c]*Student's t-test.*
NESSCA, Neurological Examination Score for Spinocerebellar Ataxias; SARA, Scale for the Assessment and Rating of Ataxia; SCA3/MJD, spinocerebellar ataxia type 3/Machado–Joseph disease.

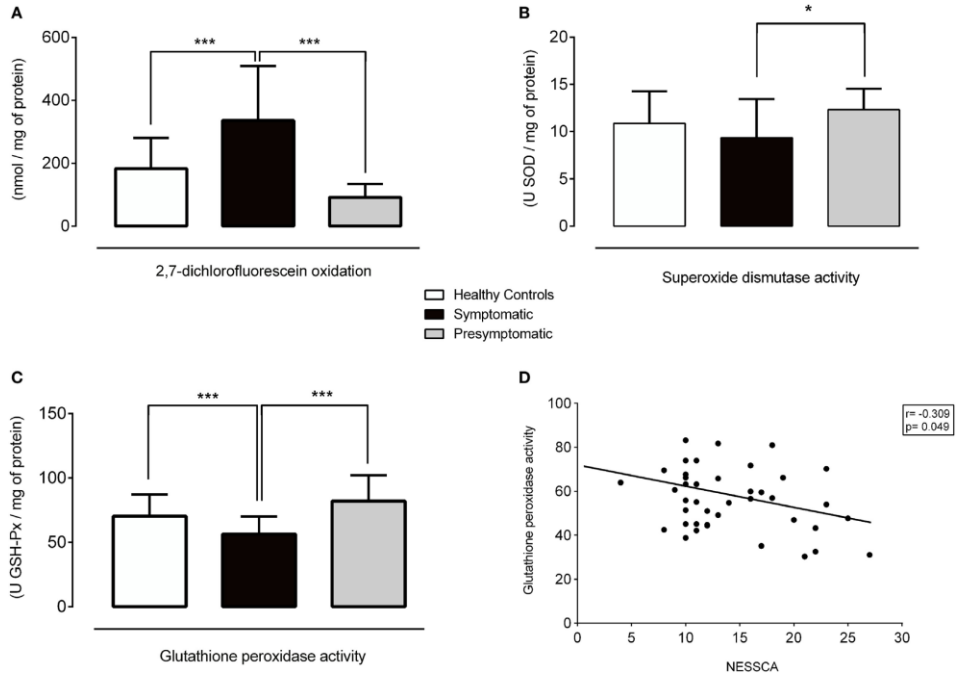

FIGURE 1 | Redox parameters in healthy controls, symptomatic, and presymptomatic SCA3/MJD individuals. **(A)** ROS levels, **(B)** SOD activity, **(C)** GSH-Px activity and **(D)** Correlation between GSH-Px and NESSCA. Values are presented as the means, and error bars represent standard error; $^{*}p < 0.05$ and $^{***}p < 0.001$. GSH-Px, glutathione peroxidase; NESSCA, Neurological Examination Score for Spinocerebellar Ataxias; ROS, reactive oxygen species; SCA3/MJD, spinocerebellar ataxia type 3/Machado–Joseph disease; SOD, superoxide dismutase.

243.80 nmol/mg of protein (95% CI, 130.64–356.96, $p < 0.001$) higher than in the presymptomatic group. The DCFH-DA levels were similar between the presymptomatic SCA3/MJD and control individuals (90.97 nmol/mg of protein, 95% CI, −21.83 to 203.79, $p = 0.161$). Refer to **Figures 1A** and **2A**.

The SOD activity was 3 U SOD/mg of protein (95% CI, 0.015–6.00, $p = 0.048$) lower in the symptomatic than that of the presymptomatic SCA3/MJD group. There were no differences in the SOD activity between the symptomatic SCA3/MJD and control groups (1.51 U SOD/mg of protein, 95% CI, −0.37 to 3.39, $p = 0.165$) or the presymptomatic SCA3/MJD and control groups (1.49 U SOD/mg of protein, 95% CI, −1.51 to 4.50, $p = 0.700$). Refer to **Figures 1B** and **2A**.

The GSH-Px activity in the symptomatic SCA3/MJD was 13.96 U GSH-Px/mg of protein (95% CI, 5.90–22.03, $p < 0.001$) lower than in the control and 20.52 U GSH-Px/mg of protein (95% CI, 6.79–34.24, $p < 0.001$) lower than in the presymptomatic SCA3/MJD group. The GSH-Px activity was similar between the presymptomatic SCA3/MJD and control groups (6.55 U GSH-Px/mg of protein, 95% CI, −7.19 to 20.30, $p = 0.762$). Refer to **Figures 1C** and **2A**.

Oxidative Stress Parameter Correlations with Clinical and Molecular Findings

The DCFH-DA levels and SOD activity did not correlate with the clinical features or molecular data in the symptomatic group (Figure S1 in Supplementary Material). The GSH-Px activity exhibited an inverse correlation with the NESSCA severity in the symptomatic group ($R = -0.309$, $p = 0.049$, **Figure 1D**), i.e., lower levels of GSP-Px activity were identified in the patients with more severe disease. No significant correlations of oxidative stress markers with predicted age of onset or CAG expansion length were identified in the presymptomatic SCA3/MJD group ($p > 0.05$ for all comparisons, Figure S2 in Supplementary Material).

DISCUSSION

This study evaluated redox parameters in a representative sample of symptomatic SCA3/MJD patients and presymptomatic carriers. The ROS marker DCFH-DA was higher in the symptomatic SCA3/MJD individuals; the activity of the antioxidant enzyme GSH-Px was lower in the symptomatic SCA3/MJD group and

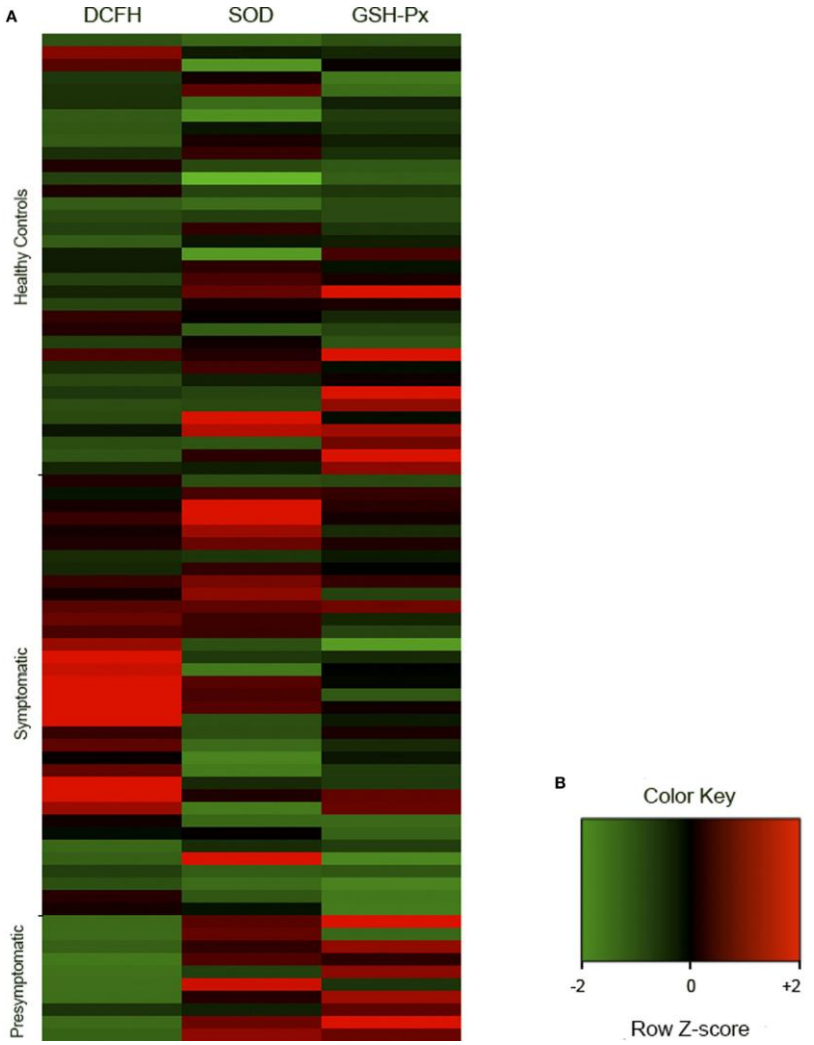

FIGURE 2 | Representative cluster of the redox analyses in healthy controls (n = 35), symptomatic (n = 35), and presymptomatic (n = 10) SCA3/MJD individuals. The results were analyzed as Z-score values. Z is negative when the sample value is below the population mean and positive when it is above the mean. **(A)** Each square represents one individual. DCFH-DA, 2′,7′-dichlorofluorescein diacetate; GSH-Px, glutathione peroxidase; SCA3/MJD, spinocerebellar ataxia type 3/Machado–Joseph disease; SOD, superoxide dismutase. **(B)** Color key of row z-score.

was associated with the disease severity; the presymptomatic carriers presented a higher activity of the antioxidant enzyme SOD than the symptomatic SCA3/MJD patients. Overall, these results indicate a pro-oxidative stress state in the early/moderate stages of SCA3/MJD and a potential antioxidant defense response in presymptomatic carriers.

In the present study, we identified higher ROS in the symptomatic SCA3/MJD patients measured by the DCFH-DA serum levels. The lack of correlations between the DCFH-DA levels and clinical or molecular data should be considered in the perspective of a peripheral marker for a disease that mainly affects the CNS. Nevertheless, our results differed from a clearly underpowered

case–control study (seven SCA3/MJD and seven control individuals) that reported no differences in the DCFH-DA levels between groups (15).

Oxidative stress damage has been involved in several pathological processes that affect various organs and tissues. Specifically, the brain is particularly vulnerable as denoted by many neurodegenerative diseases of which oxidative stress has been implicated in the pathogenesis (16, 32). As previously stated, neuronal mitochondria function may be directly impaired by polyQ aggregates, which may lead to increased ROS generation (13). Alternatively or simultaneously, ROS may increase in SCA3/MJD as a result of a direct failure of antioxidant enzymes.

In our study, we identified higher SOD activity in the presymptomatic than early/moderate stages of symptomatic SCA3/MJD individuals. Furthermore, the GSH-Px activity was lower in the symptomatic SCA3/MJD group, and these lower levels were correlated with greater disease severity as measured *via* the ataxia and non-ataxia sign scale NESSCA. Pacheco et al. (15) identified similar results, in which the thiol levels, an indirect measure of GSH-Px activity, were lower in SCA3/MJD patient sera. Therefore, the GSH-Px activity was the most promising oxidative stress disease biomarker in SCA3/MJD, and our results strengthened the findings of previous indirect studies on the GSH-Px activity and present novel data that correlated this marker with disease severity.

According to our data, significant oxidative stress was only present after disease onset, and we speculate whether a failure/exhaustion in antioxidant defense mechanisms (depicted by an increased activity of SOD in the presymptomatic stages) may play a role in disease onset. Higher peripheral SOD activity in presymptomatic individuals than controls was a remarkable finding that departs from the previous scenarios. The hypothesis of an antioxidant defense response present in presymptomatic carriers is appealing, particularly in face of preliminary evidence that suggests alterations in other pathways are present in the preclinical phases of this disease (33). Nevertheless, it remains necessary to determine whether high SOD activity in the prodromal phases represents a phenomenon common to other tissues, such as the CNS. However, we emphasize that experimental evidence indicates a link between oxidative stress and SCA3/MJD pathology. The brain has a cellular defense system against oxidative stress, which includes high levels of several antioxidant enzymes, including SOD, GSH-Px, GSH reductase, and catalase (14). GSH plays predominant roles in the removal of excess H_2O_2 from the brain (14), as well as SOD in the removal of O_2^- (32). Lower GSH levels and decreased activity of GSH reductase, catalase, and SOD were previously identified in mutant SCA3/MJD cell lines compared with wild-type cells, which suggests that mutant ataxin-3 may influence the activity of enzymatic components to efficiently remove both O_2^- and H_2O_2 (14). Ataxin-3 binds to target gene promoters and modulates transcription by interacting with transcriptional regulators. During oxidative stress, ataxin-3 and forkhead box O (FOXO) transcription factor FOXO4 translocate to the nucleus, concomitantly bind to the SOD2 gene promoter and increase the expression of the antioxidant enzyme SOD2. Mutant ataxin-3 has a reduced capability to activate FOXO4-mediated SOD2 expression (12). The downregulation of SOD2 was confirmed in pons tissue and lymphoblastoid cell lines of SCA3/MJD patients. In SCA3/MJD patient lymphoblastoid cell lines, an impairment to upregulate SOD2 expression in association with a significant increase in ROS formation and cytotoxicity were reported, which suggests that a decreased antioxidant capacity and increased susceptibility toward oxidative stress contribute to neuronal cell death (12).

The general characteristics of the recruited sample were similar to the local SCA3/MJD population (4), such as the gender proportion, age at onset, and range of CAGexp. Despite several strengths, our study has several limitations. As we designed an exploratory case–control study, no primary outcome was elected, and no sample size calculation or study power determinations were performed. We conducted an exploratory study because of the lack of data on redox markers in SCA3/MJD patients and we would not have available the number of presymptomatic individuals necessary for an adequately powered study. As our sample sizes are one of the largest on biomarker studies of this disorder, the number of recruited individuals represents one of the study's merits.

In conclusion, early/moderate stage symptomatic SCA3/MJD patients presented a similar peripheral redox profile to the previously reported SCA3/MJD cellular models: a decreased antioxidant capacity and an increased production of ROS. Additional collaborative studies with larger sample sizes of presymptomatic individuals and a prospective design may help to uncover the NH of these markers and their roles as surrogate (disease or treatment) biomarkers for future clinical trials, as well as understand the association between the failure of the antioxidant defense and disease onset and its potential therapeutic implications.

ETHICS STATEMENT

The study was approved by the Ethics in Research Committee of our institution (register number 10-513). Informed written consent was obtained from all subjects prior participation.

AUTHOR CONTRIBUTIONS

AM and JA were responsible for the design, acquisition, analysis, interpretation, drafting, and approval of the final version of the manuscript. AL, CH, VRT, AB, GS, GF, TG, AR, TM, RC, AS, RD, KD, SC, and VBL were responsible for acquisition, analysis, interpretation, and approval of the final version of the manuscript. DS and CM were responsible for interpretation, drafting, critical revision, and approval of the final version of the manuscript. LJ and LP were responsible for the design, interpretation, drafting, critical revision, and approval of the final version of the manuscript.

FUNDING

This study was supported by FAPERGS (09/0078-5 and 17/2551-0000516-3), CNPq (478888/2010-4 and 465671/2014-4), and FIPE-HCPA (10-513). JS and GF were supported by CAPES. TG, GS, LP, CR, and LJ were supported by CNPq. The authors would like to thank the patients and families who participated in the study.

SUPPLEMENTARY MATERIAL

The Supplementary Material for this article can be found online at http://journal.frontiersin.org/article/10.3389/fneur.2017.00485/full#supplementary-material.

FIGURE S1 | Correlations of redox parameters with clinical and molecular data in the symptomatic SCA3/MJD group. *$p < 0.05$. DCFH, 2′,7′-dichlorofluorescein diacetate; GSH-Px, glutathione peroxidase; NESSCA, Neurological Examination Score for Spinocerebellar Ataxias; SARA, Scale for the Assessment and Rating of Ataxia; SCA3/MJD, spinocerebellar ataxia type 3/Machado–Joseph disease; SOD, superoxide dismutase.

FIGURE S2 | Correlations of redox parameters with clinical and molecular data in the presymptomatic SCA3/MJD group. Predicted time to onset (in years) was calculated with the formula: current age—predicted age of onset [according to Ref. (28)]. DCFH, 2′,7′-dichlorofluorescein diacetate; GSH-Px, glutathione peroxidase; SCA3/MJD, spinocerebellar ataxia type 3/Machado–Joseph disease; SOD, superoxide dismutase.

REFERENCES

1. Saute JAM, Jardim LB. Machado Joseph disease: clinical and genetic aspects, and current treatment. *Expert Opin Orphan Drugs* (2015) 3:517–35. doi:10.1517/21678707.2015.1025747
2. Sequeiros J, Martins S, Silveira I. Epidemiology and population genetics of degenerative ataxias. *Handb Clin Neurol* (2012) 103:227–51. doi:10.1016/B978-0-444-51892-7.00014-0
3. de Castilhos RM, Furtado GV, Gheno TC, Schaeffer P, Russo A, Barsottini O, et al. Spinocerebellar ataxias in Brazil – frequencies and modulating effects of related genes. *Cerebellum* (2014) 13:17–28. doi:10.1007/s12311-013-0510-y
4. Souza GN, Kersting N, Krum-Santos AC, Santos AS, Furtado GV, Pacheco D, et al. Spinocerebellar ataxia type 3/Machado-Joseph disease: segregation patterns and factors influencing instability of expanded CAG transmissions. *Clin Genet* (2016) 90(2):134–40. doi:10.1111/cge.12719
5. Durr A, Stevanin G, Cancel G, Duyckaerts C, Abbas N, Didierjean O, et al. Spinocerebellar ataxia 3 and Machado-Joseph disease: clinical, molecular, and neuropathological features. *Ann Neurol* (1996) 39:490–9. doi:10.1002/ana.410390411
6. Globas C, Du Montcel ST, Baliko L, Boesch S, Depondt C, Didonato S, et al. Early symptoms in spinocerebellar ataxia type 1, 2, 3, and 6. *Mov Disord* (2008) 23:2232–8. doi:10.1002/mds.22288
7. Kieling C, Rieder CR, Silva AC, Saute JA, Cecchin CR, Monte TL, et al. A neurological examination score for the assessment of spinocerebellar ataxia 3 (SCA3). *Eur J Neurol* (2008) 15:371–6. doi:10.1111/j.1468-1331.2008.02078.x
8. Boeddrich A, Gaumer S, Haacke A, Tzvetkov N, Albrecht M, Evert BO, et al. An arginine/lysine-rich motif is crucial for VCP/p97-mediated modulation of ataxin-3 fibrillogenesis. *EMBO J* (2006) 25:1547–58. doi:10.1038/sj.emboj.7601043
9. Chai Y, Shao J, Miller VM, Williams A, Paulson HL. Live-cell imaging reveals divergent intracellular dynamics of polyglutamine disease proteins and supports a sequestration model of pathogenesis. *Proc Natl Acad Sci U S A* (2002) 99:9310–5. doi:10.1073/pnas.152101299
10. Li F, Macfarlan T, Pittman RN, Chakravarti D. Ataxin-3 is a histone-binding protein with two independent transcriptional corepressor activities. *J Biol Chem* (2002) 277:45004–12. doi:10.1074/jbc.M205259200
11. Evert BO, Araujo J, Vieira-Saecker AM, De Vos RA, Harendza S, Klockgether T, et al. Ataxin-3 represses transcription via chromatin binding, interaction with histone deacetylase 3, and histone deacetylation. *J Neurosci* (2006) 26:11474–86. doi:10.1523/JNEUROSCI.2053-06.2006
12. Araujo J, Breuer P, Dieringer S, Krauss S, Dorn S, Zimmermann K, et al. FOXO4-dependent upregulation of superoxide dismutase-2 in response to oxidative stress is impaired in spinocerebellar ataxia type 3. *Hum Mol Genet* (2011) 20:2928–41. doi:10.1093/hmg/ddr197
13. Weber JJ, Sowa AS, Binder T, Hubener J. From pathways to targets: understanding the mechanisms behind polyglutamine disease. *Biomed Res Int* (2014) 2014:701758. doi:10.1155/2014/701758
14. Yu YC, Kuo CL, Cheng WL, Liu CS, Hsieh M. Decreased antioxidant enzyme activity and increased mitochondrial DNA damage in cellular models of Machado-Joseph disease. *J Neurosci Res* (2009) 87:1884–91. doi:10.1002/jnr.22011
15. Pacheco LS, Da Silveira AF, Trott A, Houenou LJ, Algarve TD, Bello C, et al. Association between Machado-Joseph disease and oxidative stress biomarkers. *Mutat Res* (2013) 757:99–103. doi:10.1016/j.mrgentox.2013.06.023
16. Reina CP, Zhong X, Pittman RN. Proteotoxic stress increases nuclear localization of ataxin-3. *Hum Mol Genet* (2010) 19:235–49. doi:10.1093/hmg/ddp482
17. Bichelmeier U, Schmidt T, Hubener J, Boy J, Ruttiger L, Habig K, et al. Nuclear localization of ataxin-3 is required for the manifestation of symptoms in SCA3: in vivo evidence. *J Neurosci* (2007) 27:7418–28. doi:10.1523/JNEUROSCI.4540-06.2007
18. Jardim LB, Hauser L, Kieling C, Saute JA, Xavier R, Rieder CR, et al. Progression rate of neurological deficits in a 10-year cohort of SCA3 patients. *Cerebellum* (2010) 9:419–28. doi:10.1007/s12311-010-0179-4
19. Jacobi H, Bauer P, Giunti P, Labrum R, Sweeney MG, Charles P, et al. The natural history of spinocerebellar ataxia type 1, 2, 3, and 6: a 2-year follow-up study. *Neurology* (2011) 77:1035–41. doi:10.1212/WNL.0b013e31822e7ca0
20. Jacobi H, Du Montcel ST, Bauer P, Giunti P, Cook A, Labrum R, et al. Long-term disease progression in spinocerebellar ataxia types 1, 2, 3, and 6: a longitudinal cohort study. *Lancet Neurol* (2015) 14:1101–8. doi:10.1016/S1474-4422(15)00202-1
21. Saute JA, Donis KC, Serrano-Munuera C, Genis D, Ramirez LT, Mazzetti P, et al. Ataxia rating scales – psychometric profiles, natural history and their application in clinical trials. *Cerebellum* (2012) 11:488–504. doi:10.1007/s12311-011-0316-8
22. Tezenas du Montcel S, Charles P, Goizet C, Marelli C, Ribai P, Vincitorio C, et al. Factors influencing disease progression in autosomal dominant cerebellar ataxia and spastic paraplegia. *Arch Neurol* (2012) 69:500–8. doi:10.1001/archneurol.2011.2713
23. Saute JA, De Castilhos RM, Monte TL, Schumacher-Schuh AF, Donis KC, D'avila R, et al. A randomized, phase 2 clinical trial of lithium carbonate in Machado-Joseph disease. *Mov Disord* (2014) 29:568–73. doi:10.1002/mds.25803
24. Saute JA, Rieder CR, Castilhos RM, Monte TL, Schumacher-Schuh AF, Donis KC, et al. Planning future clinical trials in Machado Joseph disease: lessons from a phase 2 trial. *J Neurol Sci* (2015) 358:72–6. doi:10.1016/j.jns.2015.08.019
25. Bauer PO, Kotliarova SE, Matoska V, Musova Z, Hedvicakova P, Boday A, et al. Fluorescent multiplex PCR – fast method for autosomal dominant spinocerebellar ataxias screening. *Genetika* (2005) 41:830–7.
26. Kieling C, Prestes PR, Saraiva-Pereira ML, Jardim LB. Survival estimates for patients with Machado-Joseph disease (SCA3). *Clin Genet* (2007) 72:543–5. doi:10.1111/j.1399-0004.2007.00910.x
27. Schmitz-Hubsch T, Du Montcel ST, Baliko L, Berciano J, Boesch S, Depondt C, et al. Scale for the assessment and rating of ataxia: development of a new clinical scale. *Neurology* (2006) 66:1717–20. doi:10.1212/01.wnl.0000219042.60538.92
28. Tezenas du Montcel S, Durr A, Rakowicz M, Nanetti L, Charles P, Sulek A, et al. Prediction of the age at onset in spinocerebellar ataxia type 1, 2, 3 and 6. *J Med Genet* (2014) 51:479–86. doi:10.1136/jmedgenet-2013-102200
29. Boveris A. Determination of the production of superoxide radicals and hydrogen peroxide in mitochondria. *Methods Enzymol* (1984) 105:429–35. doi:10.1016/S0076-6879(84)05060-6
30. Wendel A. Glutathione peroxidase. *Methods Enzymol* (1981) 77:325–33. doi:10.1016/S0076-6879(81)77046-0
31. Nonose Y, Gewehr PE, Almeida RF, Da Silva JS, Bellaver B, Martins LA, et al. Cortical bilateral adaptations in rats submitted to focal cerebral ischemia: emphasis on glial metabolism. *Mol Neurobiol* (2017). doi:10.1007/s12035-017-0458-x
32. Rotilio G, Aquilano K, Ciriolo MR. Interplay of Cu,Zn superoxide dismutase and nitric oxide synthase in neurodegenerative processes. *IUBMB Life* (2003) 55:629–34. doi:10.1080/15216540310001628717

33. da Silva Carvalho G, Saute JA, Haas CB, Torrez VR, Brochier AW, Souza GN, et al. Cytokines in Machado Joseph disease/spinocerebellar ataxia 3. *Cerebellum* (2016) 15:518–25. doi:10.1007/s12311-015-0719-z

Conflict of Interest Statement: The authors declare that the research was conducted in the absence of any commercial or financial relationships that could be construed as a potential conflict of interest.

ANEXO II-C. *Cytokines in Machado Joseph Disease/Spinocerebellar Ataxia 3*

No ANEXO II-C apresentamos o artigo publicado no periódico *Cerebellum*

Cerebellum
DOI 10.1007/s12311-015-0719-z

ORIGINAL PAPER

Cytokines in Machado Joseph Disease/Spinocerebellar Ataxia 3

Gerson da Silva Carvalho[1] &Jonas Alex Morales Saute[1,7] &Clarissa Branco Haas[2] &
Vitor Rocco Torrez[2] &Andressa Wigner Brochier[2] &Gabriele Nunes Souza[1] &
Gabriel Vasata Furtado[2] &Tailise Gheno[2] &Aline Russo[1] &Thais Lampert Monte[1,8] &
Artur Schumacher-Schuh[8] &Rui D'Avila[7] &Karina Carvalho Donis[7] &
Raphael Machado Castilhos[2] &Diogo Onofre Souza[2,4,10] &
Maria Luiza Saraiva-Pereira[2,4,7,9] &Vanessa Leotti Torman[3,5] &Suzi Carney[3,5] &
Luis Valmor Portela[2,4,10] &Laura Bannach Jardim[1,2,6,7,9]

Abstract The aim of the present study is to describe the serum concentrations of a broad spectrum of cytokines in symptomatic and asymptomatic carriers of Machado Joseph disease (SCA3/MJD) CAG expansions. Molecularly confirmed carriers and controls were studied. Age at onset, disease duration, and clinical scales Scale for the Assessment and Rating of Ataxia (SARA), Neurological Examination Score for Spinocerebellar Ataxias (NESSCA), SCA Functional Index (SCAFI), and Composite Cerebellar Functional Score (CCFS) were obtained from the symptomatic carriers. Serum was obtained from all individuals and a cytokine panel Bconsisted of^A eotaxin, granulocyte-macrophage colony-stimulating factor (GM-CSF), interferon (IFN)-α, IFN-γ, interleukin (IL)-1β, IL-1RA, IL-2, IL-2R, IL-4, IL-5, IL-6, IL-7, IL-8, IL-10, IL-12, IL-13, IL-15, IL-17, interferon gamma-induced protein (IP)-10, monocyte chemoattractant protein (MCP)-1, monokine induced by gamma interferon (MIG), macrophage inflammatory protein (MIP)-a, MIP-b, regulated on activation, normal T cell expressed and secreted (RANTES) and tumor necrosis factor (TNF)-α was analyzed. In a subgroup of symptomatic carriers, the cytokine panel was repeated after 360 days. Cytokine distribution among groups was studied by discriminant analysis; changes in serum levels after 360 days were studied by generalized estimation equation. Sixty-six symptomatic carriers, 13 asymptomatic carriers, and 43 controls were studied. No differences in cytokine patterns were found between controls and carriers of the CAG expansions or between controls and symptomatic carriers only. In contrast, eotaxin concentrations were significantly higher in asymptomatic than in symptomatic carriers or in controls (p=0.001, ANCOVA). Eotaxin did not correlate with age, disease duration, CAG expansion, NESSCA score, and SARA score. Among symptomatic carriers, eotaxin dropped after 360 days (p=0.039, GEE). SCA3/MJD patients presented a benign pattern of serum cytokines. In contrast, levels of eotaxin, a peptide secreted by astrocytes, were elevated in the asymptomatic carriers, suggesting that a specific response of these cells can be related to symptom progression, in SCA3/MJD.

* Laura Bannach Jardim
ljardim@hcpa.edu.br

[1] Post-Graduate Programme in Medical Sciences, Universidade Federal do Rio Grande do Sul, Porto Alegre, RS, Brazil

[2] Post-Graduate Programme in Genetics and Molecular Biology, Universidade Federal do Rio Grande do Sul, Porto Alegre, RS, Brazil

[3] Department of Epidemiology, Universidade Federal do Rio Grande do Sul, Porto Alegre, RS, Brazil

[4] Department of Biochemistry, Universidade Federal do Rio Grande do Sul, Porto Alegre, RS, Brazil

[5] Department of Statistics, Universidade Federal do Rio Grande do Sul, Porto Alegre, RS, Brazil

[6] Department of Internal Medicine, Universidade Federal do Rio Grande do Sul, Porto Alegre, RS, Brazil

[7] Medical Genetics Service, Hospital de Clínicas de Porto Alegre (HCPA), Porto Alegre, RS, Brazil

[8] Neurology Service, Hospital de Clínicas de Porto Alegre (HCPA), Porto Alegre, RS, Brazil

[9] Instituto Nacional de Genética Médica Populacional (INAGEMP), Porto Alegre, Brazil

[10] Instituto Nacional de Ciência e Tecnologia em Excitotoxicidade e Neuroproteção (INCTEN), Porto Alegre, Brazil

Published online: 22 September 2015

Keywords Cytokines · Discriminant analysis · Eotaxin · Machado Joseph disease · Neuroprotection · Spinocerebellar ataxia type 3

Background

Machado Joseph disease, also known as spinocerebellar ataxia type 3 (SCA3/MJD), is an autosomal dominant, untreatable polyglutamine (polyQ) disorder caused by a CAG repeat expansion (CAGexp) at *ATXN3* gene. SCA3/MJD usually starts around 32–40 years [1, 2]. Gait ataxia is the main neurological deficit, but ataxia later affects speech, swallowing, and limb coordination. Pyramidal, extrapyramidal, and peripheral nerve findings also occur during disease course. After some years, patients become bedridden. The median survival time after onset is 21 years [3]. Expansion of the polyQ tract in *ATXN3* is thought to promote an altered conformation in the protein ataxin-3, leading to changes in interactions with native partners and to the formation of insoluble aggregates. The principal disease mechanisms remain unclear [4]. Mutant ataxin-3 might trigger multiple, interconnected pathogenic cascades, and an inflammatory response might be among them.

Cytokines are a large group of small soluble peptides that act as signaling molecules to regulate inflammation and modulate cellular activities such as growth, survival, and differentiation [5, 6]. In the nervous system, cytokines work as neuromodulators and regulate neurodevelopment, neuroinflammation, and synaptic transmission [6]. Microglia are the brain immune cells, responsible for orchestrating the brain innate immune response. In the disease state, activated microglia mediate neuronal and glial cell injury and death through production and release of proinflammatory cytokines, glutamate, and reactive oxygen species among others [6]. Neurodegeneration is concomitant with astrogliosis, microgliosis, and microvasculature remodeling. Though the trophic factors released initially by astrocytes during astrogliosis aid in tissue repair, these factors might amplify the inflammatory response, and a balance between repair and proinflammatory factors might modify the outcome of a neurodegenerative process [7] (Kettenmann et al. 2011).

Several studies already demonstrated an involvement of neuroinflammation in neurodegenerative diseases like Alzheimer's disease, Parkinson's disease, or amyotrophic lateral sclerosis [8–11]. In Huntington disease (HD), a polyQ disorder, there is evidence that activation of the immune system starts in the presymptomatic stage of the disease [12, 13].

Immune abnormalities were not seen in a transgenic mice model of SCA3/MJD that lacks the C-terminal part of ataxin 3 and, therefore, the polyQ stretch. However, this model mimics a neurodegenerative disorder that is pathologically distinct from human SCA3/MJD [14]. Therefore, immune abnormalities and cytokine patterns related to SCA3/MJD patients are currently unknown.

In the present exploratory study, we aimed to determine the serum concentrations of cytokines, found among presymptomatic and symptomatic individuals carrying a CAGexp at ATXN3.

Methods

Population and Clinical Evaluations

Individuals were invited to participate in this study either if they were symptomatic and previously diagnosed with SCA3/MJD or if they were asymptomatic, at 50 % risk subjects looking for presymptomatic testing in our outpatient clinics from May, 2011, to July, 2013. Molecular characterization of the CAG repeats at *ATXN3* in both symptomatic SCA3 and asymptomatic SCA3 groups was performed by amplifying region of interest using fluorescent-labeled primers. Following amplification, products were separated on an ABI3130xl Genetic Analyzer and length of CAGexp allele was determined against size standard 500 LIZ as well as positive and negative controls.

The symptomatic individuals comprised the symptomatic SCA3 group. After consent, their data was collected during baseline assessments of a randomized controlled trial where disease duration [DD] of more than 10 years was exclusion criteria [15]. At-risk individuals proved to carry a CAGexp at *ATXN3* and whose neurological examination was normally comprised the asymptomatic SCA3 group. The control group consisted of those at-risk individuals who do not carry CAGexp, plus healthy, unrelated individuals with age, gender, and environmental characteristics similar to the symptomatic individuals. Individuals with chronic or acute inflammatory, infectious, or allergic diseases were excluded.

Age at onset (AO) of the first symptoms and DD of the symptomatic individuals were noted. The clinical scales Neurological Examination Score for Spinocerebellar Ataxias (NESSCA) [16], Scale for the Assessment and Rating of Ataxia (SARA) [17], SCA Functional Index (SCAFI) [18], and Composite Cerebellar Functional Score (CCFS) [19] were applied.

This study was approved by the Ethics in Research Committee of our institution (register number 10-512).

Sample Collections

After consent, blood was collected to study peripheral cytokines. All subjects were under fasting conditions: collections were done between 8 a.m. and 4 p.m., and processing was done within 4 h. Serum was obtained by blood centrifugation at 6000*g* for 5 min, frozen immediately, and stored at −80 °C until analyses [20].

As already mentioned, the symptomatic SCA3 individuals were included in a recent phase 2 clinical trial in SCA3/MJD [15]. Due to the design of that study, other serum samples were

obtained 90 and 360 days after the first blood collection. The present cytokine panel was repeated in the samples collected at 90 and 360 days from the placebo group. Since we considered that the placebo intervention would not produce any biological effect, the placebo group of that trial comprised the prospective subgroup of symptomatic individuals of the present study.

Cytokine Measurements

We performed cytokine assessment in serum samples with the commercial kit Human Cytokine Magnetic 25-Plex Panel (Reference # LHC0009M, Invitrogen, USA). This is a solid-phase protein immunoassay that uses spectrally encoded antibody-conjugated beads as the solid support. Each bead is given a unique identification number, or bead region, allowing differentiation of one bead from another. The assay is performed in a 96-well plate format and analyzed with a Luminex® instrument, which captures beads while simultaneously measuring the quantity of associated fluorophore.

The 25-Plex Panel "consisted of" eotaxin, granulocyte-macrophage colony-stimulating factor (GM-CSF), interferon (IFN)-α, IFN-γ, interleukin (IL)-1β, IL-1RA, IL-2, IL-2R, IL-4, IL-5, IL-6, IL-7, IL-8, IL-10, IL-12, IL-13, IL-15, IL-17, interferon gamma-induced protein (IP)-10, monocyte chemoattractant protein (MCP)-1, monokine induced by gamma interferon (MIG), macrophage inflammatory protein (MIP)-a, MIP-b, regulated on activation, normal T cell expressed and secreted (RANTES), and tumor necrosis factor (TNF)-α (all measured in pg/ml).

This panel represents different functional cytokine profiles such as "cytotoxic cellular cytokines" (e.g., IL-1β, IL-2, IL-12, IL-15, IL-17, IFN-α, IFN-γ, and TNF-α), "humoural cytokines" (e.g., IL-4, IL-1RA, IL-5, IL-6, IL-10, and IL-13), "growth factors" (e.g., GM-CSF, IL-7), "chemokines" [e.g., CXCL8 (IL-8), MCP-1, CCL3 (MIP-1a), IP-10, CCL4 (MIP-1b), MIG, CCL11 (eotaxin), and CCL5 (RANTES)] and "death receptors" (e.g., IL-2R) [21].

Statistical Analyses

Since the distribution of all 25 cytokines under study was highly skewed, the obtained measurements were $\log_{10}$ normalized.

Since this is an exploratory study without an a priori hypothesis, functional groups of cytokines were not chosen to be studied. Each cytokine was treated as a unique variable. However, some cytokines covariated with others and could be excluded from the analysis. In accordance, only those cytokines that did not present collinearity (variance impact factor=VIF <0.2) were picked up for further analysis.

The distribution of the selected cytokines among groups was then compared by discriminant analysis. This analysis was performed in three settings, in order to predict whether an individual was as follows: (1) a CAGexp-carrying (symptomatic SCA3 plus asymptomatic SCA3 groups) or a CAGexp-non-carrying individual (control group), to explore the possible patterns related to the presence of a CAGexp per se; (2) a symptomatic SCA3 or an unaffected individual (control group), to explore the possible patterns related to the disease status of SCA3/MJD individuals; and (3) a symptomatic SCA3 or an asymptomatic SCA3, to explore the possible patterns related to the appearance of symptoms per se and not to the presence of a CAGexp.

A stepwise analysis (using Wilk's lambda method and with p-in=0.05, p-out=0.10) was done in order to identify the best or most useful cytokines for distinguishing between groups.

The cross-validated classification accuracy rate of the discriminant analyses shows the proportion of the original grouped cases that would be correctly classified by the cytokine panel. Cross-validated classification accuracy rates ≥20 % higher than the proportional by chance accuracy rate were considered good. The proportion by chance of the accuracy rate was computed by squaring and summing the proportion of cases in each group.

If a given cytokine was associated to any status under study (carrying a CAGexp at *ATXN3* gene or being symptomatic), its serum levels along 90 and 360 days after baseline evaluation were studied by generalized estimation equation (GEE), in the prospective symptomatic subgroup.

Results

Sixty-six individuals comprised the symptomatic SCA3 group; 13, the asymptomatic SCA3 group; and 43, the control group (9 related and 34 unrelated to SCA3/MJD individuals). Clinical and demographic characteristics are described in Table 1.

Twenty-seven out of 63 symptomatic individuals were followed for 360 days. Their gender proportion, age, AO, DD, CAGexp, NESSCA, SARA, and ataxia severity scores were similar to the overall group of symptomatic individuals (data not shown).

The cytokines that did not present collinearity (VIF <0.2) and that were selected for further analysis were the log10 of eotaxin, IFN-α, IFN-γ, IL-1β, IL-2, IL-5, IL-6, IL-8, IL-12, IL-13, IL-17, IP-10, TNF-α, and RANTES, all reported as picogram per milliliter.

Comparisons Between the CAGexp-Carrying and CAGexp-Non-Carrying Individuals

Seventy-nine individuals (66 symptomatic SCA3 plus 13 asymptomatic SCA3) comprised the CAGexp-carrying group, whereas the 43 controls comprised the non-carrying group.

The 19 identified cytokines were not significantly different between groups. The panel was able to correctly classify 61.5 % of individuals.

Table 1 Clinical and molecular characteristics of the three subgroups under study

	Asymptomatic	Symptomatic (those with 360-day follow-up)	Controls
N	13	66 (27)	43
Females	8	33 (15)	25
Age	33.15±8.2*	40.7±9.5* (40.3±9)	40.9±14
M±SD Age at onset		34.8±9 (32.2±8.9)	
M±SD CAG expanded repeats	73.3±3	74.91±3.1 (75.5±2.8)	
M±SD Disease duration		5.9±2.5 (6.13±2.5)	
M±SD NESSCA baseline		14.3±4.8 (15±5.1)	
M±SD SARA baseline		10.7±4 (11.6±4)	
M±SD Ataxia severity at baseline		2.17±0.75 (2.2±0.6)	
M±SD			

Only significant differences between comparisons were described

M±*SD* mean±standard deviation

*$p<0.05$, *t* test

The discriminant function did not reveal a significant association between groups and any predictors (the cytokines under study), accounting for 17.1 % of between-group variability. The cross-validated classification showed that, overall, 52.1 % were correctly classified, which is lower than 66.0 % (the proportional by chance accuracy rate times 1.20 or $(0.355^2+0.645^2)*1.20$).

Comparisons Between Symptomatic SCA3 and the Unaffected Individuals

The 66 symptomatic SCA3 individuals were compared against the 43 controls.

Again, the 19 identified cytokines were not significantly different between groups. The panel was only able to correctly classify 63.3 % of individuals.

The discriminant function did not reveal a significant association between groups and any predictors, accounting for 16.2 % of between-group variability. The cross-validated classification showed that, overall, 42.2 % were correctly classified, which is lower than 65.3 % (the proportional by chance accuracy rate times 1.20 or $(0.394^2+0.606^2)*1.20$).

Comparisons Between the Symptomatic and the Asymptomatic Carriers of CAGexp: Eotaxin as a Biomarker of Disease Status

The 66 symptomatic SCA3 individuals were compared against the 13 asymptomatic carriers of CAGexp. Since both groups showed significant differences between their age, age was included in the discriminant function.

Although the discriminant function revealed a significant association between groups and all predictors, it accounted for 47.0 % of between-group variability. The cross-validated classification showed that, overall, 85.9 % were correctly classified, which is lower than 88.7 % (the proportional by chance accuracy rate times 1.20 $(0.154^2+0.846^2)*1.20$).

The stepwise analysis identified eotaxin, IFN-γ, and age as the most important predictors. The discriminant function revealed a significant association between groups and eotaxin, but it accounted for 31.1 % of between-group variability. The cross-validated classification showed that, overall, 91.0 % were correctly classified using those three variables, which is higher than 88.7 %, the proportional by chance accuracy rate times 1.20.

Age differences between these groups were expected, however, and could act as a confounder. To study eotaxin and IFN-γ individually, ANCOVA was done, using age as covariate. Means of log IFN-γ in asymptomatic ($M=-0.9$, standard error (SE)=0.2) and in symptomatic SCA3 ($M=-0.5$, SE=0.1) groups were not significantly different ($p=0.152$). In contrast, mean of log eotaxin in asymptomatic carriers ($M=2.3$, SE=0.2) was significantly larger than the value obtained in symptomatic SCA3 group ($M=1.3$, SE=0.1, $p<0.001$). In other words, the higher values of eotaxin among asymptomatic SCA3 individuals were not explained by differences in ages between groups (Table 1). Serum concentrations of log eotaxin are depicted in Fig. 1.

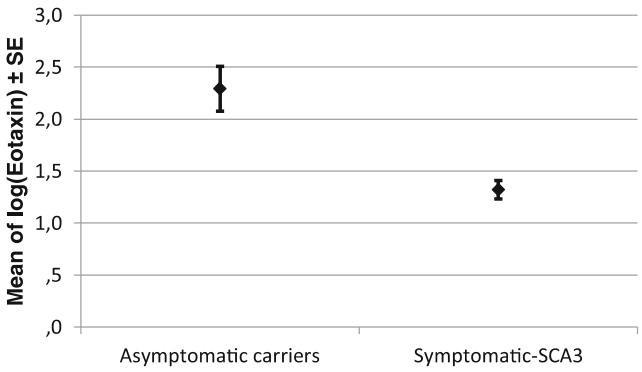

Fig. 1 Comparison of serum concentrations of eotaxin in asymptomatic carriers of *ATXN3* CAG expansions with those found in symptomatic individuals and in controls

Serum log eotaxin levels of SCA3 symptomatic individuals were very similar to control values, whereas levels in SCA3 asymptomatic individuals were higher than SCA3 symptomatic and control groups.

Among the asymptomatic carriers, no correlation was found between eotaxin levels and one of its main peripheral sources, number of peripheral eosinophils (rho=−0.07, p=0.8, Spearman test).

A post hoc analysis was done in order to clarify if any of the cytokines excluded from the analysis covariated with eotaxin. None of them (GM-CSF, IL-1RA, IL-2R, IL-4, IL-7, IL-10, IL-15, MCP-1, MIG, MIP1a, MIP1b) presented a relevant correlation with eotaxin (rhos between 0.2 and 0.3).

Possible Associations of Eotaxin with Age, Disease Severity and Duration, and CAGexp: Eotaxin Progression During Time

Log eotaxin did not correlate with age or with any of the parameters of disease severity: DD, CAGexp, NESSCA, SARA, SCAFI, and CCFS (data not shown). Log eotaxin means obtained in subgroups of gait ataxia severity were compared, and no differences were found (data not shown). Although not a good candidate for a SCA3/MJD biomarker, the same analyses were done for log IFN-γ: no significant associations were observed (data not shown).

Clinical and molecular characteristics of the prospective symptomatic subgroup were similar to the other symptomatic SCA3 individuals (Table 1). In this subgroup, GEE was used to analyze if there was a change of log eotaxin along time. Log eotaxin presented a significant reduction in a 360-day interval (p=0.039), but not in 90 days (p=0.398) (Fig. 2). The same analysis was done for log IFN-γ: no significant changes were observed (data not shown).

Discussion

Our study did not disclose an altered pattern of cytokines in SCA3/MJD, as occurs in diseases related to microglia activation. In contrast, the asymptomatic status of SCA3/MJD was associated with increased levels of only one cytokine, eotaxin, a peptide secreted by astrocytes to repel circulating immune cells and also on peripheral tissues mainly by T lymphocytes (Th2) [6, 22].

Few studies have been done on the role of microglia and astrocytes, cells that secrete cytokines in response to the disease processes, in SCA3/MJD and other polyQ SCAs [23–28]. A transgenic mouse expressing the expanded human ataxin-3 with 94 CAGs showed astrogliosis but not microglial activation [23]. In a conditional Tet-Off mouse model using the full-length human ataxin-3 cDNA with 77 CAGs, ataxin-3 was predominantly detected in glial cells of the cerebellum—not in neurons. This model showed that glial cells expressing expanded ataxin-3 can secondarily alter Purkinje cell function [24]. Pathological studies in humans disclosed that microglial cells might be activated in degenerated brainstem nuclei of SCA3/MJD patients, an effect that might be related to late stages of the disease [25, 26]. Distribution of reactive astrocytes is quite interesting. While present in affected and in preserved, nondegenerated gray matter regions such as thalamic and vestibular nuclei, reactive astrocytes were absent from some severely degenerated nuclei, such as lateral and interstitial vestibular nuclei, and pulvinar and reticular nuclei, in thalamus [27, 28]. Similar findings were obtained in other polyQ SCAs [25]. The possible astrocyte and microglial activation on cytokines was never studied, in SCA3/MJD.

We have chosen to perform a large exploratory study covering 25 cytokines belonging to different functional groups, in order to detect those that could be related to this disease. Unfortunately, only 13 asymptomatic carriers with normal neurological examination accepted to participate in this study. The low acceptance of presymptomatic testing among

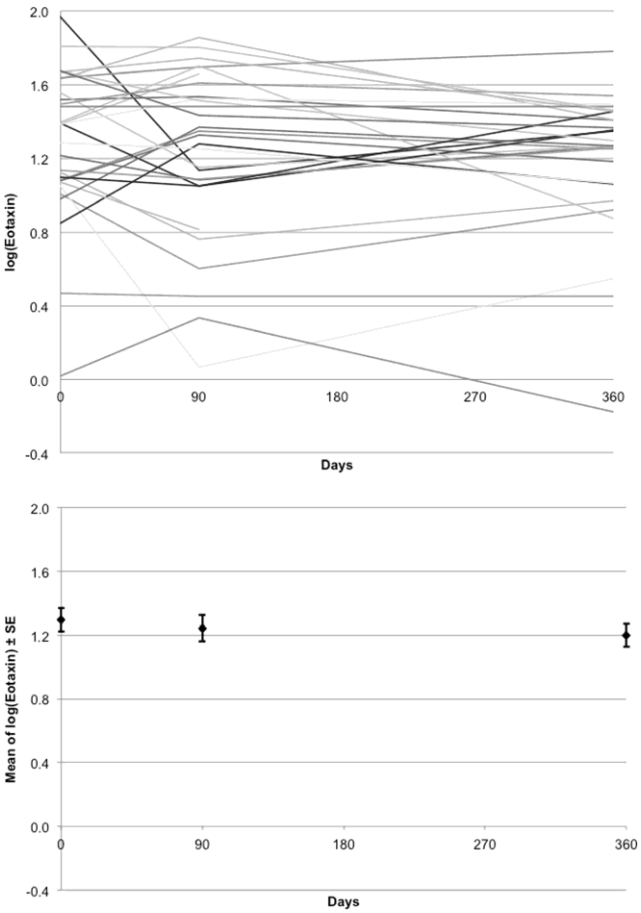

Fig. 2 Eotaxin progression during a 360-day interval in 27 SCA3 symptomatic individuals. **a** Log eotaxin changes: each *line* represents one individual. **b** Mean of log eotaxin changes in the overall group of symptomatic individuals

Brazilians might explain these numbers [29]. Even so, an unbiased analysis was able to show that eotaxin serum levels in asymptomatic carriers of the mutation were significantly higher than those measured in symptomatic patients and higher than those found in controls. Moreover, eotaxin serum levels seemed to progressively drop among symptomatic individuals. If that is true, one would expect an association between eotaxin levels and DD among the symptomatic individuals. The lack of association in the present study may have been due to the low DD (up to 10 years) of the symptomatic subjects recruited.

Many different cell types can produce eotaxin: in CNS, astrocytes and, peripherally, lymphocytes, endothelial cells, and others [6, 22, 30]. On periphery, eotaxin is strongly chemotactic for eosinophils, as well as for basophils and Th2 cells [31]. As we measured serum eotaxin levels in SCA3/MJD, the first question would be if eotaxin crosses the blood-brain barrier (BBB) from periphery and/or if there is a brain efflux of eotaxin that may reflect CNS immune changes. Studies performed in vitro showed that eotaxin can cross the BBB in both directions [20]. Since SCA3/MJD was never related to any allergic cascade, we decided to not discuss the possible relationship of peripheral sources of eotaxin with our findings.

Eotaxin is secreted by astrocytes in an attempt to keep away circulating immune cells [6, 32]. Astrocytes are the primary cell type found in glia scar formation. They help the resolution of inflammation by reducing the secretion of pro-inflammatory cytokines and increasing anti-inflammatory processes [6]. Increased numbers of reactive astrocytes and activated microglial cells are present in SCA3/MJD [25, 26]. In polyQ SCAs, including SCA3/MJD, reactive astrocytes are often seen in affected and apparently preserved gray areas. In

contrast, astrocytes are frequently absent from some of the totally degenerated gray matter areas. If these astrocyte losses reflect that functional capacities are exhausted or that they could be targets of the disease processes and could ultimately degenerate similarly to neurons remains to be tested [26].

The present data shows that serum concentrations of eotaxin are higher in asymptomatic than in symptomatic carriers of a CAGexp at *ATXN3* and in controls. Since there is no evidence in the literature in favor of a peripheral activation of the immune system in SCA3/MJD, a possible interpretation is that eotaxin is highly secreted by astrocytes during the presymptomatic period. Among the anatomical structures studied in detail, there is evidence that unaffected regions show astrogliosis [27, 28]. Maybe, astrogliosis might start during the presymptomatic period. These concentrations drop as time passes, maybe when astrocytes get exhausted or degenerated and undergone cell death. This might roughly coincide with the symptomatic period. If the eotaxin measured in peripheral serum is portraying the eotaxin secreted by astrocytes, then our preliminary data matches with the theory that the progressive loss of astrocytes would be related to the disease process, in SCA3/MJD and other polyQ disorders, and to the start of symptoms. The astrocyte vanishing from the destroyed brain grays, in polyQ SCAs, suggests that after their functional capacities are exhausted, the progression of symptoms would appear [26]. In this context, eotaxin either might play a direct protective role in the presymptomatic phase of the disease or might only be a biomarker of astrocyte dysfunction.

These are very speculative hypotheses. Understanding the role of cytokines in neurodegenerative diseases is complicated by several factors. The first is the distance between the serum and the central nervous system. The second is the cytokine dual roles in neuroprotection and neurodegeneration. The example of IL-6, a neurotrophin that promotes neuronal survival in some cases and brain diseases in others [33], should refrain us to attribute a clear neuroprotective role to eotaxin, with the present evidence.

Conclusion

The study of cytokines in neurodegenerative diseases such as SCA3/MJD might enlighten the understanding of the disease process of this and other polyQ disorders. Moreover, changes in cytokine patterns could be used as a biomarker of disease state/progression. This exploratory study raised significant new information about cytokines in SCA3/MJD. There is no evidence of a generalized cytokine change associated with the disease. In contrast, serum levels of eotaxin, a cytokine secreted by astrocytes, were shown to be elevated in asymptomatic carriers; these levels decreased among symptomatic individuals in a progressive way. Eotaxin might be a good candidate biomarker of the presymptomatic state. In order to confirm this, further prospective studies, especially those measuring eotaxin in cerebrospinal fluid and those relating eotaxin with brainstem atrophy, are needed.

Acknowledgments We thank the patients who participated in the study. We thank HCPA and its Postgraduate Research Group (GPPG).

Compliance with Ethical Standards

Funding This study was supported by FAPERGS (09/0078-5), CNPq (478888/2010-4), and FIPE-HCPA (09-418; 10-512). DOS, LVP, MLSP, and LBJ were supported by CNPq.

Conflict of Interest The authors declare that they have no competing interests.

Ethical Approval All procedures performed were in accordance with the ethical standards of the institutional and/or national research committee and with the 1964 Helsinki declaration and its later amendments or comparable ethical standards.

Informed Consent Informed consent was obtained from all individual participants included in the study.

Authors' Contributions GSC conceived the study, recruited subjects, organized the data bank, and reviewed the manuscript. JAMS participated in the recruitment of subjects, performed neurological examinations and clinical scales, organized the data and the sample banks, reviewed the statistical analysis, and helped to draft the manuscript. CBH, VRT, and AWB carried out the cytokine assays and reviewed the manuscript. GNS, AR, TLM, ASS, RDA, KCD, and RMC performed neurological evaluations and clinical scales and reviewed the manuscript. GVF, TCG, and MLSP carried out the molecular genetic studies, helped organizing the sample bank, and reviewed the manuscript. VLT and SC performed the statistical analysis and helped to draft the manuscript. DOS participated in the design of the study, helped in obtaining funding, and reviewed the manuscript. LVP participated in the design and coordination of the study and helped to draft the manuscript. LBJ conceived and coordinated the study and drafted the manuscript. All authors read and approved the final manuscript.

References

1. Bettencourt C, Lima M. Machado-Joseph disease: from first descriptions to new perspectives. Orphanet J Rare Dis. 2011;6:35.
2. de Castilhos RM, Furtado GV, Gheno TC, Schaeffer P, Russo A, Barsottini O, et al. Rede Neurogenetica. Spinocerebellar ataxias in Brazil—frequencies and modulating effects of related genes. Cerebellum. 2014;13(1):17–28.
3. Kieling C, Prestes PR, Saraiva-Pereira ML, Jardim LB. Survival estimates for patients with Machado-Joseph disease (SCA3). Clin Genet. 2007;72(6):543–5.
4. Costa MC, Paulson HL. Toward understanding Machado-Joseph disease. Prog Neurobiol. 2012;97(2):239–57.
5. Devi LA. G-protein-coupled receptor dimers in the lime light. Trends Pharmacol Sci. 2000;21(9):324–6.
6. Ramesh G, MacLean AG, Philipp MT. Cytokines and chemokines at the crossroads of neuroinflammation, neurodegeneration, and neuropathic pain. Mediators Inflamm. 2013;2013:480739.
7. Kettenmann H, Hanisch UK, Noda M, Verkhratsky A. Physiology of microglia. Physiol Rev. 2011;91(2):461–553.

8. Harry GJ, Kraft AD. Neuroinflammation and microglia: considerations and approaches for neurotoxicity assessment. Exp Opin Drug Metab Toxicol. 2008;4(10):1265–77.
9. Hirsch EC, Hunot S. Neuroinflammation in Parkinson's disease: a target for neuroprotection? Lancet Neurol. 2009;8(4):382–97.
10. Lobsiger CS, Cleveland DW. Glial cells as intrinsic components of non-cell-autonomous neurodegenerative disease. Nat Neurosci. 2007;10(11):1355–60.
11. Hofmann KW, Schuh AF, Saute J, Townsend R, Fricke D, Leke R, et al. Interleukin-6 serum levels in patients with Parkinson's disease. Neurochem Res. 2009;34(8):1401–4.
12. Björkqvist M, Wild EJ, Thiele J, et al. A novel pathogenic pathway of immune activation detectable before clinical onset in Huntington's disease. J Exp Med. 2008;205(8):1869–77.
13. van der Burg JM, Björkqvist M, Brundin P. Beyond the brain: widespread pathology in Huntington's disease. Lancet Neurol. 2009;8(8):765–74.
14. Hübener J, Casadei N, Teismann P, Seeliger MW, Björkqvist M, von Hörsten S, et al. Automated behavioral phenotyping reveals presymptomatic alterations in a SCA3 genetrap mouse model. J Genet Genom. 2012;39(6):287–99.
15. Saute JA, de Castilhos RM, Monte TL, Schumacher-Schuh AF, Donis KC, D'Ávila R, et al. A randomized, phase 2 clinical trial of lithium carbonate in Machado-Joseph disease. Mov Disord. 2014;29(4):568–73.
16. Kieling C, Rieder CR, Silva AC, Saute JA, Cecchin CR, Monte TL, et al. A neurological examination score for the assessment of spinocerebellar ataxia 3 (SCA3). Eur J Neurol. 2008;15:371–6.
17. Schmitz-Hübsch T, du Montcel ST, Baliko L, Berciano J, Boesch S, Depondt C, et al. Scale for the assessment and rating of ataxia: development of a new clinical scale. Neurology. 2006;66:1717–20.
18. Schmitz-Hübsch T, Giunti P, Stephenson DA, Globas C, Baliko L, Saccà F, et al. SCA Functional Index: a useful compound performance measure for spinocerebellar ataxia. Neurology. 2008;71:486–92.
19. du Montcel ST, Charles P, Ribai P, Goizet C, Le Bayon A, Labauge P, et al. Composite cerebellar functional severity score: validation of a quantitative score of cerebellar impairment. Brain. 2008;131:1352–61.
20. Erickson MA, Morofuji Y, Owen JB, Banks WA. Rapid transport of CCL11 across the blood–brain barrier: regional variation and importance of blood cells. J Pharmacol Exp Ther. 2014;349(3):497–507.
21. Szodoray P, Alex P, Brun JG, Centola M, Jonsson R. Circulating cytokines in primary Sjögren's syndrome determined by a multiplex cytokine array system. Scand J Immunol. 2004;59(6):592–9.
22. Baruch K, Ron-Harel N, Gal H, Deczkowska A, Shifrut E, Ndifon W, et al. CNS-specific immunity at the choroid plexus shifts toward destructive Th2 inflammation in brain aging. Proc Natl Acad Sci U S A. 2013;110(6):2264–9.
23. Silva-Fernandes A, Costa Mdo C, Duarte-Silva S, Oliveira P, Botelho CM, Martins L, et al. Motor uncoordination and neuropathology in a transgenic mouse model of Machado–Joseph disease lacking intranuclear inclusions and ataxin-3 cleavage products. Neurobiol Dis. 2010;40:163–76.
24. Boy J, Schmidt T, Wolburg H, Mack A, Nuber S, Bottcher M, et al. Reversibility of symptoms in a conditional mouse model of spinocerebellar ataxia type 3. Hum Mol Genet. 2009;18:4282–95.
25. Evert BO, Vogt IR, Kindermann C, Ozimek L, de Vos RA, Brunt ER, et al. Inflammatory genes are upregulated in expanded ataxin-3-expressing cell lines and spinocerebellar ataxia type 3 brains. J Neurosci. 2001;21:5389–96.
26. Rüb U, Schöls L, Paulson H, Auburger G, Kermer P, Jen JC, et al. Clinical features, neurogenetics and neuropathology of the polyglutamine spinocerebellar ataxias type 1, 2, 3, 6 and 7. Prog Neurobiol. 2013;104:38–66.
27. Rüb U, de Vos RA, Brunt ER, Schultz C, Paulson H, Del Tredici K, et al. Degeneration of the external cuneate nucleus in spinocerebellar ataxia type 3 (Machado-Joseph disease). Brain Res. 2002;953(1–2):126–34.
28. Rüb U, Brunt ER, de Vos RA, Del Turco D, Del Tredici K, Gierga K, et al. Degeneration of the central vestibular system in spinocerebellar ataxia type 3 (SCA3) patients and its possible clinical significance. Neuropathol Appl Neurobiol. 2004;30(4):402–14.
29. Rodrigues CS, de Oliveira VZ, Camargo G, Osório CM, de Castilhos RM, Saraiva-Pereira ML, et al. Presymptomatic testing for neurogenetic diseases in Brazil: assessing who seeks and who follows through with testing. J Genet Couns. 2012;21(1):101–12. doi:10.1007/s10897-011-9383-8.
30. Waddell A, Ahrens R, Steinbrecher K, Donovan B, Rothenberg ME, Munitz A, et al. Colonic eosinophilic inflammation in experimental colitis is mediated by Ly6C(high) CCR2(+) inflammatory monocyte/macrophage-derived CCL11. J Immunol. 2011;186(10):5993–6003.
31. van Dooren FH, Duijvis NW, te Velde AA. Analysis of cytokines and chemokines produced by whole blood, peripheral mononuclear and polymorphonuclear cells. J Immunol Methods. 2013;396(1–2):128–33.
32. Cardona AE, Gonzalez PA, Teale JM. Chemokines mediate leukocyte trafficking into the central nervous system during murine neurocysticercosis: role of $\gamma\delta$ T cells in amplification of the host immune response. Infect Immun. 2003;71(5):2634–42.
33. Erta M, Quintana A, Hidalgo J. Interleukin-6 a major cytokine in the central nervous system. Int J Biol Sci. 2012;8:1254–66.

ANEXO II-D. *Neurological impairment among heterozygote women for X-linked Adrenoleukodystrophy: a case control study on a clinical, neurophysiological and biochemical characteristics*

No ANEXO II-D apresentamos o artigo publicado no periódico *Orphanet Journal of Rare Diseases*

Habekost et al. Orphanet Journal of Rare Diseases 2014, 9:6
http://www.ojrd.com/content/9/1/6

ORPHANET JOURNAL OF RARE DISEASES

RESEARCH Open Access

Neurological impairment among heterozygote women for X-linked Adrenoleukodystrophy: a case control study on a clinical, neurophysiological and biochemical characteristics

Clarissa Troller Habekost[1,11], Pedro Schestatsky[5,7], Vitor Felix Torres[7], Daniella Moura de Coelho[6], Carmen Regla Vargas[4,6], Vitor Torrez[2], Jean Pierre Oses[10,12], Luis Valmor Portela[2,3,12], Fernanda dos Santos Pereira[8], Ursula Matte[1,9,11] and Laura Bannach Jardim[1,5,6,8,11*]

Abstract

Background: Neurologic impairments in female heterozygotes for X-linked Adrenoleukodystrophy (X-ALD) are poorly understood. Our aims were to describe the neurological and neurophysiological manifestations of a cohort of X-ALD heterozygotes, and to correlate them with age, disease duration, mutations, X-inactivation and serum concentrations of a marker of neuronal damage, neuron-specific enolase (NSE).

Methods: All 45 heterozygotes identified in our region, with previous VLCFA and molecular diagnosis, were invited to be evaluated through myelopathy scales JOA and SSPROM, nerve conduction studies and somatosensory evoked responses. X inactivation pattern was tested by HUMARA methylation assay. Serum NSE was measured by eletrochemiluminescense.

Results: Thirty three heterozygote women were recruited: 29 (87%) were symptomatic. Symptomatic and asymptomatic women presented different m ± sd ages (43.9 ± 10.2 versus 24.3 ± 4.6), JOA (14.5 ± 1.7 versus 16.6 ± 0.2) and SSPROM (86.6 ± 7.9 versus 98.4 ± 1.1) scores ($p < 0.05$). Both JOA ($r = -0.68$) and SSPROM ($r = -0.65$) correlated with age, irrespectively of the disease status ($p = 0.0001$, Spearman). Delayed latencies in the central ascending conduction studies on the lower limbs were present in 72% of all heterozygotes, and correlated with SSPROM ($r = -0.47$, $p = 0.018$, Spearman). NSE values were higher in heterozygote than in control women (12.9 ± 7 and 7.2 ± 7 ng/ml, $p = 0.012$, Mann-Whitney U). Mutation severity and inactivation patterns were not associated with neurologic status.

Conclusion: Neurologic manifestations, clearly related to age, were quite common in the present cohort. JOA and SSPROM scales were able to discriminate the asymptomatic from the symptomatic heterozygotes. Both scales might be useful tools to follow disease progression, in future studies.

Keywords: X-linked adrenoleukodystrophy, X-ALD heterozygote females, X-ALD carriers, JOA, SSPROM, Neuron-specific enolase, Evoked potentials, Nerve conduction, X inactivation, Spastic paraplegia

* Correspondence: ljardim@hcpa.ufrgs.br
[1]Post-Graduation Program in Genetics and Molecular Biology, Universidade Federal do Rio Grande do Sul (UFRGS), Porto Alegre, Brazil
Full list of author information is available at the end of the article

Background

X-linked adrenoleukodystrophy (X-ALD, OMIM #300100) is the most common peroxisomal disorder worldwide [1,2]. Affecting the metabolism of saturated very long chain fatty acids (VLCFAs), X-ALD is caused by a defect in *ABCD1* gene that codes for ALD protein [3], a peroxisomal membrane protein that belongs to the ATP-binding cassette superfamily of membrane transport proteins [4]. *ABCD1* mutations give rise to obvious phenotypes in hemizygote men, such as the classical cerebral form of ALD (CALD) and the adrenomyeloneuropathy (AMN), among others [4].

A very limited number of studies addressed manifestations in female carriers; some authors stated that affected women are under recognized and undertreated [5]. Early reports said that 20 to 50% of heterozygotes might present a mild to severe myeloneuropathy that resembles AMN, this clinical picture being related to ageing [6]. The myelopathic component of AMN is characterized by a distal axonopathy that affects the dorsal column and the corticospinal tract [7]. Neurophysiologic studies showed central and peripheral abnormalities and suggested the prominence of axonal dysfunction [8].

VLCFA were established a long time ago as biomarkers for X-ALD. Elevated plasma VLCFA levels are the diagnostic gold-standard for X-ALD in men and present 15-20% of false negative results in women, for whom a molecular investigation is the main diagnostic tool [4].

In addition to diagnostic concerns, there are no reasonable mechanistic explanations for the variability regarding the presence and absence of neurological impairments in heterozygote females. Although brain VLCFA levels correlated with CALD in hemizygotes [9], plasma VLCFA levels have never been related to X-ALD phenotypes in men and women [4]. It is well known that genotypes do not correlate with phenotypes, in X-ALD [4]. Skewed X chromosome inactivation was also investigated, bringing contradictory results [10-12]. Alterations in oxidative stress parameters such as thiobarbituric acid-reactive substances [13] have been described in female carriers, without further exploring their potential associations with phenotypes.

Therefore, clinical and biochemical biomarkers of disease progression in heterozygotes for X-ALD are lacking. In this sense, we aimed to describe the symptomatic status of our X-ALD heterozygote cohort; to measure the neurological manifestations through myelopathy scales JOA and SSPROM, peripheral nerve conduction studies and somatosensory evoked responses; to measure plasma levels of a neuron disease marker, neuron-specific enolase (NSE); and to look for associations between these parameters and independent variables such as age, age at onset, mutations, X inactivation pattern and plasma VLCFA.

Methods

Population and clinical evaluations

All women previously identified as heterozygotes for X-ALD, in South Brazil, were invited to participate in this study. All had molecular analyses and VLCFA dosages performed in our institution, as reported elsewhere [14]. To be included, they had to be over 18 years old and give the informed consent. Exclusion criteria were the presence of any abnormality on the following exams at recruitment: lymphocytes count, hemoglobin, erythrocytes median corpuscular volume, sedimentation rate, vitamin B12, thyroid stimulating hormone, proteinogram, VDRL (Venereal disease research laboratory), FTA-Abs (Fluorescent Treponemal Antibody- absorption), antibodies anti-HTLV (Human T lymphotropic virus) and Anti-HIV (Human Immunodeficiency Virus), oxalacetic and glutamic pyruvic transaminases, qualitative urine test, thrombocytes, glucose and creatine.

The interview started with an open question about any disability or presence of symptoms in the heterozygote. After that, the interviewer (CTH) described the symptoms of spasticity, paraparesis, sensory losses and loss of sphincter control, and explained that these symptoms could be present in heterozygote females. After that, the interviewer asked again about the presence and age at onset (AO) of motor disability, sensory losses and/or loss of sphincter control and the answer to this was taken into account. Heterozygote women were then classified according to their responses; as symptomatic if complaints of neuropathic pain, paresthesia, sphincter dysfunction or paresis were present, or as asymptomatic if these complaints were absent. Data such as age, AO, disease duration (DD), family and ABCD1 mutations were collected.

Neurological impairment and disability were evaluated through two myelopathy scales: the Japanese Orthopaedic Association (JOA) [15] and the Severity Score System for Progressive Myelopathy (SSPROM) [16]. JOA includes questions about motor disability of upper and lower limbs, about sensory losses and about sphincter function. SSPROM includes questions about these same domains, plus questions about motor strength and tonus/reflexes. In this sense, both scales measure disability as well as neurological impairment.

We elected two SSPROM domains to measure disability. SSPROM's motor disability domain was based on and mirrors the Overall Disability Sum Score [17], while SSPROM's sphincter domain was based and recapitulates the "sphincter dysfunction" domain of Kurtzke functional systems scores [18]. An overall disability evaluation was then measured by these two SSPROM domains (0 to 50 points; Table 1). Since a minimally important difference has not been determined for the disability parameters so far, we have

Table 1 Clinical characteristics of the local cohort of X-ALD heterozygote women

	X-ALD heterozygotes			p*
	All heterozygotes participant	Symtomatic	Asymtomatic	
N (families)	(16) 33	29	4	
Age at examination	41.2 ± 11.9	43.9 ± 10.2	24.3 ± 4.6	0.005
		(24–61)	(20–30)	
Age at onset of symptoms		39.4 ± 10 (21–59)		
Disease duration		4.5 ± 3.3		
JOA (range: -2 to17)	14.8 ± 1.8	14.5 ± 1.7	16.6 ± 0.2	0.005
SSPROM (range: 0 to 100)	88 ± 8.4	86.6 ± 7.9	98.4 ± 1.1	0.001
SSPROM Motor Disability (range: 0 to 30)	27.6 ± 2.6	27.3 ± 2.6	30 ± 0	0.023
SSPROM Motor Strength (0 to 20)	18.9 ± 2	19.1 ± 1.3	17.5 ± 5	ns
SSPROM sensory losses (0 to 20)	16.4 ± 2.4	16.1 ± 2.3	18.5 ± 9	ns
SSPROM spasticity/ hyperreflexia (0 to 10)	6.1 ± 2.1	5.7 ± 1.8	9.4 ± 1.2	0.05
SSPROM sphincter contro (0 to 30)	27.6 ± 2.6	17.8 ± 2.3	20 ± 0	ns

*Mann-Whitney U.

arbitrated that women with an overall score ≤ 47 points were already disabled.

In order to produce a "disease severity score" where the neurological impairment was corrected by the disease duration, the SSPROM reciprocate of each woman was divided by disease duration. This severity score was then compared among groups stratified by risk factors such as mutation position, mutation severity, NSE and inactivation patterns.

Blood samples were taken and neurophysiological studies (described below) were performed within 15 days of evaluation.

Neurophysiological studies

Motor and sensory nerve conduction studies in several nerves were performed in the right side of the body (Table 2). Motor conduction velocity (m-NCV), distal latency and amplitude for both compound muscle action potential (CMAP) and sensory nerve action potential (SNAP) were measured according to standard techniques in which normal values were considered within 2-SD from the mean [19].

Somatosensory evoked responses (SSER) were measured using the 10/20 electrode placement international system and recorded according to standard techniques [19]. The latencies of N8, P40 and N50 were recorded after tibial nerve stimulation, and N9 and N20 after median nerve stimulation. Only P40 and N20 latencies were included into regression analyses. Normal latency values were considered according to Chiappa [20] and based on the patient's height. The upper limits of normal values were given in Table 3.

Both, nerve conduction studies and SSER were performed using a Nihon –Kohden (*Neuropack S1* MEB-9400 K) 4 channel EMG/EP system.

VLCFA

Plasma docosanoic (C22:0), tetracosanoic (C24:0) and hexacosanoic (C26:0) acids were obtained previously to the present study, and were analyzed as described by others [21]. Values of C26:0 (in μm/L) and of discriminant factor 3,805(C24:0/C22:0) + 5,296(C26:0/C22:0) + 5,15(C26:0) [22] were studied in the present heterozygote females. The discriminant factor's value of 10.86 discriminated X-ALD heterozygote from normal homozygote women, with 15% of false-negative results.

Enolase quantification

Serum NSE was measured using an eletrochemiluminescent assay provided by Roche DiagnosticsR, Indianapolis, IN, a double sandwich assay that uses an antibody anti-NSE bound with ruthenium (luminescent label). The reaction and quantification were performed by Elecsys-2010 (Roche). No hemolyzed samples were used. The assay was carried out in duplicate and the confidence variance was within 5%. NSE concentrations were also measured in thirteen unrelated, normal women used as a control group.

Inactivation studies

Genomic DNA was obtained from peripheral leukocytes by the salting out procedure [23]. X-inactivation patterns were assessed for skewing with the human androgen-receptor locus (HUMARA) methylation assay [24]. Prior to digestion, informative women were identified by PCR at HUMARA locus and capillary electrophoresis. For the informative women (n = 20), digestion of 100 ng genomic DNA with the methylation-sensitive restriction endonuclease, *Hpa*II, and subsequent PCR amplification of the HUMARA polymorphic CAG repeat was used to determine X-inactivation status in X-ALD heterozygotes.

Table 2 Nerve conduction studies according to the presence or absence of symptoms of 22 ×-ALD heterozygote women

Neuroconduction studies, right side (Mean ± sd) (range)		All 22 heterozygotes	Presence of symptoms		p*
			Symptomatic (20)	Asymptomatic (2)	
Motor conduction velocity (m/s)	Median	57 ± 6.2 (47–73)	56.9 ± 6.5	58.9 ± 2.2	ns
	(results above the cutoff value of 49,2)		(2)	(0)	
	Fibular	48.1 ± 5 (40–55)	47.3 ± 4.9	53.2 ± 1	ns
	(results above the cutoff value of 45.3)		(3)	(0)	
	Tibial	49.5 ± 4.6 (44–63)	49.2 ± 4.6	54.4	ns
	(results above the cutoff value of 39.9)		(0)	(0)	
Sensitive conduction velocity (m/s)	Median	49.4 ± 3.9 (42–59)	49.2 ± 4	52 ± 2	ns
	(results above the cutoff value of 51.7)		(12)	(0)	
	Ulnar	52.6 ± 6 (44–66)	52.8 ± 6.3	51.3 ± 0.6	ns
	(results above the cutoff value of 53.8)		(3)	(0)	
	Fibular superficial	53.7 ± 5.7 (44–64)	53.1 ± 5.4	58.4 ± 7.5	ns
	(results above the cutoff value of 35)		(0)	(0)	
Motor conduction amplitude (mV)	Median	9 ± 3.6 (2–16)	9 ± 3.7	9.2 ± 0.5	ns
	(results under the cutoff value of 3.3)		(1)	(0)	
	Fibular	4 ± 1.9 (1–7)	4 ± 1.8	3.9 ± 3.2	ns
	(results under the cutoff value of 1.6)		(1)	(0)	
	Tibial	7.7 ± 4.7 (2 to 19)	7.6 ± 5	8.1 ± 2.3	ns
	(results under the cutoff value of 2,8)		(1)	(0)	
Sensitive conduction amplitude (μV)	Median	14.5 ± 5.8 (5 to 29)	14.5 ± 5.9	15.2 ± 7	ns
	(results under the cutoff value of 15.1)		(3)	(0)	
	Ulnar	11.3 ± 6 (5 to 27)	11.4 ± 6.4	10.9 ± 3.3	ns
	(results under the cutoff value of 5.8)		(0)	(1)	
	Fibular	15.3 ± 6.6 (5 a 30)	15.3 ± 6.5	15.4 ± 11	ns
	(results under the cutoff value of 10)		(2)	(1)	

*Mann-Whitney U.

The degree of chromosome X inactivation was calculated using the formula [(d1/u1) / (d1/u1 + d2/u2)], where d = digested, u = undigested sample, and the two allele peaks (1 and 2) are compared [25]. Inactivation ratios less than 70:30 were considered random. Ratios greater than or equal to 70:30 and less than or equal to 90:10 were considered moderately skewed. Ratios greater than 90:10 were considered highly skewed [26].

Statistical analyses

Patient characteristics are given as mean ± SD and range, when applicable. Categorical variables were represented by absolute and relative frequencies and were compared through Fisher exact test. The majority of continuous variables did not show a normal distribution on the Shapiro-Wilk test, and therefore were tested by Mann-Whitney U, Spearman correlation and, when applicable,

Table 3 Somatosensory evoked responses according to the presence or absence of symptoms of 25 ×-ALD heterozygote women

Somatosensory evoked responses		All 25 heterozygote females	Presence of symptoms		p
			Symptomatic women: 23	Asymtomatic women: 2	
Upper Limbs (N20, or somatosensory cortex contralateral to the wrist stimulated) in ms	Mean ± sd	19.2 ± 1.1	20.1 ± 4.2	18 ± 0.9	ns *
	Above the cutoff value of 20.5 ms	6/25	6/23	0/2	ns #
Lower Limbs (P40, or somatosensory cortex ipsilateral to the tibial nerve stimulated) in ms	Mean ± sd	38 ± 2,5	55.3 ± 32.8	38.9 ± 3.8	ns *
	Above the cutoff value of 41,5 ms	18/25	17/23	1/2	ns #

* Mann-Whitney U; m/s = meters per second; mV – milivolts; μV = microvolts.

by stepwise linear regression. Statistical significance was defined as $p < 0.05$. All statistical tests were performed in PASW 18.3.

Results

Clinical findings

Forty five heterozygote women (belonging to 25 families) had been detected by molecular studies in our institution, from 2008 to 2013. Thirty three heterozygotes (or 73% of the total heterozygotes detected in our region) gave their consent and were included in this study. The another 27% (12 women) were lost: six were not found by two phone calls and letter, two refused to participate in the study and another four fulfilled exclusion criteria. The mean ± sd ages of the 33 participants and of the 12 non-participants, in 2013, were of 41.2 ± 11.9 and 40.9 ± 15, respectively (ns, t test). Twenty-nine of the 33 participants classified themselves as symptomatic and four, as asymptomatic, after learning about X-ALD symptoms in females. Their general characteristics are present in Table 1.

Symptomatic were significantly older and presented worse JOA and SSPROM scores and higher disability scores than asymptomatic women. Significant differences in SSPROM scores were due to a high proportion of symptomatic females (27/29) with spasticity/hyperreflexia; and to motor disabilities (Table 1). The autoclassification and the disability scores did not perfectly match: normal scores in the overall disability evaluation were obtained in all four asymptomatic but also in 15/29 symptomatic women. Overall disability was related to SSPROM and JOA scores, but not to age, age at onset of symptoms, neurophysiologic studies and other biomarkers (data not shown).

Among symptomatic women, although SSPROM correlated with age and DD, only DD was maintained on linear regression ($r = -0.73$, $p = 0.0001$, Spearman; $B = -1.91$, $EP = 0.28$). When all heterozygote women were analyzed together, the association with age was confirmed ($r = -0.65$, $p = 0.0001$, Spearman; $B = -0.43$, $EP = 0,10$, by Linear regression) (Figures 1A and 1C).

Similar associations were found regarding to JOA. Among symptomatic women, although JOA scores were at first correlated with age, AO and DD, only DD was significantly related to JOA on stepwise linear regression ($r = -0.61$, $p < 0.001$, Spearman; $B = -0.37$; $EP = 0.07$).

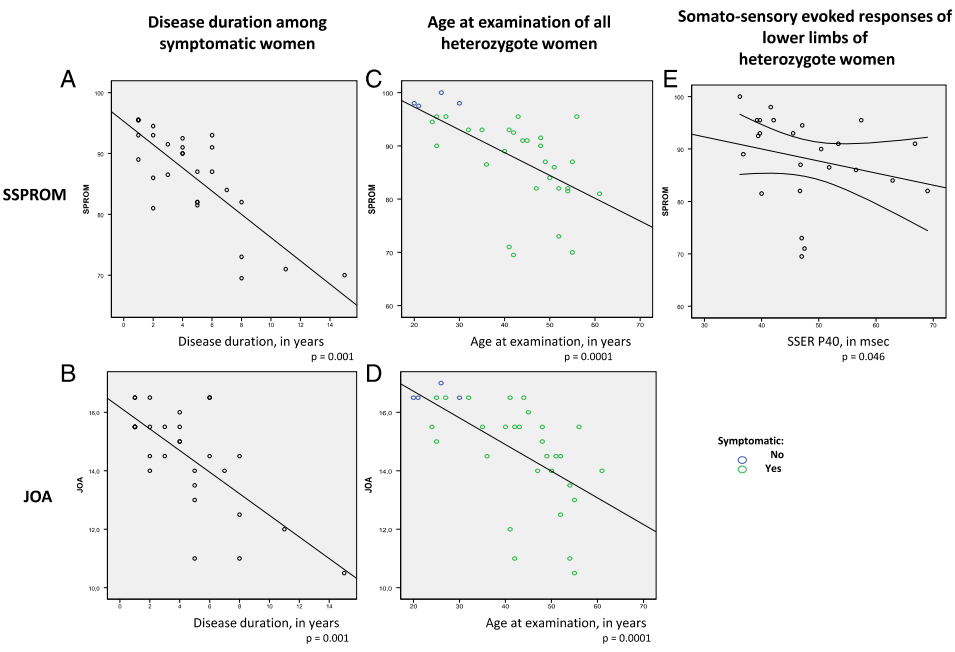

Figure 1 Associations relating JOA and SSPROM scales to independent variables age, disease duration and somato-sensory evoked responses. (A and B) Disease duration of symptomatic heterozygotes. **(C and D)** Age at examination all heterozygotes. **(E)** Somato-sensory evoked responses of lower limbs of all heterozygotes.

When all heterozygotes were analyzed together, JOA correlated with age (r = −0.68, p = 0.0001, Spearman; B = −0.09; EP = 0.02, Linear regression) (Figures 1B and 1D).

Mean ± sd of disease severity, or 1/(SSPROM x DD), among symptomatic women, were 3.7 ± 2.6. This score did not correlate with age or any other parameters.

Symptomatic classification produced more associations with independent parameters than the disability classification, in this cohort. Due to that, it was maintained as the stratification criteria between the present heterozygote women, when necessary.

Nerve conduction studies

Twenty-two out of 33 heterozygotes (20 symptomatic and 2 asymptomatic women) performed neurophysiologic studies. The others denied for personal reasons. Nineteen (including one asymptomatic heterozygote) presented at least one altered proof. Results are presented in Table 2.

All m-NCV and most of s-NCV were normal, and there were no correlations between NCVs and symptomatic status, age, AO, DD, disability status, JOA, SSPROM, disease severity, inactivation studies or plasma NSE concentrations (data not shown). Twelve out of 20 symptomatic heterozygotes showed reduced s-NCV of the median nerve, measured on the elbow. This finding was unrelated to any variable under study (data not shown).

No evidence of generalized axonal damage was found in any of the women studied, since the majority of CMAPs and SNAPs amplitudes were between the normal range. The amplitude of fibular superficial nerve SNAPs correlated with AO among the heterozygotes (r = 0.55, p = 0.015, Spearman).

Somatosensory evoked responses

Twenty-five heterozygote females (including those 22 females with nerve studies) were tested for SSE. Eighteen (17 symptomatic) presented delayed latencies in the central ascending conduction studies starting on the lower limbs (evoked potential P40) (Table 3). Latencies of the evoked potentials were not related to age, disability, disease severity or to the symptomatic status of the heterozygote women (ns, Spearman and Mann-Whitney U tests). SSPROM correlated weakly with lower limbs evoked potential latencies (r = −0.47, p = 0.018, Spearman, Figure 1E).

Mutations found in *ABCD1* gene

The mutations detected on *ABCD1* gene are depicted on Additional file 1: Table S1. These mutations were stratified according to their exonic position in the gene as well as divided according to their severity in missense or nonsense/frameshift. Mutation severity or position did not correlate either to age at onset of symptoms or to disease severity (Mann-Whitney U and Kruskal-Wallis, data not shown).

X Chromosome inactivation patterns

Twenty heterozygotes were informative in the technique applied to determine the inactivation pattern. Six had a skewed inactivation pattern of 70:30 or more. Skewed inactivation was not associated to symptomatic state (ns, Fisher exact test), disability, SSPROM, JOA, disease severity (ns, Spearman) or AO (ns, Linear Regression). A curious trend to relate larger skewing with age was also seen (r = 0.37, p = 0.1, Spearman).

NSE

The medium ± sd values of NSE were higher in heterozygotes than in controls (12.9 ± 7 versus 7.2 ± 7 ng/ml, p = 0.012, Mann-Whitney U, Figure 2). Both heterozygote and control groups had similar ages (41.2 ± 11.9 and 35.5 ± 10.4 years, ns, M-W U).

NSE was not correlated with age, either among all women or just among heterozygotes. No correlations were found between NSE and AO, disability or symptomatic status, inactivation studies, position of mutation in ABCD1 gene, SSPROM, JOA, disease severity, evoked responses or other neurophysiology parameters (data not shown).

VLCFA

VLCFA had been determined at the time of diagnosis of the present 33 heterozygotes, sometimes several years before the present evaluation. Their mean ± sd ages at the collection were of 30 ± 11.3 (range: 7 to 43) years-old. In the case of symptomatic women, for whom the symptom onset has been determined as year zero, blood collections were done at a −3.8 ± 4.5 (range: -12 to 3) years from the start of their symptoms. Correlations of VLCFA levels with age at the time of blood collection and with time from disease start were then tested. There were direct correlations between age and both C26:0 and VLCFA discriminant factor (r = 0.58, p = 0.011 and r = 0.60, p = 0.007, Spearman, Additional file 2: Figure S1).

Discussion

We examined 73% of all known heterozygote women for X-ALD followed in our institution, and detected significant clinical and neurophysiologic impairments in 87% of them. The clinical scales JOA and SSPROM were able to differentiate symptomatic from asymptomatic heterozygotes. Both scales were associated with DD of the symptomatic cases and with age in the overall group. Abnormalities in somatosensory evoked responses, mostly from the lower limbs, were quite frequent. A plasma protein related to neuronal damage, NSE, was associated with the heterozygote state. All these might be candidates as

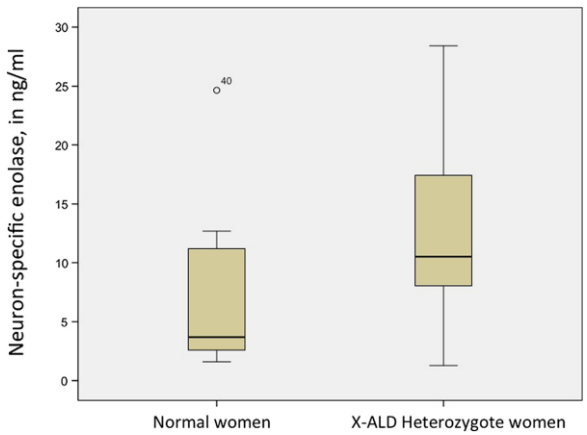

Figure 2 NSE among the X-ALD heterozygotes and the control women.

biomarkers for disease progression in heterozygotes for X-ALD.

Quantifying physical disability and neurologic burden is essential to understanding the progression rate of any disease [5]. In the present report, three levels of consequences related to the heterozygote state for X-ALD were measured: subjective perception, neurologic impairment and disability. Being symptomatic is a yes/or/no subjective perception. Neurologic impairment was measured by JOA and SSPROM scales, and by neurophysiologic studies. Disability reflects dysfunctions on performance and activity; we measured it by using specific domains of SSPROM. Disability needs an arbitrary cutoff. Disability scores obtained in the present group were very mild. Due to that, we decided to include even small disabilities in the dichotomic, positive group. We have then stratified heterozygote women both by their symptomatic and disability states.

We have obtained 29 symptomatic and 4 asymptomatic women; in contrast, there were 14 disabled and 19 non-disabled women. Although the disability stratification seemed to produce more even groups, it failed to be associated with age or with DD. In contrast, symptomatic status correlated with age, JOA, and SSPROM; moreover, DD - in other words, the duration of symptoms - correlated with both JOA and SSPROM. Therefore, symptomatic classification produced more useful information than its counterpart (disability).

Neurological impairment was better evaluated by clinical scales than by neurophysiology. Both JOA and SSPROM scales were able to discriminate symptomatic from asymptomatic heterozygotes, with almost no overlap, correlated very well with DD in the symptomatic group, and with age in the overall group.

The lack of any substantial alterations on peripheral neurophysiology reported here corroborates the findings of Schmidt and Cols [8]. One interesting finding was the direct correlation of fibular SNAP with AO. Reduced SNAP is commonly related to an inherent susceptibility of the fibular nerve for entrapments. Why did it correlate with AO, is an issue that deserves investigation in other heterozygotes.

After clinical scores, the SSER of lower limbs have shown the most prevalent abnormalities in heterozygote women. Similar results have been seen by others [8,27-30] SSER of lower limbs correlated with SSPROM and this might be taken as an external validation for SSPROM usefulness among X-ALD heterozygotes. On the other hand, SSER were not associated with any other measurement of disease progression like age and disease duration.

X chromosome inactivation has been studied as a modifying factor that could influence clinical presentation in women with X linked disorders. Relating a skewed inactivation in peripheral leukocytes to a neuronal disorder, as in the heterozygote women with X-ALD, is a complex hypothesis. If this association would exist, at least two possible mechanisms should be invoked: a good mirroring between neurons and leukocytes, where a skewed X inactivation in neurons would be related to differences in clinical presentation; and/or an intercellular mechanism, operating from skewed cells other than neurons. Differently from some authors [12] but similar to others [11], we did not find any association between inactivation and

symptomatic status or neurological scores. We observed a trend relating an increased skewing with age, which is in accordance with literature [31].

VLCFA also increased with age, at least in this cohort, whose blood collections had been done between 7 and 43 years of age. Other authors have observed a similar finding in this age group, with decreasing VLCFA concentrations in women older than 50 years old [32]. Although both VLFCA and skewing inactivation increased with age in our group, no association was found with increasing neurological symptoms.

NSE is a cytoplasmatic glycolytic enzyme found in neurons and cells with neuroendocrine differentiation. Since NSE is not physiologically secreted, an increase of its serum concentrations can be associated with structural damage to neuronal cells [33]. NSE concentrations were higher in heterozygote women than in controls, in the present study. Since NSE was not associated with symptomatic or disability status, nor with any variable related to disease progression, we were not able to show a clear potential for NSE as a biomarker for disease progression in this disease.

According to former studies, around 50% of X-ALD heterozygotes showed some degree of neurologic involvement [6]. Our results were quite different: 87% were symptomatic, with neurological impairments as measured by JOA and SSPROM scores. Our large proportion of symptomatic women was quite surprising. Although one cannot rule out a selection bias favoring the recruitment of symptomatic heterozygotes, the similitude between the mean ages of the recruited and of the non-recruited heterozygote women works against this conjecture. Our rates might be explained by different measurements of neurological burden: perhaps former reports relied on disabilities rather than impairments. Our experience showed that disabilities were mild in general, with the exception of sphincter dysfunctions (Table 1). Impairments, on the other hand, were clearly present, the major impact being the corticospinal involvement (Table 1).

Emotional issues should also be remembered. Male X-ALD is a catastrophic disease for families. A mother or a female caregiver of an affected boy usually lives in very stressful conditions, where priorities are put in hemizygote men rather than in her well-being. Maybe the actual numbers of symptomatic heterozygote females had been previously underestimated, due to a hasty report of these women about their healthy states. The hypothesis that the majority of heterozygote females will present a neurologic impairment is not negligible. Moreover, the associations between JOA and SSPROM with age might suggest that the symptomatic status is a matter of time and that, as heterozygote females grow older, they get symptomatic.

With the prominent involvement of pyramidal tracts, X-ALD presenting in symptomatic heterozygotes and as male AMN, can be seen as one form of complicated spastic paraplegia (SPG) [34]. Therapeutic trials in men and women with AMN and in SPGs in general are expected in a near future, and it will be important to decide what scales to use on them. Recently, some studies have measured the neurological impairment of SPGs by the Spastic Paraplegia Rating Scale (SPRS) [35]. In contrast, we have used two instruments fitted to measure both disability and impairment, scales that might be called disease severity scoring systems (or 3S): the scales JOA and SSPROM. SSPROM was developed to follow metabolic progressive myelopathies such as AMN; so far, only the present and the description studies have used it [16]. JOA was developed to follow cervical compression myelopathies [15], and it is probably the most used neurologic scale for myelopathies so far. For a clinical trial, several properties of the chosen scale will be essential to guarantee the best design, such as validity, reliability and sensitivity to change. At this very moment, it is not clear what scale will be best fitted to a future trial for AMN. Comparisons of these characteristics among different scales are needed and should be done in a near future.

Conclusions

Neurologic impairments are frequent and are clearly related to age and to the CNS involvement, in heterozygote females. SSER of lower limbs and plasma NSE concentrations were altered in the majority of heterozygote females. Since they did not differentiate between symptomatic and asymptomatic heterozygotes, nor were related to age or disease duration, we cannot postulate them as good candidates as biomarkers of disease progression. VLFCA and skewing inactivation were also unable to separate symptomatic from asymptomatic heterozygotes. Both increased with age, but dissociated from the increasing neurological symptoms. Among the number of potential biomarkers of disease progression, JOA and SSPROM presented the most robust associations with disease duration and age. Besides that, SSPROM correlated with SSER of lower limbs. We suggest that JOA and SSPROM might be valuable instruments in future natural history studies in heterozygotes for X-ALD.

Additional files

Additional file 1: Table S1. Mutations found at ABCD1 gene in the present X-ALD heterozygote women, and the distribution of ages at examination and at onset of symptoms.

Additional file 2: Figure S1. Associations between age and (6A) C26:00 plasma levels and (6B) VLCFA discriminant factor 3,805(C24:0/C22:0) + 5,296(C26:0/C22:0) + 5,15(C26:0).

Abbreviations
AMN: Adrenomyeloneuropathy; AO: Age at onset; C22:0: Docosanoic acid; C24:0: Tetracosanoic acid; C26:0: Hexacosanoic acid; CALD: Cerebral form of ALD; CMAP: Compound muscle action potential; DD: Disease duration; HUMARA: Human androgen-receptor locus; JOA: Japanese Orthopaedic Association scale of myelopathy; m-NCV: Motor conduction velocity; NSE: Neuron-specific enolase; SNAP: Sensory nerve action potential; SPG: Spastic paraplegia; SPRS: Spastic Paraplegia Rating Scale; SSER: Somatosensory evoked responses; SSPROM: Severity Score System for Progressive Myelopathy; VLCFA: Very long chain fatty acids; X-ALD: X-linked Adrenoleukodystrophy.

Competing interests
The authors declare that they have no competing interests.

Authors' contributions
CTH conceived the study, participated in the design of the study, carried out the recruitment, interviews and clinical studies, and helped to draft the manuscript. PS carried out the SSER studies and participated in the analysis. PS and VTF carried out peripheral neurophysiology studies and participated in the analysis of the data. DMC performed VLCFA analyses and helped in the coordination of data. CRV performed VLCFA analyses and helped in the acquisition of funding. VT performed NSE analyses and participated in the analysis of data. LVP performed NSE studies and helped in the acquisition of funding. FSP carried out the molecular genetic studies and participated in the analysis. UM participated in the molecular analysis and in the coordination of data. LBJ conceived the study, participated in the design and coordination of the study, performed the statistical analysis, and drafted the manuscript. All authors read and approved the final manuscript.

Acknowledgements
We would like to thank the patients and their families for taking part in this study. We would also like to thank Raphael M. Castilhos and Deborah Blank for their technical assistance and contribution in early stages of this project; Karina C. Donis, André dos Anjos and Jonas Alex Saute for their contribution in recruiting some patients; and Ana Louzada for her technical assistance in the neurophysiological studies. This work was supported by Fundo de Incentivo à Pesquisa do Hospital de Clínicas de Porto Alegre (FIPE-HCPA), Project GPPG HCPA 110308; and by Instituto Nacional de Ciência e Tecnologia em Excitotoxicidade e Neuroproteção (INCTEN), Porto Alegre, Brazil. CTH were funded by INAGEMP - Instituto Nacional de Genética Médica Populacional. Pereira FS, Matte U, Portela LV and Jardim LB are funded by CNPq – Conselho Nacional de Desenvolvimento Científico e Tecnológico.

Author details
[1]Post-Graduation Program in Genetics and Molecular Biology, Universidade Federal do Rio Grande do Sul (UFRGS), Porto Alegre, Brazil. [2]Post-Graduation Program in Biochemistry, Universidade Federal do Rio Grande do Sul (UFRGS), Porto Alegre, Brazil. [3]Department of Biochemistry, Universidade Federal do Rio Grande do Sul (UFRGS), Porto Alegre, Brazil. [4]Department of Analysis, Universidade Federal do Rio Grande do Sul (UFRGS), Porto Alegre, Brazil. [5]Department of Internal Medicine, Universidade Federal do Rio Grande do Sul (UFRGS), Porto Alegre, Brazil. [6]Medical Genetics Service, Hospital de Clínicas de Porto Alegre, Porto Alegre, Rio Grande do Sul, Brazil. [7]Neurology Service, Hospital de Clínicas de Porto Alegre, Porto Alegre, Rio Grande do Sul, Brazil. [8]Laboratory of Genetic Identification, Hospital de Clínicas de Porto Alegre, Porto Alegre, Rio Grande do Sul, Brazil. [9]Laboratory of Gene Therapy, Hospital de Clínicas de Porto Alegre, Porto Alegre, Rio Grande do Sul, Brazil. [10]Laboratório de Neurociências Clínicas, Centro de Ciências da Vida e da Saúde, Universidade Católica de Pelotas, Pelotas, Brazil. [11]Instituto Nacional de Genética Médica Populacional (INAGEMP), Porto Alegre, Brazil. [12]Instituto Nacional de Ciência e Tecnologia em Excitotoxicidade e Neuroproteção (INCTEN), Porto Alegre, Brazil.

Received: 2 December 2013 Accepted: 3 January 2014
Published: 13 January 2014

References

1. Bezman L, Moser AB, Raymond GV, Rinaldo P, Watkins PA, Smith KD, Kass NE, Moser HW: **Adrenoleukodystrophy: incidence, new mutation rate, and results of extended family screening.** *Ann Neurol* 2001, **49**(4):512–517.
2. Dubois-Dalcq M, Feigenbaum V, Aubourg P: **The neurobiology of X-linked adrenoleukodystrophy, a demyelinating peroxisomal disorder.** *Trends Neurosci* 1999, **22**(1):4–12. Review.
3. Mosser J, Lutz Y, Stoeckel ME, Sarde CO, Kretz C, Douar AM, Lopez J, Aubourg P, Mandel JL: **The gene responsible for adrenoleukodystrophy encodes a peroxisomal membrane protein.** *Hum Mol Genet* 1994, **3**(2):265–271.
4. Moser H, Smith K, Watkins P, Powers J, Moser A: **X-linked adrenoleukodystrophy.** In *The metabolic and molecular bases of inherited disease.* Edited by Scriver C, Beaudet A, Sly W, Valle D. New York, N.Y: McGraw-Hill; 2001:3257–3301.
5. Jangouk P, Zackowski KM, Naidu S, Raymond GV: **Adrenoleukodystrophy in female heterozygotes: underrecognized and undertreated.** *Mol Genet Metab* 2012, **105**(2):180–185.
6. Moser HW, Moser AB, Naidu S, Bergin A: **Clinical aspects of adrenoleukodystrophy and adrenomyeloneuropathy.** *Dev Neurosci* 1991, **13:**254–261.
7. Zackowski KM, Dubey P, Raymond GV, Mori S, Bastian AJ, Moser HW: **Sensorimotor function and axonal integrity in adrenomyeloneuropathy.** *Arch Neurol* 2006, **63:**74–80.
8. Schmidt S, Träber F, Block W, Keller E, Pohl C, von Oertzen J, Schild H, Schlegel U, Klockgether T: **Phenotype assignment in symptomatic female carriers of X-linked adrenoleukodystrophy.** *J Neurol* 2001, **248**(1):36–44.
9. Asheuer M, Bieche I, Laurendeau I, Moser A, Hainque B, Vidaud M, Aubourg P: **Decreased expression of ABCD4 and BG1 genes early in the pathogenesis of X-linked adrenoleukodystrophy.** *Hum Mol Genet* 2005, **14**(10):1293–1303. Epub 2005 Mar 30.
10. Migeon BR, Moser HW, Moser AB, Axelman J, Sillence D, Norum RA: **Adrenoleukodystrophy: evidence for X linkage, inactivation, and selection favoring the mutant allele in heterozygous cells.** *Proc Natl Acad Sci U S A* 1981, **78**(8):5066–5070.
11. Watkiss E, Webb T, Bundey S: **Is skewed X inactivation responsible for symptoms in female carriers for adrenoleucodystrophy?** *J Med Genet* 1993, **30**(8):651–654.
12. Maier EM, Muntau AC KS, Wichers M, Braun A, Roscher AA: **Symptoms in carriers of adrenoleukodystrophy relate to skewed X inactivation, Ann.** *Neurol* 2002, **52:**683–688.
13. Deon M, Sitta A, Barschak AG, Coelho DM, Terroso T, Schmitt GO, Wanderley HY, Jardim LB, Giugliani R, Wajner M, Vargas CR: **Oxidative stress is induced in female carriers of X-linked adrenoleukodystrophy.** *J Neurol Sci* 2008, **266**(1–2):79–83.
14. Pereira FS, Matte U, Habekost CT, de Castilhos RM, El Husny AS, Lourenço CM, Vianna-Morgante AM, Giuliani L, Galera MF, Honjo R, Kim CA, Politei J, Vargas CR, Jardim LB: **Mutations, clinical findings and survival estimates in South American patients with X-linked adrenoleukodystrophy.** *PLoS One* 2012, **7**(3):e34195.
15. Yanenobu K, Abumi K, Negata K, *et al*: **Interobserver and Intraobserver Reliability of the Japanese Orthopaedic Association Scoring System for Evaluation of Cervical Compression Myelopathy.** *Spine* 2001, **26:**1890–1895.
16. Castilhos RM, Blank D, Netto CB, Souza CF, Fernandes LN, Schwartz IV, Giugliani R, Jardim LB: **Severity score system for progressive myelopathy: development and validation of a new clinical scale.** *Braz J Med Biol Res* 2012, **45**(7):565–572.
17. Merkies ISJ, Schmitz PIM, van der Meché FGA, *et al*: **Clinimetric evaluation of a new overall disability scale in immune mediated polyneuropathies.** *J Neurol Neurosurg Psychiatry* 2002, **72:**596–601.
18. Kurtzke JF: **Rating neurologic impairment in multiple sclerosis: An expanded disability status scale (EDSS).** *Neurology* 1983, **33:**1444–1452.
19. Dumitru D, Amato AA: **Acquired neuropathies.** In *Electrodiagnostic Medicine.* 2nd edition. Edited by Dumitru D, Zwarts MJ, Amato A. Philadelphia: Hanley and Belfus Inc; 2002:937–1041.
20. Chiappa KH: *Evoked Potentials in Clinical Medicine.* New York: Raven Press; 1997.
21. Moser HW, Moser AB: **Measurement of saturated very long chain fatty acid in plasma.** In *Techniques of diagnostic human biochemical genetics.* Edited by Hommes FA. New York: Wiley; 1991.
22. Moser AB, Kreiter N, Bezman L, Lu S, Raymond GV, Naidu S, Moser HW: **Plasma very long chain fatty acids in 3,000 peroxisome disease patients and 29,000 controls.** *Ann Neurol* 1999, **45**(1):100–110.
23. Miller SA, Dykes DD, Polesky HF: **A simple salting out procedure for extracting DNA from human nucleated cells.** *Nucleic Acids Res* 1988, **16**(3):1215.

24. Allen RC, Zoghbi HY, Moseley AB, Rosenblatt HM, Belmont JW: **Methylation of HpaII and HhaI sites near the polymorphic CAG repeat in the human androgen-receptor gene correlates with X chromosome inactivation.** *Am J Hum Genet* 1992, **51**(6):1229–1239.
25. Sharp A, Robinson D, Jacobs P: **Age- and tissue-specific variation of X chromosome inactivation ratios in normal women.** *Hum Genet* 2000, **107**:343–349.
26. Landgraf JMA, Cottle A, Plenge RM, Friez M, Schwatrz CE, Longshore J, Willard HF: **X Chromosome-Inactivation Patterns of 1,005 Phenotypically Unaffected Females.** *Am. J. Hum. Gent* 2006, **79**:493–499.
27. Moloney JB, Masterson JG: **Detection of adrenoleucodystrophy carriers by means of evoked potentials.** *Lancet* 1982, **2**:852–853.
28. Garg BP, Markand ON, DeMyer WE, Warren C Jr: **Evoked response studies in patients with adrenoleukodystrophy and heterozygous relatives.** *Arch Neurol* 1983, **40**:356–359.
29. Shimizu H, Moser HW, Naidu S: **Auditory brainstem response and audiologic findings in adrenoleukodystrophy: its variant and carrier.** *Otolaryngol Head Neck Surg* 1988, **98**:215–220.
30. Restuccia D, Di Lazzaro V, Valeriani M, Oliviero A, Le Pera D, Colosimo C, Burdi N, Cappa M, Bertini E, Di Biase A, Tonali P: **Neurophysiological abnormalities in adrenoleukodystrophy carriers.** *Evidence of different degrees of central nervous system involvement, Brain* 1997, **120**(7):1139–1148.
31. Mengel-From J, Thinggaard M, Christiansen L, Vaupel JW, Orstavik KH, Christensen K: **Skewed X inactivation and survival: a 13-year follow-up study of elderly twins and singletons.** *Eur J Hum Genet* 2012, **20**(3):361–364.
32. Stradomska TJ, Tylki-Szymańska A: **Decreasing serum VLCFA levels in ageing X-ALD female carriers.** *J Inherit Metab Dis* 2001, **24**(8):851–857.
33. Tort AB, Portela LV, Rockenbach IC, Monte TL, Pereira ML, Souza DO, Rieder CR, Jardim LB: **S100B and NSE serum concentrations in Machado Joseph disease.** *Clin Chim Acta* 2005, **351**(1–2):143–148.
34. Finsterer J, Löscher W, Quasthoff S, Wanschitz J, Auer-Grumbach M, Stevanin G: **Hereditary spastic paraplegias with autosomal dominant, recessive, X-linked, or maternal trait of inheritance.** *J Neurol Sci* 2012, **318**(1–2):1–18.
35. Schüle R, Holland-Letz T, Klimpe S, Kassubek J, Klopstock T, Mall V, Otto S, Winner B, Schöls L: **The Spastic Paraplegia Rating Scale (SPRS): a reliable and valid measure of disease severity.** *Neurology* 2006, **67**(3):430–434.

doi:10.1186/1750-1172-9-6
Cite this article as: Habekost *et al.*: Neurological impairment among heterozygote women for X-linked Adrenoleukodystrophy: a case control study on a clinical, neurophysiological and biochemical characteristics. *Orphanet Journal of Rare Diseases* 2014 **9**:6.